

March 1985

DEVELOPMENT OF AN ADJUSTABLE BUOYANCY  
BALLON TRACER OF ATMOSPHERIC MOTION

Phase I. Systems Design and Demonstration of Feasibility

ATMOSPHERIC SCIENCES RESEARCH LABORATORY  
OFFICE OF RESEARCH AND DEVELOPMENT  
U.S. ENVIRONMENTAL PROTECTION AGENCY  
RESEARCH TRIANGLE PARK, NORTH CAROLINA 27711

DEVELOPMENT OF AN ADJUSTABLE BUOYANCY  
BALLON TRACER OF ATMOSPHERIC MOTION

Phase I. Systems Design and Demonstration of Feasibility

by

B. D. Zak, H. W. Church, A. L. Jensen,  
G. T. Gay, and M. D. Ivey

Sandia National Laboratories  
Albuquerque, New Mexico 87185

Interagency Agreement DW930214

Project Officers

J. S. Irwin and R. G. Lamb  
Meteorology and Assessment Division  
Atmospheric Sciences Research Laboratory  
Research Triangle Park, NC

ATMOSPHERIC SCIENCES RESEARCH LABORATORY  
OFFICE OF RESEARCH AND DEVELOPMENT  
U.S. ENVIRONMENTAL PROTECTION AGENCY  
RESEARCH TRIANGLE PARK, NORTH CAROLINA 27711

# NOTICE

The information in this document has been funded by the United States Environmental Protection Agency under Interagency Agreement DW930214 to Sandia National Laboratories. It has been subject to the Agency's peer and administrative review, and it has been approved for publication as an EPA document. Mention of trade names or commercial products does not constitute endorsement or recommendation for use.

## ABSTRACT

An Adjustable Buoyancy Balloon Tracer of Atmospheric Motion is a research tool which allows one to follow atmospheric flows in both the horizontal and the vertical, including the weak, sustained vertical motion associated with meso- and synoptic-scale atmospheric disturbances. The design goals for the Balloon Tracer to be developed here specify a lifetime  $\geq 3$  days, tracking range  $\geq 1000$  km, a ceiling altitude  $\geq 500$  mb (5.5 km), and the capability to respond to mean vertical flows as low as 1 cm/s. The balloon tracer is also to measure and telemeter selected meteorological variables, to be sufficiently inexpensive to permit use in significant numbers, and to be serviced by a ground system capable of handling several balloon tracers at a time. While the balloon tracer has applications throughout the atmospheric sciences, the immediate motivation for this effort is to meet the need to evaluate the accuracies of existing air pollution transport models, to establish source-receptor relationships to distances of order 1000 km, and to assess the inherent limits on the predictability of source impact at long distances. The authors have proposed a generic design for such a system. They also have subjected the proposed design to theoretical analysis, have constructed a prototype, and have conducted a series of tests with the prototype to evaluate the concept. They conclude without reservation that a system meeting the design goals is feasible, and are proceeding to build that system in Phase II of this project.

## CONTENTS

Abstract. . . . .	iii
Figures . . . . .	vii
Acronyms. . . . .	x
Acknowledgements. . . . .	xi
1. Summary . . . . .	1
2. Introduction. . . . .	11
3. Concept and Theoretical Analysis. . . . .	14
a. Buoyancy Control. . . . .	14
b. Control Strategies. . . . .	21
4. Systems Design. . . . .	27
a. Tracking and Data Handling. . . . .	28
b. Balloon Envelope. . . . .	32
c. Payload . . . . .	33
d. Ground Support Station. . . . .	44
e. Control Algorithm . . . . .	47
5. Demonstration of Technical Feasibility: The Testbed Prototype . . . . .	48
a. Approach. . . . .	48
b. Balloon Envelope. . . . .	49
c. Payload . . . . .	50
d. Vertical Anemometer . . . . .	60
e. Prototype Ground System . . . . .	63
6. Experimental Results. . . . .	66
a. Laboratory. . . . .	66
b. Tower . . . . .	73
c. Ambient Atmosphere. . . . .	90
7. Future Work . . . . .	93
8. Conclusions and Discussion. . . . .	97
References . . . . .	102

## Appendices:

A.	Federal Aviation Regulations, Part 101 . . . .	105
B.	Pumpdown Speed in a Standard Atmosphere. . . .	110
C.	Superpressure as a Function of Equilibrium Altitude . . . . .	112
D.	Effect of Temperature Swing on Balloon Pressure . . . . .	115
E.	Energy Required for Pumpdown . . . . .	116
F.	Lift and Maximum Altitude. . . . .	118
G.	Trajectories: Isentropic and Actual . . . . .	121
H.	The ARGOS Satellite-Based Data Collection and Platform Location System . . . . .	125
I.	Pumpdown Speed with an Arbitrary Lapse Rate. . . . .	140
J.	Diffusive Spread of a Marked Air Parcel and Its Implications for Lagrangian Experiments. .	142

## FIGURES

<u>Number</u>	<u>Page</u>
1-1 Prototype Adjustable Buoyancy Balloon Tracer being readied for flight . . . . .	3
3-1 Schematic Diagram of the Adjustable Buoyancy Balloon	16
3-2 Sulfur Hexafluoride Concentration versus time on board the LAMP (Lagrangian Measurement Platform) during the Tennessee Plume Study . . . . .	25
3-3 Trajectory of LAMP during the TPS. . . . .	26
4-1 Number of ground stations required for 1000 km square area, and VHF radio range as a function of balloon altitude . . . . .	29
4-2 Buoyancy control plumbing. . . . .	34
4-3 NCAR microprocessor data system for balloon application. . . . .	38
4-4 ARGOS PTT (Platform Transmitter Terminal) for balloon application. . . . .	40
4-5 NCAR ARGOS Antenna . . . . .	42
4-6 Paper lithium battery. . . . .	43
4-7 Diagram of ground support station for an operational tracer system. . . . .	46
5-1 Block diagram of testbed prototype payload . . . . .	52
5-2 Airsonde and tethersonde circuit boards side by side	55
5-3 Preferred sensor placement relative to the balloon .	56
5-4 Gilian pump, Klippard valve, and Japan Remote Control RC receiver and servo. . . . .	58
5-5 Assembled testbed prototype payload. . . . .	59
5-6 High sensitivity vertical anemometer for relative vertical air motion measurement . . . . .	61
5-7 Vertical air motion observed with MacCready anemometer on DaVinci II balloon flight. . . . .	62

5-8	Block diagram of prototype ground station. . . . .	64
5-9	Prototype ground station . . . . .	65
6-1	Combined speed of two Gilian pumps at 6 VDC versus backpressure. . . . .	69
6-2	Combined current consumption of two Gilian pumps at 6 VDC versus backpressure . . . . .	71
6-3	Vent valve flow as a function of superpressure . . .	72
6-4	Tower of Solar Central Receiver Test Facility, the interior of which was used to test the testbed prototype PLT. . . . .	74
6-5	Interior of the Solar Tower with reference levels indicated . . . . .	75
6-6	Dimensions and reference levels of testbed prototype PLT for Solar Tower tests. . . . .	76
6-7	Valve-up number one. . . . .	78
6-8	Pumpdown number one. . . . .	79
6-9	Temperature vs altitude on pumpdown number one . . .	80
6-10	Internal temperature, ambient temperature, and superpressure on pumpdown number one . . . . .	81
6-11	Valve-up number two. . . . .	83
6-12	Pumpdown number two. . . . .	85
6-13	Temperature vs. altitude on pumpdown number two. . . . .	86
6-14	Testbed prototype PLT during an "open air tower" test . . . . .	91
6-15	Testbed prototype PLT during a slack-tether flight test . . . . .	92
7-1	Lagrangian experiment instrumented aircraft measurement pattern . . . . .	96
G-1	Comparison of twelve-hour isobaric and isentropic trajectories . . . . .	124



J-1	Dimensionless diffusion parameter D versus dimensionless parameter T proportional to time . . .	145
J-2	$\epsilon^{1/3}$ versus time for the DaVinci II flight . . . . .	147
J-3	" $\epsilon$ -meter" used to make turbulence measurements on DaVinci II . . . . .	148

## ACRONYMS

ADAS	-	Atmospheric Data Acquisition System
AGL	-	Above Ground Level
AIR	-	Atmospheric Instrumentation Research (Inc.)
CNES	-	Centre National d'Etudes Spatiales (France)
CVB	-	Constant Volume Balloon
DME	-	Distance-Measuring Equipment
DOE	-	U.S. Department of Energy
EPA	-	U.S. Environmental Protection Agency
FAA	-	Federal Aviation Administration
GHOST	-	Global Horizontal Sounding Technique
HF	-	High Frequency
LAMP	-	Lagrangian Measurement Platform
LORAN	-	Long Range (radio) Navigation
LUT	-	Local User Terminal (ARGOS)
MSL	-	(Above) Mean Sea Level
NASA	-	National Aeronautics and Space Administration
NCAR	-	National Center for Atmospheric Research
NOAA	-	National Oceanic and Atmospheric Administration
PGS	-	Prototype Ground Station
PLT	-	Physical Lagrangian Tracer
PTT	-	Platform Transmitter Terminal (ARGOS)
RC	-	Radio Control
RV	-	Recreational Vehicle
SNL	-	Sandia National Laboratories
TP	-	Testbed Prototype
TPS	-	Tennessee Plume Study
UHF	-	Ultra High Frequency
VOR	-	VHF Omni-directional Range
VHF	-	Very High Frequency
WMO	-	World Meteorological Organization

## ACKNOWLEDGMENTS

The authors wish to thank R. G. Lamb and J. S. Irwin of the Atmospheric Sciences Research Laboratory, U.S. Environmental Protection Agency, whose interest in broadening and deepening understanding of atmospheric processes important to air pollution sparked this project. We gratefully acknowledge the substantial contributions of V. E. Lally, E. Lichfield, S. Stenlund, and N. Carlson of the National Center for Atmospheric Research for generously sharing with us their wealth of experience with superpressure balloons and supporting systems. R. Enderson and T. Markhart of Raven Industries, D. Call of Atmospheric Instrumentation Research, Inc., and A. L. Morris and D. Street of Ambient Analysis, Inc., all went far beyond the call of duty in assisting us with this effort. We also wish to thank J. Otts of Sandia National Laboratories for making the solar tower available for system testing, S. Sawyer, also of Sandia, for her dedication and skill in preparing this report, and P. S. Homann, for assuring that it all came together properly. The following individuals graciously consented to review and comment on this document: J. S. Irwin and R. G. Lamb of the U.S. Environmental Protection Agency, E. F. Danielson of NASA Ames Research Center, V. E. Lally and E. Lichfield of the National Center for Atmospheric Research, J. K. Angell and C. R. Dickson of the NOAA Air Resources Laboratory, P. B. MacCready of AeroVironment, Abdul Alkezweeny of Pacific Northwest Laboratory, and D. S. Ballantine of the DOE Office of Health and Environmental Research. We are particularly indebted to A. L. Morris of Ambient Analysis, who not only reviewed this report, but also checked the equations describing balloon behavior. This research was funded by the U.S. Environmental Protection Agency in part through the National Acid Precipitation Assessment Program.



## 1. SUMMARY

An Adjustable Buoyancy Balloon tracer of atmospheric motion is a physical Lagrangian tracer, an airborne instrumentation system that follows the flow of air, and that can be tracked electronically (Figure 1-1). Such a system has been desired for decades by researchers in the atmospheric sciences to aid in understanding the dynamics of the atmosphere, and to cast light on long range air pollution. The present effort, however, is motivated primarily by the more immediate need to establish source-receptor relationships to distances of order 1000 km, to evaluate the accuracies of existing air pollution transport models, and to assess the inherent limits on the predictability of source impacts at long distances.

The Adjustable Buoyancy Balloon system must operate under Federal Aviation Regulations Part 101, which covers unmanned free balloons. FAR 101 divides such balloons into two classes. Those which offer little hazard to aircraft because of their limited size, weight, and density are explicitly exempted from most of the other stipulations of the regulation. So-called "weather balloons" (radiosondes) fall in this category. Hundreds of such balloons are launched twice a day from sites all over the US and around the world to provide data on meteorological conditions aloft. Balloons not meeting the conditions contained in the exemption clauses of FAR 101 are subject to strict regulation, and are treated much like other aircraft. It is highly desirable for the balloon tracer to operate under the exemption clauses, in that certain other provisions of FAR 101 would severely limit the usefulness of a balloon tracer which was not exempt. Even though the Adjustable Buoyancy Balloon system will be exempt, it will nevertheless carry a radar reflector and an FAA

transponder so the FAA can keep track of its location.

In addition to meeting the exemption conditions of FAR 101, the design goals for the balloon tracer are:

- Lifetime  $\geq$  3 days
- Tracking range  $>$  1000 km
- Telemetry of selected meteorological parameters
- Ground system capable of handling several PLTs at a time
- Ceiling altitude  $\geq$  500 mb (5.5 km)
- Follows mean vertical flows as low as 1 cm/s
- Sufficiently inexpensive to permit use in significant numbers.

The project is divided into two phases:

Phase I: Systems Design and Demonstration of Feasibility.

Phase II: Development of an Operational Prototype.

This report covers work on Phase I. Phase II is now proceeding.

The design of the Adjustable Buoyancy Balloon Tracer is based upon an idea put forward by V. Lally of the National Center for Atmospheric Research in 1967. Here the outer skin of a spherical balloon is made of a high modulus of elasticity material which expands very little as pressure in the balloon increases. Hence, the volume of the balloon is very nearly constant as long as the pressure of the gas inside is greater than the ambient pressure. A thin polyethylene bag, or "ballonet", separates the interior into two compartments. One of these compartments is filled with helium, the lift gas. The other is filled with air. The air serves as ballast. A pump and valve permit additional air to be taken into the balloon, or to be released. When the balloon is at its

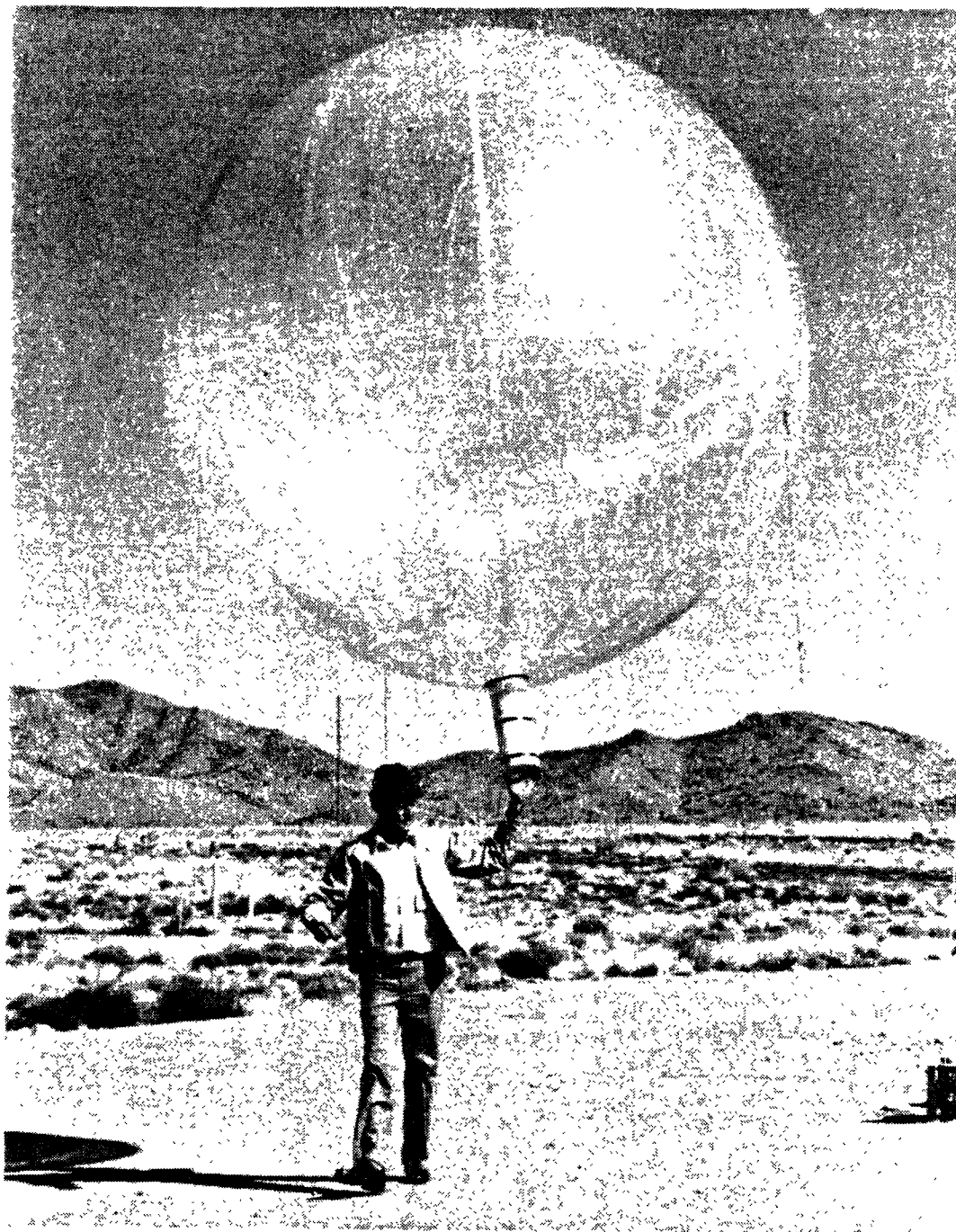


Figure 1-1. Prototype Adjustable Buoyancy Balloon Tracer being readied for flight. Payload weighs 2.36 kg (5.2 lbs) including batteries, and is constructed of styrofoam covered with 0.6 oz fiberglass. It meets the exemption clauses of FAR 101.

equilibrium altitude, and more air is pumped in, it becomes heavier, and sinks to a lower altitude. When air is released through the valve, the balloon becomes lighter, and rises to a higher altitude.

Expressions have been derived in the appendices which describe the rate at which pumping and valving change the equilibrium altitude, the behavior of the excess of internal over ambient pressure (superpressure) as a function of equilibrium altitude, the effect of temperature changes on balloon pressure, the energy required for pumpdown, how the ceiling altitude is determined by system parameters, and a procedure for properly filling the balloon to obtain the desired characteristics. All of these calculations confirm that a properly-designed balloon system of the type proposed by Lally can meet the design goals.

Given this means of adjusting the buoyancy of a constant volume balloon, the balloon will become a tracer for atmospheric motion if the buoyancy is periodically adjusted so that the balloon follows the vertical motion of the air. The nature of balloons is such that they naturally follow horizontal air motions. Hence, if a system is constructed to also follow the vertical motions, that system will follow the overall flow.

There are two basic approaches to the altitude control problem. The first is to continuously measure the vertical velocity of the air relative to the balloon, and to adjust the buoyancy so that, on average, the relative velocity of the air is zero -- that is, so that on average, the balloon and the air move together. The second approach is to take advantage of the very nearly adiabatic nature of atmospheric flows. When flows are adiabatic, the potential temperature is



constant along each air parcel trajectory. In this approach, the buoyancy of the balloon is adjusted so that the potential temperature is kept constant. As long as this condition is met, the balloon will move along with the air surrounding it.

The approach to altitude control based on relative vertical air motion is most direct, but if it were to be used continuously for three days, the air motion measurements would have to be extraordinarily accurate. Under most atmospheric conditions, the approach based on potential temperature is quite satisfactory, but under certain conditions -- when the system is in a layer of air in which active convective mixing is taking place -- potential temperature does not offer an adequate guide for altitude control. Under convective mixing conditions, the air surrounding the balloon consists of turbulent air flows moving both up and down. The mixing makes the potential temperature uniform with altitude within the mixed layer.

When convective mixing engulfs a "parcel" of air, the main effect is to disperse it, and to spread it out in the vertical, mixing it with air from all the surrounding parcels. If a balloon tracer is embedded in an air parcel which is subjected to convective mixing, as long as the balloon remains in the mixed layer, it is within the confines of the now greatly-expanded "parcel". Following the expanding parcel during convective mixing makes less stringent demands on the buoyancy control system than does following a parcel in the absence of convective activity. Hence, a number of different control strategies are satisfactory during these periods.

Thus it appears that a hybrid control approach will yield best results. Different control strategies will be employed

under different meteorological conditions. On the basis of the data from the onboard sensors, an onboard microcomputer will determine which control strategy will be implemented at any given time.

Having confirmed on paper that the Adjustable Buoyancy Balloon Tracer is viable in principle, we proceeded to formulate a preliminary design for an operational system. The major elements of the design are the tracking and data handling system, the balloon envelope itself, the balloon payload, and the ground support station.

Tracking and data reception will be handled by the ARGOS satellite-based data collection and platform location system. ARGOS is a joint undertaking of NASA, NOAA, and Centre National d'Etudes Spatiales (CNES, France). It makes use of NOAA satellites, and both US and French ground support facilities, to service fixed and moving platforms collecting environmental data. ARGOS has the advantages that it is well-proven, has a high data recovery rate, that lightweight hardware designed for use on balloons is commercially available, and that it provides world-wide coverage.

The balloon envelope design was undertaken in consultation with NCAR and in collaboration with Raven Industries, the maker of NCAR's high altitude constant volume balloons. The initial design adopted is for a spherical balloon of 2.9 m diameter,  $12.5 \text{ m}^3$  volume, made of 3 mil bilaminated polyester (mylar) film with a 1 mil polyethylene ballonet inside. The balloon was designed to carry up to a 4.5 kg (10 lb) payload to 600 mb, and to have an operational superpressure limit in excess of 80 mb. With a lighter payload, the ceiling altitude will exceed the design goal of 500 mb (5.5 km; 18,000 ft).

The payload consists of a buoyancy adjustment subsystem, sensors, a microprocessor or microcomputer, a telemetry subsystem, a radio command subsystem, tracking aids, and batteries. The buoyancy adjustment subsystem is just the pumps, valves and associated plumbing mentioned earlier. The initial list of sensors numbers 12, and includes those necessary to follow either a zero relative vertical velocity, or a constant potential temperature altitude control strategy. The microprocessor or microcomputer processes all data, formats it for ARGOS transmission, and uses it in a control algorithm to determine what altitude control measures should be taken to follow the mean vertical air flow -- no action, vent air, or pump more air in. The telemetry subsystem is, in ARGOS parlance, a platform transmitter terminal (PTT). The radio command subsystem is an HF radio receiver and command decoder enabling the user to override the onboard computer control. The tracking aids consist of an FAA transponder, a radar reflector, and a strobe to aid in visual tracking. The batteries are state of the art flexible ("paper") lithium batteries with high power-to-weight ratio.

The Ground Support Station (GSS) consists of an ARGOS local user terminal (LUT), an ARGOS uplink receiver, a radio-theodolite or LORAN tracking system, a command transmitter, and a desktop computer with associated peripherals. The LUT allows one to receive data from the balloon tracer in real time via re-transmission from the satellite whenever the satellite is within range of the tracer and within range of the LUT. The ARGOS uplink receiver allows one to listen directly to the data stream being transmitted by the balloon tracer when it is within radio range of the ground station. The radiotheodolite or LORAN system provides for local tracking of the tracer when it is being used within radio range. The command transmitter is a multi-band transmitter

capable of transmitting commands to the balloon tracer over long distances. The computer receives, formats, archives, and displays the location and meteorological data as desired. It also includes a modem to provide for data reception by phone.

The GSS accommodates three modes of use: (a) satellite/worldwide; (b) hybrid/regional; and (c) ground-based/local. In the satellite/worldwide mode, location and meteorological data are received from the tracer via the satellite either through the LUT or through NOAA facilities accessed by phone. The LUT gives one the data in real time, whereas the data are available from NOAA approximately 6 hours later. Data are only received by the satellite when it is within radio range of the balloon tracer -- about 10 minutes every 2-4 hours. Depending upon the design of the balloon tracer payload, the data transmitted may be only the current values of the measurements being made by the sensors, or it may be all the values recorded over the previous several hours.

In the hybrid/regional mode, the uplink receiver and other remotely-located uplink receivers are strategically located so that the balloon tracer is within radio range of at least one everywhere within the region of interest. Consequently, continuous real-time data reception and archiving are available over the region covered by the uplink receiver network. Tracking is still accomplished by satellite.

In the ground-based/local mode, the satellite link is not used at all. The balloon tracer is locally tracked, and the data acquired directly by the uplink receiver. This mode of use is limited by radio range.

Demonstration of technical feasibility was accomplished by fabrication and evaluation of a "testbed prototype" (TP)

balloon tracer. The TP is sufficiently similar to the flight system proposed in the preliminary systems design so as to establish feasibility, but does not meet all of the design goals itself. The major differences between the TP and an operational balloon tracer are that the TP is designed for local use only, and that it incorporates elements which make changing the control algorithm easy.

The TP consists of a balloon much like those for the operational tracer system, and a payload consisting of a buoyancy adjustment subsystem, an AIR (Atmospheric Instrumentation Research, Inc.) airsonde circuit board located inside the balloon, an AIR tethersonde circuit board located externally, a radio control command receiver, batteries and a strobe.

The TP is flown under the control of a prototype ground station which consists of an AIR ADAS (Atmospheric Data Acquisition System) unit, an HP85 desktop computer, an HP3421 data acquisition and control unit, and a radio command transmitter. The ADAS receives the data from the airsonde and tethersonde which give data on conditions inside the balloon and in the ambient atmosphere, respectively. The HP85 processes, archives, and analyzes the data. The control algorithm is resident in the HP85. Altitude control actions are transmitted back to the TP via the HP3421 and the command transmitter. This arrangement allows the control program to be written in a high-level language, and to be altered on the ground with a few keystrokes, even when the TP is in flight. Almost exclusive use of minimally-modified commercially-available elements in the TP design made demonstration of feasibility possible within project time and resource constraints.

The Phase I experimental program was limited to the minimum necessary to demonstrate that the concept of the Adjustable Buoyancy Balloon Tracer is viable. Initially, measurements were made in the laboratory on individual components to determine if their performance was satisfactory. Next, the testbed prototype underwent tests in an enclosed tower. Finally, testing began in the ambient atmosphere.

The most telling results were obtained in the tower. The tower is part of the Solar Central Receiver Test Facility at Sandia National Laboratories. It offers an enclosed volume roughly 10 m square by 52 m high. Since it is enclosed, it provides a more controlled environment than does the ambient atmosphere, making it easier to interpret test results.

Measurements were made on several pumpdown and valve-up cycles in the tower. The results made clear that the theory developed does indeed describe the behavior of the balloon tracer. They also made clear that the tracer's behavior is more complex than is obvious from the expressions derived under the assumption of dynamic equilibrium. The equilibrium theory may be thought of as describing the behavior of the equilibrium altitude of the balloon tracer, rather than its actual instantaneous position as a function of time. The balloon tracer oscillates around its equilibrium altitude, as its other parameters oscillate around their equilibrium values. The dynamic effects influence the details, but not the gross features of tracer balloon behavior.

In the final section of the report, the authors re-examine the design goals in light of the theoretical analysis, their experience in designing and building the testbed prototype balloon tracer, and the experimental results. They conclude

without reservation that an Adjustable Buoyancy Balloon Tracer of atmospheric motion meeting the design goals is feasible. They are proceeding in Phase II to turn this conviction into operational hardware.

## 2. INTRODUCTION

An Adjustable Buoyancy Balloon Tracer of Atmospheric Motion is a physical Lagrangian tracer (PLT) -- that is, an airborne instrumentation system that follows the flow of air in its vicinity, and that can be tracked electronically.<sup>1</sup> For decades, such a system has been desired by researchers to aid in understanding the dynamics of the atmosphere, and more recently, to cast light on long-range air pollution: acid deposition, regional haze and oxidant episodes, and associated problems of international diplomacy. The present effort is primarily motivated by the need to establish source-receptor relationships to distances of order 1000 km, to evaluate the accuracies of available air pollution transport models, and to assess the inherent limits on the predictability of source impacts at that distance. In a more basic sense, however, it addresses an underlying broad need in atmospheric science for a convenient means of following atmospheric flows.

The need for a physical Lagrangian tracer has led to extensive work with constant volume balloons (CVBs) reviewed by Tatom and King (1977) and more recently by Zak (1983). CVBs follow the horizontal motions of the volume of air in which they are embedded, but not the vertical motions. Coupled with wind shear, this characteristic limits their

---

<sup>1</sup> For a detailed discussion of the meaning of the term "Lagrangian" and of how the concept depends upon the spatial scale of application, see Zak (1983).

usefulness -- hence the search for a better tracer of atmospheric motion (Danielson, 1961; see also Appendix G).

PLTs are necessarily balloon-borne systems, and consequently must operate under Federal Aviation Regulations Part 101: Moored Balloons, Kites, Unmanned Rockets, and Unmanned Free Balloons (Appendix A). The purpose of this regulation is to strictly limit the hazard to air navigation which such systems might otherwise represent. According to FAR 101, its provisions apply to any unmanned free balloon that:

- (i) Carries a payload package that weighs more than four pounds and has a weight/size ratio of more than three ounces per square inch on any surface of the package, determined by dividing the total weight in ounces of the payload package by the area in inches of its smallest surface;
- (ii) Carries a payload package that weighs more than 6 pounds;
- (iii) Carries a payload of two or more packages, weighing more than 12 pounds; or
- (iv) Uses a rope or other device for suspension of the payload that requires an impact force of more than 50 pounds to separate the suspended payload from the balloon.

Consequently, to be exempt from the other provisions of FAR 101, an unmanned free balloon must either:

- (a) Carry a payload package weighing less than four pounds;
- (b) Carry a payload package weighing less than six pounds, and have an areal density of less than three ounces per square inch;



- (c) Carry multiple payload packages each one of which satisfies (a) or (b) above, the total weight of which does not exceed 12 pounds, and which are connected by a suspension with a breaking strength of less than 50 pounds.

The philosophy is that, to be exempt from the more restrictive provisions of FAR 101, an unmanned free balloon should represent no more hazard to air navigation than a large bird in flight. Under these regulations, the National Weather Service, together with the Weather Services of other nations around the world through WMO, routinely launch hundreds of radiosonde balloons without incident twice daily. Radiosondes measure the meteorological conditions aloft from the surface to beyond 60,000 feet above many major airports and certain other selected sites.

It is highly desirable for a PLT to operate under the exemption clauses of FAR 101. Certain other provisions of FAR 101 would severely limit the usefulness of a PLT which was not exempt. Even though there is no FAA requirement to do so on an exempt balloon, the PLT will also carry a radar reflector and an FAA transponder. In this way the FAA will be able to keep track of its altitude and location.

The intended uses also provide other PLT design goals:

- Lifetime  $\geq$  3 days.
- Tracking range > 1000 km in the northeastern quadrant of the United States.
- Telemetry of relative vertical air motion, pressure, temperature, and humidity.
- Ground system capable of handling several PLTs at a time.
- Capable of establishing specified ascent and descent rates under radio command.

- Capable of reaching altitudes up to 500 mb (5.5 km).
- Capable of following mean vertical flows as low as 1 cm/s with "acceptable" fidelity.
- Sufficiently inexpensive to permit use in significant numbers on an expendable basis.

The project as currently funded is divided into two phases:

Phase I: Systems Design and Demonstration  
of Feasibility

Phase II: Development of an Operational  
Prototype.

Phase I involves concept development, theoretical analysis, design, fabrication, and limited testing of a testbed prototype PLT -- a system capable of establishing feasibility, but which is not intended to meet all of the design goals for an operational PLT. Note that the operational PLT to be developed in Phase II is still designated as a prototype. This is because for subsequent use, it is probable that a manufacturer of flight instrumentation would be called upon to fabricate the PLTs. These could differ in detail from the Phase II prototype. This report covers work on Phase I.

### 3. CONCEPT AND THEORETICAL ANALYSIS

#### a. Buoyancy Control

Balloon systems obey Archimedes' Principle: A body immersed in a fluid is buoyed up by a force equal to the weight of the fluid displaced. This implies that a balloon system will be in equilibrium when the weight of the air it displaces is equal to the weight of the system.

Constant volume balloon systems have a unique characteristic. The equilibrium condition is met only at one well-defined altitude, and the CVB seeks that altitude. If it should find itself above the equilibrium altitude, the CVB will experience a net downward force due to gravity because the ambient air is less dense at the higher altitude, and the volume of air displaced is fixed. Likewise, if it should be below its equilibrium altitude, it will experience a net upward force, since then the buoyancy force exceeds the gravitational force. Thus, CVBs tend to oscillate around their equilibrium altitude. In atmospheric flows which have zero average vertical velocity, CVBs follow the horizontal flow at their equilibrium altitude. However, in flows in which the vertical component is significant, a CVB will not adequately follow the vertical flow. Consequently, wind shear can result in large horizontal as well as vertical displacements between a CVB and the volume of air it was intended to follow -- as much as 1300 km in 12 hours (Danielson, 1961; Appendix G). For long range applications, CVBs also suffer from the problem that they have no mechanism for dealing with high terrain -- they need to be flown above the altitude of the highest terrain likely to be encountered.

Nevertheless, CVBs offer the best approximation to a PLT of any passive balloon system. To improve on the CVB, it is necessary to go to an active system. If, for instance, a CVB is designed to sense its deviation from the vertical flow, and to adjust its buoyancy to keep its average vertical motion relative to the air near zero, then one has a system which follows both horizontal and vertical flows. This is the principle of the adjustable buoyancy balloon tracer. To create a PLT, one must develop a means of adjusting the buoyancy of a CVB, and a means of sensing deviation from the mean vertical flow.

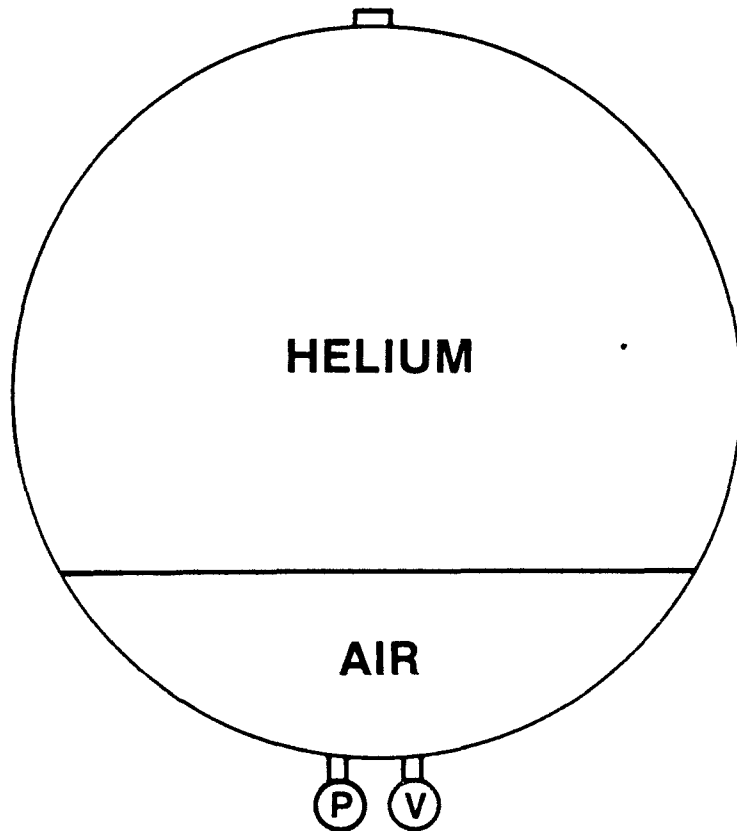


Figure 3-1. Schematic Diagram of the Adjustable Buoyancy Balloon. The outer skin of the balloon is made of a material which expands very little as the internal pressure increases. A thin polyethylene inner balloon, or "ballonet", keeps the helium lift gas separate from the air ballast. A pump (P) permits more ballast air to be taken on. A valve (V) permits ballast air to be vented. The total volume remains nearly constant, so pumping or valving changes the average density of the system, and thus its altitude.

The first problem was solved in principle by Lally (1967) of the National Center for Atmospheric Research. He proposed a CVB with an inner bladder, or ballonet, to contain the lift gas (helium). The remainder of the volume of the CVB was filled with air (Figure 3-1). A system of pumps and valves allowed air to be pumped in or to be released, respectively increasing the mean density of the balloon and thereby decreasing the equilibrium altitude, or decreasing the mean density and thus increasing the equilibrium altitude. Lally's concept forms the basis of this project. It was tried by the French on stratospheric balloons with some success, but was not developed further (Blamont et al, 1974).

We examine the behavior of this proposed PLT system in a standard atmosphere. In Appendix B, an expression is derived for the rate at which the equilibrium altitude can be changed by pumping or valving in a standard atmosphere. This rate  $v_p$  has the dimensions of a velocity, and for convenience, we choose to call it the "pumpdown speed". In the absence of inertial effects and drag forces, it would be the actual vertical speed with which the balloon would move under pumping or valving. It is given by:

$$v_p = \frac{dz}{dt} = -1.042 \times 10^4 \frac{S}{V} (1 - 2.256 \times 10^{-5} z) \quad (3-1)$$

Here  $z$  is the equilibrium altitude in metres MSL,  $S$  is the speed (volume flow) of the pump or valve in cubic metres per second, and  $V$  is the volume of the balloon in cubic metres.

Consider a system with volume  $12.5 \text{ m}^3$ , and pumping speed  $7.0 \text{ l/min}$  ( $1.2 \times 10^{-4} \text{ m}^3/\text{s}$ ). These are the approximate parameters for the testbed prototype PLT system. The pumpdown speed at sea level in a standard atmosphere given by (3-1) is

10 cm/s. Sustained average vertical flows in the atmosphere are typically less than 10 cm/s. Of course, higher pumping speeds are feasible, and one can release air through a valve far more rapidly, so a PLT capable of responding to higher vertical velocities can be built. However, for the long range applications presently in mind, where the interest is in following macro-scale, rather than micro-scale flows, this pumpdown speed appears to be adequate.

Another relationship important to PLT behavior is the rate at which the superpressure in the balloon varies with equilibrium altitude. This rate influences the altitude range over which a PLT system could be used. In Appendix C, an expression is derived which gives superpressure,  $P_s$ , as a function of equilibrium altitude in a standard atmosphere. Note that superpressure is the difference between the absolute pressure inside and outside the balloon. It is given by:

$$P_s = 2.396 \times 10^4 \frac{C}{V} (1 - 2.256 \times 10^{-5} z) \quad (3-2)$$

Here superpressure is given in millibars, and C is a constant satisfying the above equation for the initial superpressure  $P_{s0}$  specified at some altitude,  $z_0$ . For our testbed PLT, assuming a superpressure of 35 mb at 1000 m MSL,

$$C = 1.868 \times 10^{-2} \quad (3-3)$$

Since

$$\frac{dP_s}{dz} = -.541 \frac{C}{V} \quad (3-4)$$

we find  $dP_s/dz = -8.1 \times 10^{-4}$  mb/m. This is a remarkable result. As long as the PLT is maintained at neutral buoyancy by inhaling or exhaling air, a change in altitude of 10 km

results in a change in superpressure of only 8.1 mb. Thus, our prototype PLT with a design maximum superpressure of 80 mb could easily function anywhere between sea level and 500 mb (5.5 km) without difficulty from over- or under-pressurization. .

It should be recognized that all preceding calculations have implicitly assumed that the gas in the balloon is at the same temperature as the ambient air at the balloon altitude. This is not necessarily the case. A diurnal temperature swing due to radiative effects as great as  $\pm 6^{\circ}\text{C}$  at 900 mb, and  $-10^{\circ}\text{C}$  to  $+15^{\circ}\text{C}$  at 500 mb, is to be expected (Lally, 1985). This is based on experience in the GHOST program.

The effect of balloon temperature differing from ambient temperature is calculated in Appendix D. We find:

$$\Delta P_b = \Delta T [3.52 (1 - 2.256 \times 10^{-5} z)^{4.255} + 83.24 \frac{C}{V}] \quad (3-5)$$

where  $\Delta T$  is the temperature difference between the balloon gas and the ambient temperature, and  $\Delta P_b$  is the pressure difference induced by the temperature difference. For our prototype system, a  $\Delta T$  of  $6^{\circ}\text{C}$  ( $-6^{\circ}$  at night,  $+6^{\circ}$  during the day) results in a superpressure difference of  $\pm 20$  mb at 900 mb. The expected temperature swing at 500 mb results in a superpressure swing of from  $-21$  to  $+32$  mb at 500 mb. Somewhat smaller pressure swings can be expected when the balloon is shadowed by cloud on an otherwise sunny day. Thus, if the superpressure is 35 mb when the system is at temperature equilibrium at 1 km, the superpressure would fall to below 15 mb at night, and rise at midday to above 55 mb at 1 km, or 65 mb at 5.5 km.

Another challenge to the control system is condensation

and liquid water adhesion to the skin of the balloon. If it should rain, should the dew point depression become zero, or should nighttime cooling of the balloon exceed the dew point depression, water on the skin of the balloon would add weight which would have to be counteracted by the control system. According to Lally (1967), a properly treated balloon surface will retain only 5 g/m<sup>2</sup> of water. An untreated surface may retain up to ten times as much. The relationship between surface area and volume for a sphere is

$$A = 4.836 V^{2/3} \quad (3-6)$$

Our prototype PLT has a surface area of 26 m<sup>2</sup>, which implies 130 g of water to carry if the surface is properly treated. This is the equivalent of about 110 liters of air ballast at sea level. So for a 12.5 m<sup>3</sup> balloon, about 9 mb of superpressure would be required which could later be valved off to compensate for the added weight.

A more serious challenge to altitude control is ice formation in clouds above the freezing level. The hope here is that surface treatment will ameliorate the problem. In addition, use of a partially-aluminized balloon could raise the balloon temperature day and night (Lally, 1975). If these strategies are not sufficiently effective, use of the PLT under ice-forming conditions may not be feasible.

Power requirements are another concern. All power needs must be met by on-board power sources. Furthermore, because of the weight constraints imposed by FAR 101, it is not feasible to expand the battery complement without limit. Whereas the sensors, microprocessor, and other electronics onboard can be reduced to very low power consumption levels, the minimum pumpdown energy expenditure is fixed by the physics of the situation, and by the efficiency of the pump.



In Appendix E, we have calculated the energy required per metre ( $dW/dz$ ) to pump the balloon down, assuming a perfectly efficient pump. The result is

$$\frac{dW}{dz} = 2.30 \times 10^2 \text{ C} \quad (3-7)$$

For our prototype system, with 35 mb overpressure at 1 km, we find  $dW/dz$  is 4.3 joules/meter. So, to pump the system down 1 km requires 4300 joules, or 1.2 watt hours. This is an encouraging result. Lithium batteries have energy densities between 100 and 200 watt-hours/pound, depending upon the type of battery. Even allowing for pump inefficiency, long pumpdowns should be feasible with modest battery complements.

Having confirmed that the adjustable buoyancy balloon system is likely to work, the practical questions arise as to how to go about filling the system in a way designed to give proper lift, and what the maximum altitude is that the system can attain. Both of these questions are addressed in Appendix F. For the testbed prototype, with approximate balloon envelope weight of 4.5 kg, and payload weight of <2.7 kg (6 pounds), and with a desired superpressure of 35 mb at 1000 m MSL, the "required lift" at that altitude as defined in Appendix F is 7.75 kg, assuming a surface temperature of 282° K. This would be provided by 0.31 kilogram-moles of helium (6.95 m<sup>3</sup> at STP). Properly filled, the prototype PLT would have a service ceiling of 6.2 km MSL, well above the 500 mb level (5.5 km).

#### b. Control Strategies

We turn now to the second problem to be overcome in creating a PLT, developing a means of sensing deviation of the system from the mean vertical air flow. There are two

approaches. The first is to measure the relative vertical air velocity, and to integrate that velocity with time to obtain relative vertical displacement. The second is to take advantage of the near-adiabatic nature of atmospheric flows, and to use potential temperature, or equivalent potential temperature, as the control parameter. Both approaches have advantages and disadvantages.

The first approach is very direct. It yields the desired information with few if any assumptions. On the other hand, it places very stringent demands upon the relative vertical velocity measurement. If the measurement involves an average systematic bias of only 1 cm per second consistently in the same direction, the control system will create a relative vertical displacement which grows linearly with time at the rate of 36 m/hour. On the other hand, if the error is entirely random, the uncertainty  $\sigma_z$  in the total relative displacement is given by

$$\sigma_z = \sqrt{N} \sigma_v \Delta t \quad (3-8)$$

where  $\sigma_v$  is the uncertainty in each relative vertical velocity measurement,  $\Delta t$  is the time required for each measurement, and  $N$  is the total number of measurements made. If  $\sigma_v = 1$  cm/s,  $\Delta t = 60$  s, and  $N = 4320$  (for a 72-hour flight), then  $\sigma_z$  is only 39.5 m -- quite acceptable. However, measurement error is always a mix of both random and systematic error, with the proportions of the mix dependent upon the details of the measurement technique.

Use of the near-adiabatic character of atmospheric flows poses less of a measurement problem. In the absence of liquid water and of diabatic heating or cooling, the potential temperature  $\theta$  is conserved -- that is, trajectories are

isentropic (Holton, 1979). Potential temperature  $\theta$  is given by:

$$\theta = T(1000/P)^{R_a/c_p} \quad (3-9)$$

Here  $R_a$  is the gas constant for unsaturated air,  $c_p$  is the specific heat at constant pressure for air, and  $R_a/c_p = .286$ . Differentiating and evaluating the expression for potential temperature, one finds that at the surface, in a standard atmosphere,

$$\frac{\partial \theta}{\partial z} = 3.3 \times 10^{-3} \text{ } ^\circ/\text{m} \quad (3-10)$$

So, if one controls  $\theta$  to  $\pm 0.1^\circ$ ,  $z$  is controlled to  $\pm 31$  m -- quite adequate for our purposes.

However, diabatic effects do occur. In the region of interest below 500 mb, they are strongest near the surface, and decrease with height above ground. Throughout most of the troposphere, diabatic heating and cooling is of order  $1^\circ/\text{day}$  (Wallace and Hobbs, 1977). Depending upon meteorological conditions, this may be net heating, net cooling, or interim variation with no net gain or loss. In the absence of a means of taking these effects into account, they would limit the accuracy with which an isentropic trajectory reflects air motion.

In the presence of liquid water, condensation and evaporation occur with the result that potential temperature is no longer conserved even if the flow is adiabatic. However, "equivalent potential temperature" (Holton, 1979; Wallace and Hobbs, 1977) is conserved in both wet and dry processes. It could be used for altitude control in the presence of liquid water. The equivalent potential temperature of saturated air is given by:

$$\theta_e \approx \theta \exp (Lq_s/c_p T)$$

(3-11)

where  $L$  is the latent heat of condensation, and  $q_s$  is the saturation mixing ratio of water vapor in air.

It would be quite convenient to use potential temperature (or equivalent potential temperature when the relative humidity is 100%) as the buoyancy control parameter for a PLT. However, in a well-mixed layer,  $\partial\theta/\partial z$  goes to zero. Hence,  $\theta$  is not useful in this situation. Thus, for pollutant transport studies in the daytime mixed layer, some other control strategy would have to be used -- like relative vertical displacement. On the other hand, during daytime mixing, pollutants rapidly become uniformly distributed throughout the layer. Hence, precisely where the PLT is in the layer matters little (see Appendix J). Over flat terrain in the mixed layer, the PLT could be flown as a passive CVB, or programmed to maintain constant pressure altitude.

There is good evidence from previous experiments that this is the case. In the DaVinci III experiment, a balloon flew parallel to the plume from a large power plant for 14 hours in the daytime mixed layer. This was confirmed by periodic instrumented-aircraft plume cross sections. Statistically significant divergence between the plume centerline and the balloon was observed, if at all, not until the evening hours (Zak et al, 1981). Also, in the Tennessee Plume Study (Gay et al, 1981; Zak, 1981), a balloon was launched into the plume from a power plant the effluent of which had been spiked with sulfur hexafluoride. The balloon stayed in the plume during the mixing period for the subsequent 8 hours for which it remained airborne. This was confirmed by observing the concentrations of  $SF_6$  on board the balloon as a function of

## SULFUR HEXAFLUORIDE TRACER

AUGUST 20, 1978 LAMP FLIGHT

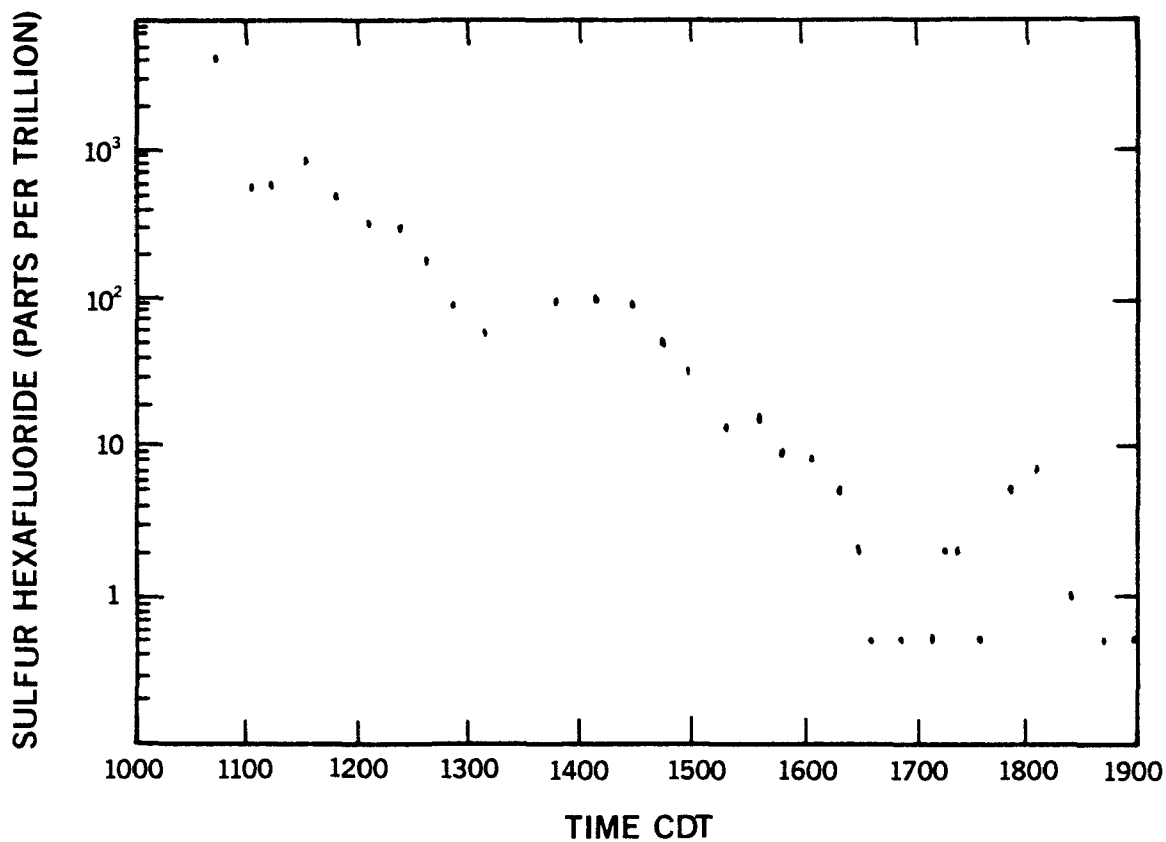


Figure 3-2. Sulfur hexafluoride concentration versus time measured on board the LAMP (Lagrangian Measurement Platform) balloon during the Tennessee Plume Study (Gay et al, 1981). The balloon was launched into a power plant plume spiked with SF<sub>6</sub>.

# TRAJECTORY FOR AUGUST 20, 1978 FLIGHT

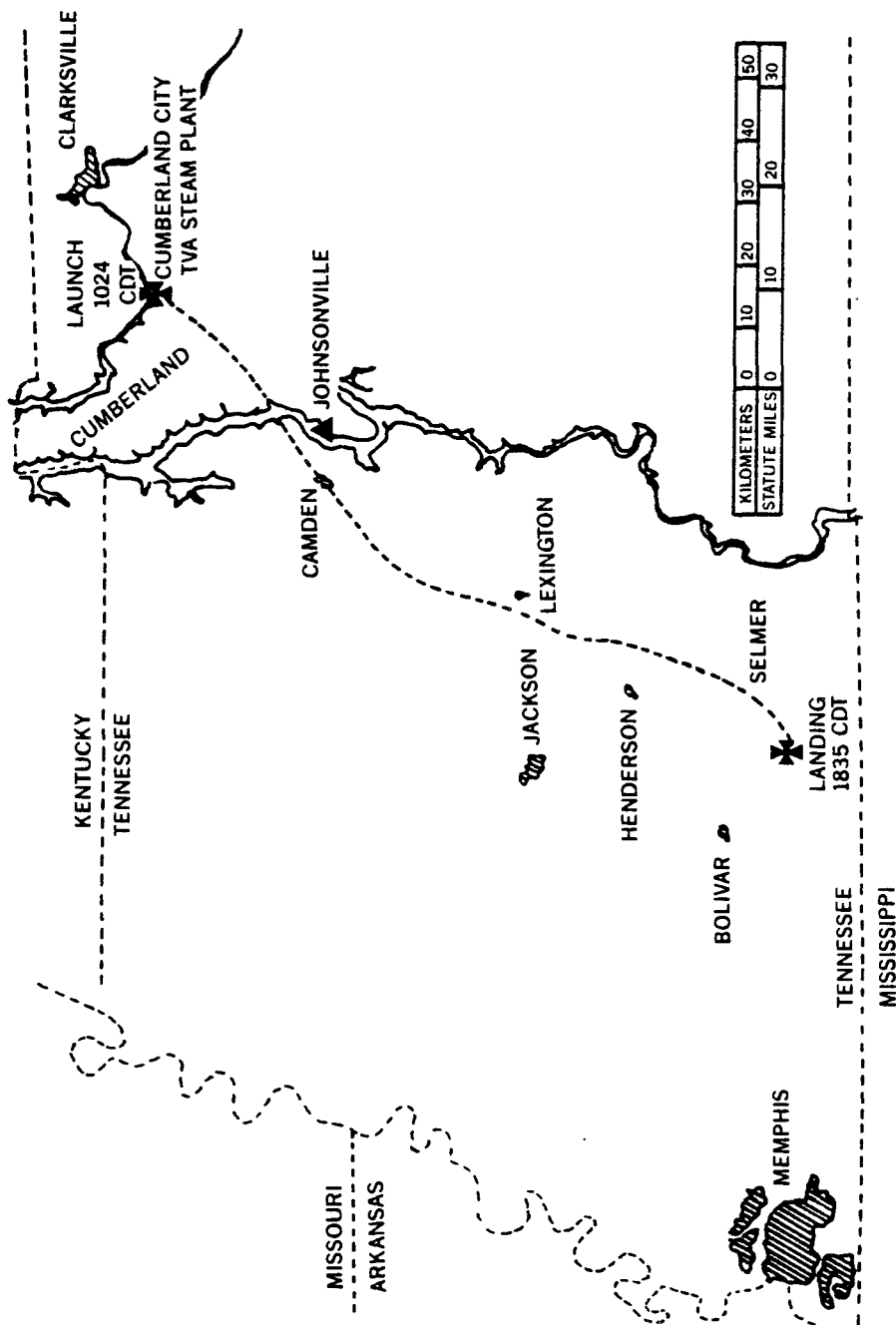


Figure 3-3. Trajectory of the LAMP during the Tennessee Plume Study.

time (Figures 3-2 and 3-3), as well as by instrumented aircraft cross-sections of the plume in the vicinity of the balloon.

It is when atmospheric stability suppresses mixing that buoyancy control is important. Danielson (1961) has shown that under these conditions, even in the presence of diabatic effects, isentropic trajectories yield far better approximations to air parcel motion than do isobaric trajectories (Appendix G). Danielson remarks that a passive CVB trajectory approximates an isobaric trajectory.

From the foregoing discussion, it appears that a hybrid control algorithm will yield the best results, with different control strategies to be used for different situations -- convective mixing, stable and dry, stable and wet, and perhaps others. The output of onboard sensors will determine which option is selected at a given time during a flight. In the testbed prototype PLT, the initial altitude control scheme makes use of potential temperature. At the same time, a sensitive vertical anemometer has been developed which permits exploration of control algorithms based upon measured relative vertical displacement.

#### 4. SYSTEMS DESIGN

A major task during Phase I was development of a conceptual design for a complete operational system capable of meeting the design goals listed in Section 1. This was accomplished. The preliminary systems design, and the rationale for each of the major decisions it embodies, are presented in this section. Note, however, that the generic design presented here is not rigid. As we proceed with Phase

II, it is possible, even likely, that some features of the design will be modified as work progresses.

a. Tracking and Data Handling

A fundamental systems design decision concerns how the PLTs are to be tracked, and how the data acquired are to be received. Tracking techniques considered include Omega, LORAN, FAA VOR/DME, special DME, Automatic Direction-Finding (ADF), radar, and satellite techniques. Each system has its pros and cons, but all but the satellite techniques suffer from a common problem. For all of the others, tracking and data reception can be accomplished only when the PLTs are within radio range of an appropriately-equipped ground or airborne station. For the VHF frequencies, this implies line-of-sight for reliable communications. HF frequencies propagate to longer ranges than VHF, but other problems militate against their use.

If one presumes tracking by ground stations rather than specially-equipped aircraft, a large number of such stations are required to track over the desired 1000 km x 1000 km area. This is because line-of-sight communication is limited by the curvature of the earth. The number of ground stations for a specified minimum flight altitude is given in Figure 4-1. Note that for a flight altitude of 1 km, approximately 35 ground stations would be required. With this ground network, one would sacrifice data from PLTs which are carried below 1 km. Ground stations capable of both data reception and tracking would likely cost \$50-100 K each, exclusive of installation and maintenance. Thus a ground network could be very costly. The alternative of tracking and data reception using specially-equipped aircraft involves lower capital, but higher operating costs, and is not consistent with being able



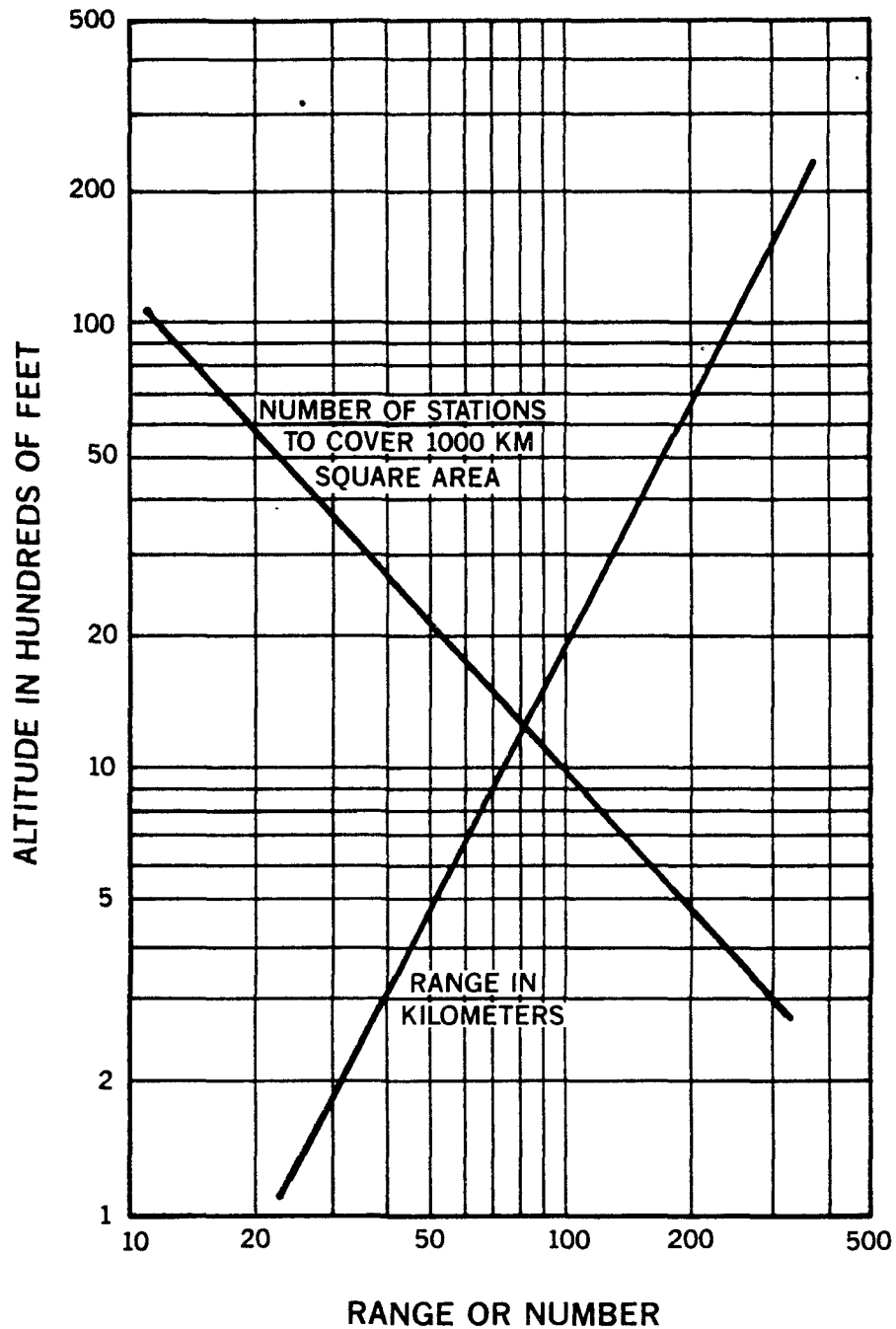


Figure 4-1. Number of ground stations required to cover a 1000 km x 1000 km area, and VHF radio range as a function of balloon altitude. Radio range  $d$  in miles is given by  $\sqrt{2h}$ , where  $h$  is altitude in feet.

to track several widely-dispersed PLTs simultaneously.

There exists, however, a satellite-based tracking and data handling system well-suited to our needs. It is called ARGOS, and is a joint undertaking of NASA, NOAA, and of Centre National d'Etudes Spatiales (CNES, France). Appropriately, the ARGOS system is primarily intended for applications concerned with environmental data collection. An overview of the ARGOS system is included as Appendix H, so only a brief description of its application to our effort is given here.

The ARGOS satellite-based data collection and platform location system makes use of NOAA satellites, a pair of which orbit at an altitude of 850 km with periods of 101 minutes. The PLT payload will carry an ARGOS platform transmitter terminal (PTT). The PTT about once a minute broadcasts a series of data frames on 401.65 MHz. If a PLT Ground Support Station (GSS) or properly equipped aircraft is within line of sight of the PLT, the data stream can be received directly with an ARGOS uplink receiver. The GSS as currently envisioned will be described in detail later.

For long range experiments, the satellite link is most convenient. The data from the PLT will be received by the satellite as it comes within view (within 2500 km). The satellite, in addition to storing the data on board for later retransmission to Service ARGOS, also retransmits the data immediately on 136.77 or 137.77 MHz. The GSS will receive those data along with position information via an ARGOS Local User Terminal (LUT). This takes place only when the marker is within view of the satellite and when the satellite is within view of the LUT. For the northeastern US, on average, this happens 10 times per day (minimum: 8; maximum: 12). The satellite "sees" an area 5000 km wide on each pass. While the

radio link exists, data can be transmitted for approximately 10 minutes. These can be both real-time and archived data taken since the last satellite pass. Thus the LUT provides location and other data every 2-3 hours. The location accuracy obtained using the LUT link is about 3-5 km.

Once during each orbit, each NOAA satellite dumps its data to a Service ARGOS ground station, from which they are transferred to the World Meteorological Organization Service ARGOS data processing center in Toulouse, France. After processing, the data are transferred to a NOAA satellite data center in Suitland, Maryland. Typically 4-6 hours after data is broadcast from the PLT, they will be available to the GSS via modem and telephone lines from NOAA Suitland. The location accuracy from this delayed link is considerably better than from the LUT -- typically  $\pm 700$  m. Service ARGOS can handle more than 200 PTTs simultaneously.

It is important to note that the use of ARGOS does not preclude continuous data reception. If either a ground network or airborne data reception units with ARGOS uplink receivers are provided for a given experiment, continuous data will be obtained. However, long range experiments can be done without such facilities. Hence, the minimum investment needed for an ARGOS-based PLT system is much smaller than for systems based on other tracking and data-handling options.

Other advantages of ARGOS which led to its selection are: it already exists -- it doesn't have to be developed from scratch; it is very well proven -- it works with close to 100% data recovery; lightweight PTTs designed for use on balloons are commercially available, as are uplink receivers and local user terminals; ARGOS offers world-wide coverage -- it's not limited to the northeastern U.S.; and finally, the resources

available for this project do not permit the development of an analogous system based upon some other tracking option.

b. Balloon Envelope

Balloon design was undertaken in consultation with the National Center for Atmospheric Research, and in collaboration with Raven Industries, the maker of NCAR's high altitude constant volume balloons. Three different CVB shapes were considered: cylindrical, tetrahedral, and spherical. Cylindrical and tetrahedral balloons are simpler to fabricate, and hence offer the potential for lower unit cost. On the other hand, the spherical shape provides the lowest surface area per unit enclosed volume, and the lowest skin stress for a given superpressure and skin thickness.

Raven carried out a detailed design study on all three shapes. They found that the increased skin thickness necessary to accommodate the higher stresses in the first two shapes considerably increased balloon weight. Thus, those balloons would have to have been considerably larger in order to carry the desired payload plus the weight of the balloon itself. In part as a result, the cost difference between the three designs was only about 10%. The smaller size of the spherical balloon, its significantly lower surface area, and the long experience of both Raven and NCAR with spherical-design CVBs made the choice obvious.

The calculated parameters for the respective designs to meet the specifications for the testbed prototype system are given below:

#### Sphere

Volume	12.47 m <sup>3</sup>
Diameter	2.88 m
Material	3.3 mil polyester (bilaminated)
Ballonet	1.0 mil polyethylene
Weight	4.1 kg

#### Tetrahedron

Volume	19.84 m <sup>3</sup>
Diameter	4.24 m
Material	4.8 mil polyester (bilaminated)
Ballonet	1.0 mil polyethylene
Weight	8.2 kg

#### Cylinder

Volume	23.80 m <sup>3</sup>
Diameter	1.83 m
Length	7.32 m
Material	4.2 mil polyester (bilaminated)
Ballonet	1.0 mil polyethylene
Weight	11.8 kg

Balloons of these designs are able to carry a 4.5 kg payload to a pressure altitude of 600 mb with a superpressure of 80 mb, and with a maximum skin stress of 10,000 psi. A lighter payload, of course, could be carried to higher altitude.

#### c. Payload

The operational PLT payload will consist of the following elements:

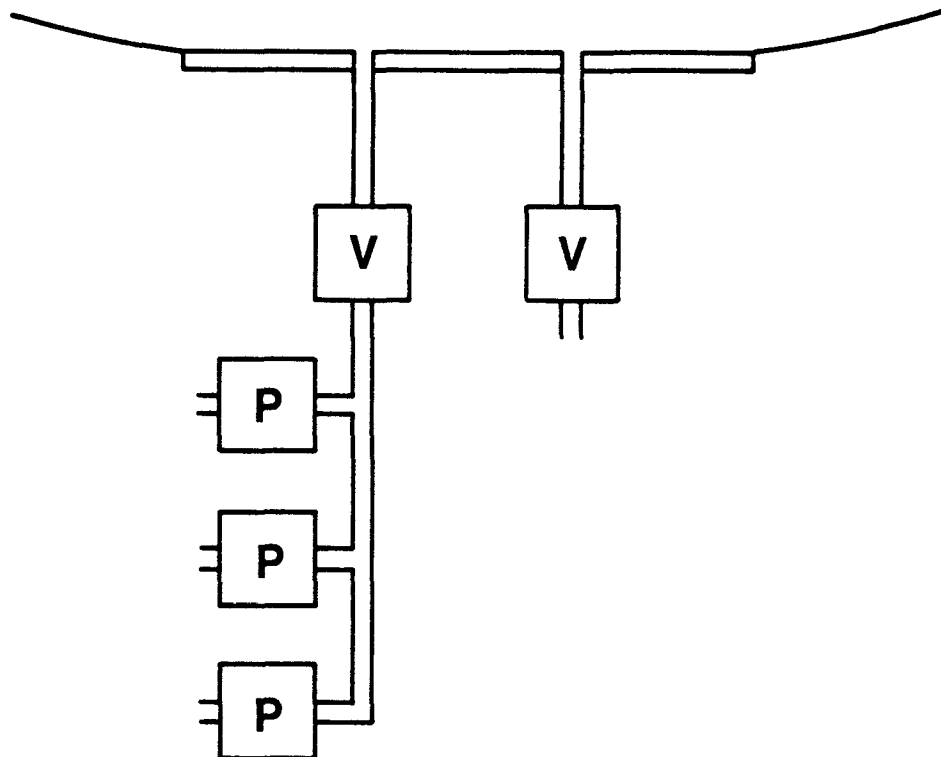


Figure 4-2. Buoyancy Control Plumbing. Pumps (P) and valves (V) are electrically-operated. For the Testbed Prototype, only 2 pumps are used, but for the Operational Prototype, 3 will be incorporated to gain a 50% increase in pumdown speed. A valve is in series with the pumps to avoid leakage through the pumps when they are not operating.

- Buoyancy adjustment subsystem
- Sensors
- Microprocessor or microcomputer
- Telemetry subsystem
- Radio command subsystem
- Tracking aids
- Batteries

These are described below.

The buoyancy control subsystem is just the set of pumps and valves necessary to change the amount of air ballast carried by the PLT. The buoyancy control plumbing is shown in Figure 4-2. The pumps used in the testbed prototype are adequate for our purposes, but the manufacturer may be able to further optimize them. A valve is in series with the pumps because the pumps do not prevent backflow when off.

The list of sensors which are either essential or desirable is quite long:

- Ambient pressure
- Ambient temperature (aspirated)
- Ambient humidity (aspirated)
- Vertical anemometer
- Balloon orientation
- Rain sensor
- Internal pressure
- Internal temperature
- Skin strain
- Upward-looking radiometer
- Voltage
- Mass flow

According to the specified design goals, ambient pressure, temperature, and humidity are to be measured and reported. They are standard meteorological measurements that are already made on the testbed prototype. Minor improvements in the sensors will be made, but no major problems are anticipated.

The vertical anemometer needs to be an order of magnitude more sensitive than standard meteorological instruments. Sonic, hot wire, ionic, and propeller anemometers were considered. A sonic anemometer would certainly be able to make the measurement with adequate accuracy. However, weight, cost, and power consumption considerations for commercially available sensors make this choice somewhat unattractive. The hot wire anemometer suffers from the difficulties that it does not give direction of flow, and that power consumption is typically high. Ionic anemometers are in an early stage of development (Barat, 1982). At the level of accuracy we require, they suffer from drift problems, and are not commercially available.

That leaves the propeller anemometer. It was recalled that some years ago P. B. MacCready developed a very sensitive vertical anemometer under contract to SNL for the DaVinci experiments (MacCready, 1977; MacCready and Mullen, 1981). Gill (1979) has also developed a similar device. The MacCready design shows promise of being able to meet our needs at low cost, weight, and power consumption, using commercially-available components. It is being further developed for the testbed prototype, and will be discussed in Section 5. If it should not live up to its promise, it may be necessary to fall back on the sonic anemometer.

If a propeller anemometer is used, rotation of the balloon itself would be a source of error. Consequently, it would be



necessary to keep track of the balloon orientation. Fortunately, a convenient electronic compass is available and has been incorporated into the testbed prototype.

It is likely that a different control algorithm would be required in rain than under other conditions. Hence a rain sensor is incorporated.

Pressure and temperature measurements within the balloon will be made to assess its condition, and to aid experimenters in understanding the dynamics and thermodynamics of the system. Skin strain will also be measured with the same view in mind.

In Section 3, during consideration of an isentropic control strategy, it became clear that it would be advantageous to be able to estimate and correct for diabatic effects. A simple upward-looking radiometer capable of sensing solar insolation during the day, and of measuring radiant energy loss at night, might provide adequate information for such an estimate.

The state of health of the payload will be reflected in the values of selected reference voltages. Hence a "voltmeter" will be required.

Finally, mass flow into and out of the balloon will be a function not only of the pump and valve used, but of the ambient pressure and the superpressure as well. Kurz Instruments of Carmel Valley, California, has recently put on the market a small sensor and associated electronics which seems suitable to our needs. It could simplify the control problem.

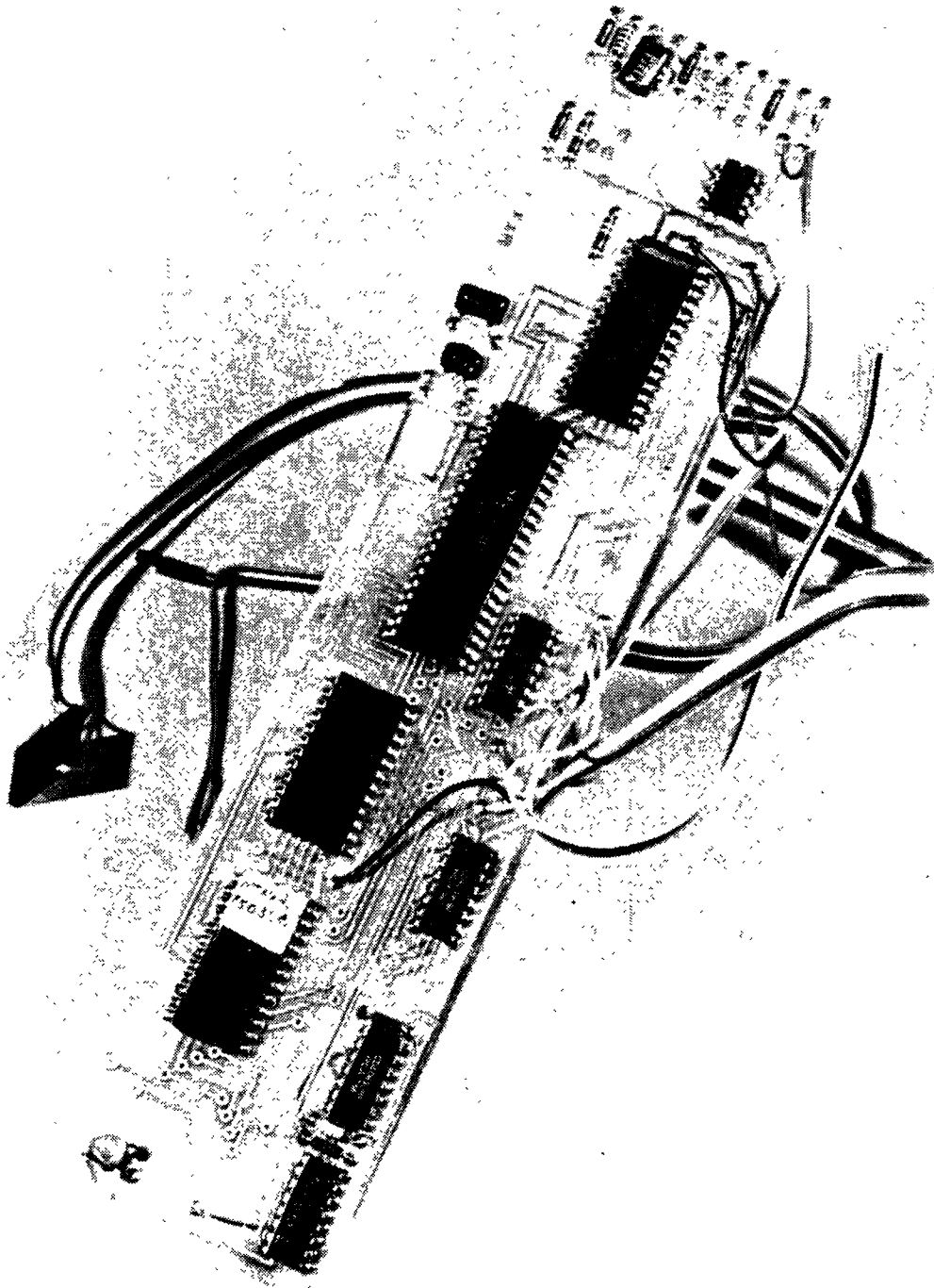


Figure 4-3. NCAR microprocessor data system for balloon application, shown approximately actual size.

Returning now to the main list of payload elements, note that the microprocessor or microcomputer is the heart of the system. Its function is to analyze the sensor data in accordance with the control algorithm, and to operate the pump and valve appropriately. It may have other functions as well -- processing the sensor output, formatting the sensor data for transmission, and whatever other data-handling and control tasks may be necessary on the payload.

Microprocessor technology has advanced so rapidly that it may be possible to incorporate an entire microcomputer on a single printed circuit board addressable in a high level language, rather than a microprocessor with read only memory. If so, this would greatly increase the flexibility of the system.

Microprocessor-based data systems have been used by Lally's group and others for sophisticated data archiving, manipulation, and reporting via ARGOS. A typical system is shown in Figure 4-3. One would expect the operational prototype PLT microprocessor or microcomputer system to be similar.

Having made the choice of ARGOS for tracking and data collection, the telemetry system becomes well-defined. An existing, commercially-available ARGOS PTT designed for balloon application is shown in Figure 4-4. It is similar to the unit to be incorporated into the operational PLT, except that the new unit does not require a constant temperature cell. An ARGOS antenna is shown in Figure 4-5.

The design goals call for the capability to establish specified ascent or descent rates upon radio command. The only other command capability deemed necessary is to cause the

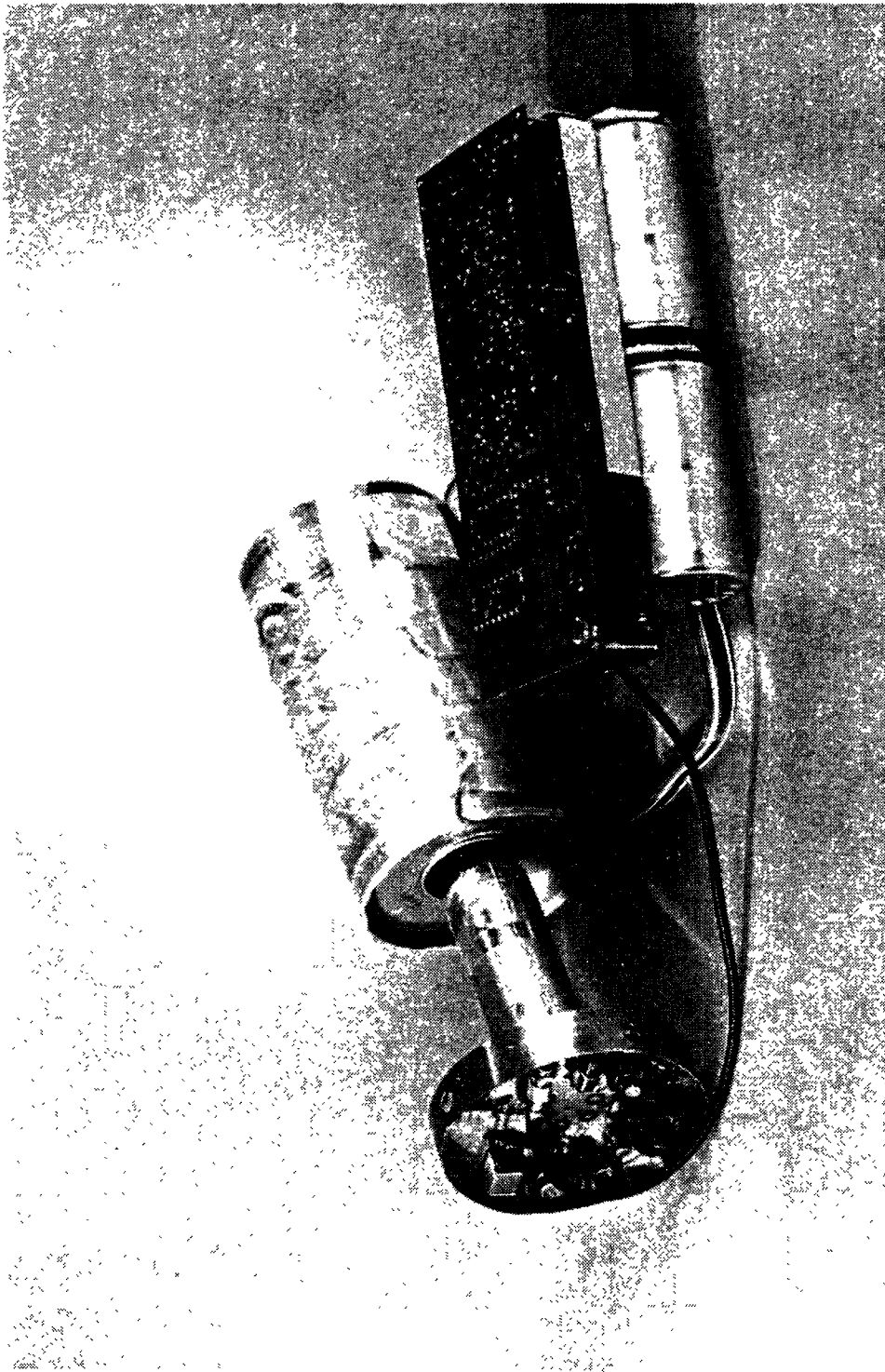


Figure 4-4. ARGOS Platform Transmitter Terminal (PTT) designed for balloon application (shown half size). This unit includes batteries (below) and a constant temperature chamber (left) for the transmitter crystal. Unit to be used does not require the chamber, and will use paper batteries.

balloon to descend rapidly -- commonly called "cutdown". Command transmitters, receivers, and decoders are in common use at SNL and at NCAR, and are not anticipated to present a problem. The system to be used would most likely provide protection against radio interference or command misinterpretation. This is done by automatically transmitting the coded command twice. The command is not acted upon unless the replicate transmissions received are confirmed to be identical. The encoding permits selection of the balloon to which the command is addressed if several are simultaneously airborne, as well as selection of the action to be initiated.

It is planned to incorporate a radio command system which operates at HF, rather than VHF or UHF frequencies to get around the requirement for line of sight between the transmitter and the balloon system. At the high power level available from a ground-based transmitter, HF signals can be received at great distances, frequently, around the world; more about this later.

While the ARGOS system provides primary tracking data to the experimenters, it is also desirable to provide an independent means for FAA Air Traffic Control to identify and track each balloon on their radar screens. This is done by incorporating a commercially-available FAA transponder. The transponder need not operate continuously. Rather, the microprocessor will cycle it on and off frequently to reduce average power consumption. To permit radar-equipped aircraft to see the PLT, it will also carry a very light-weight radar reflector. At night, a lightweight strobe light will operate.

Much of the above equipment requires electrical power which can only be provided by batteries (in this application, solar cells are not feasible). The power requirements, though

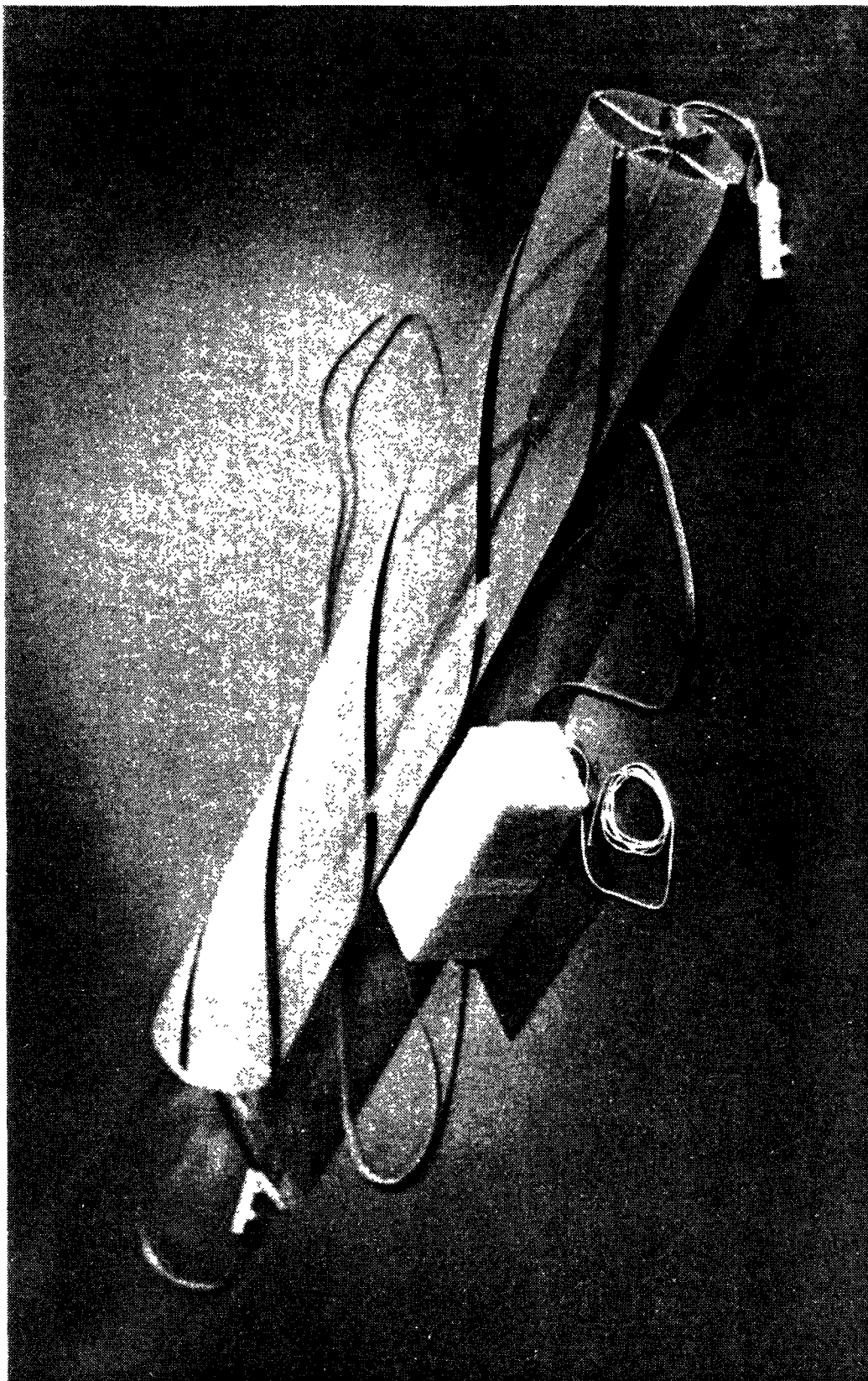


Figure 4-5. NCAR ARGOS antenna. It consists of spirals of foil on mylar. It is 7.6 cm (3 in) in diameter, 0.6 m (2 ft) in length, and weighs 62 g (2.2 oz).

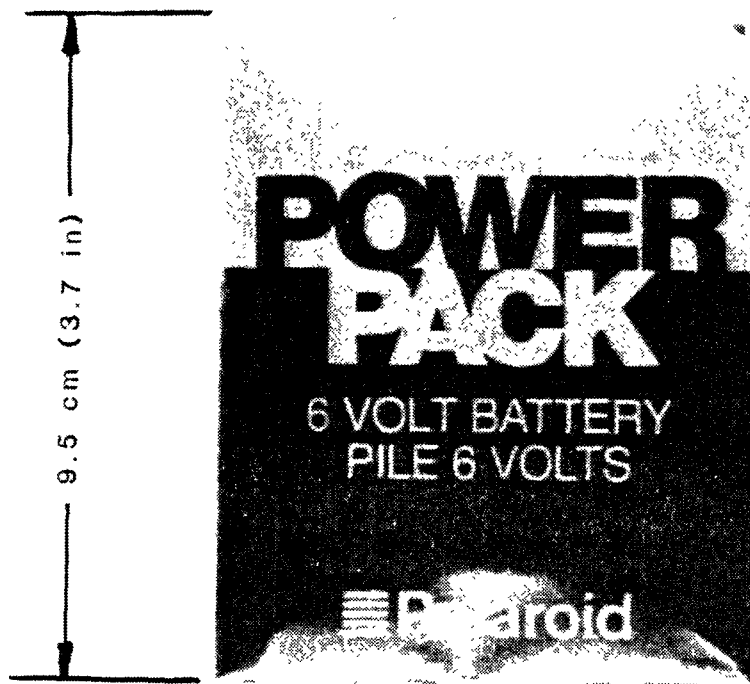


Figure 4-6. "Paper" lithium battery. The battery shown here has a 1.2 Ahr (7.2 Whr) capacity, weighs 34 g (1.2 oz), and is 0.46 cm (0.18 in) thick.

modest for short to intermediate operating periods, become considerable when a three-day lifetime is considered. Fortunately, great advances have been made in recent years in lithium battery technology. Lithium batteries based on several different chemical reactions are commercially available, all with energy densities of about 100-200 watt hours/pound. Several of these have eliminated the overheating hazards associated with earlier lithium batteries. Thus for a 72-hour flight, an average power consumption of 3-6 watts is obtainable with a 1 kg battery pack. This appears to be adequate to our needs if care is taken in electrical systems design.

A development of particular note is that of "paper" batteries (Margolin, 1982). These batteries are made of paper, thin plastic materials, metal foils, and electrolytes. They are deformable, rather than rigid. They are attractive from the point of view of further reducing the potential hazard to aircraft even beyond the requirements of FAR 101. Figure 4-6 shows a typical paper lithium battery.

#### d. Ground Support Station

As presently conceived, the GSS will accommodate three distinct modes of use of the PLT. The mode we have focused upon to this point makes exclusive use of the ARGOS satellite for tracking and data handling. This mode provides data whenever one of the NOAA satellites is within view of the PLT -- about ten minutes every two to three hours. If the PLT is equipped for data archiving, one can receive, store and transmit via ARGOS all the data acquired since the last satellite pass.



In some applications, however, it is desirable to have continuous real-time data. Over a limited geographical area, this can be accomplished by locating "up-link" receivers at towers or other high points around the region of interest. They will receive data from all PLTs within line-of-sight. The data can be accessed by telephone modem. If it is not necessary to have continuous tracking information, but only continuous data from the on-board sensors, this can be accomplished at modest cost -- \$10-\$15 K per site for the hardware. Here tracking would still be done only by the satellites. The GSS can accommodate this mode of use provided that it is equipped with appropriate telephone service.

The final mode of use provides for continuous tracking and data reception for short range experiments in which the PLT remains within radio range of the GSS -- tens of kilometers, depending upon PLT altitude. In this case, it is possible to continuously track the PLT with a radiotheodolite or LORAN tracking system. If a radiotheodolite were used, it could track only one PLT at a time, so if more than one PLT were involved in the experiment, they would have to be observed sequentially, or more than one radiotheodolite would be needed. The LORAN tracking systems may be more attractive. For experiments of a very local nature, either could be replaced by an optical theodolite equipped with shaft encoders.

The three modes of use are designated, respectively: (a) satellite/world-wide; (b) hybrid/regional; (c) ground-based/local. In typical long range use, one would expect the modes to be combined, especially if several PLTs are released from a single site, and the GSS is located at that site. Each PLT would be tracked locally while it remained within range, and thereafter by satellite.

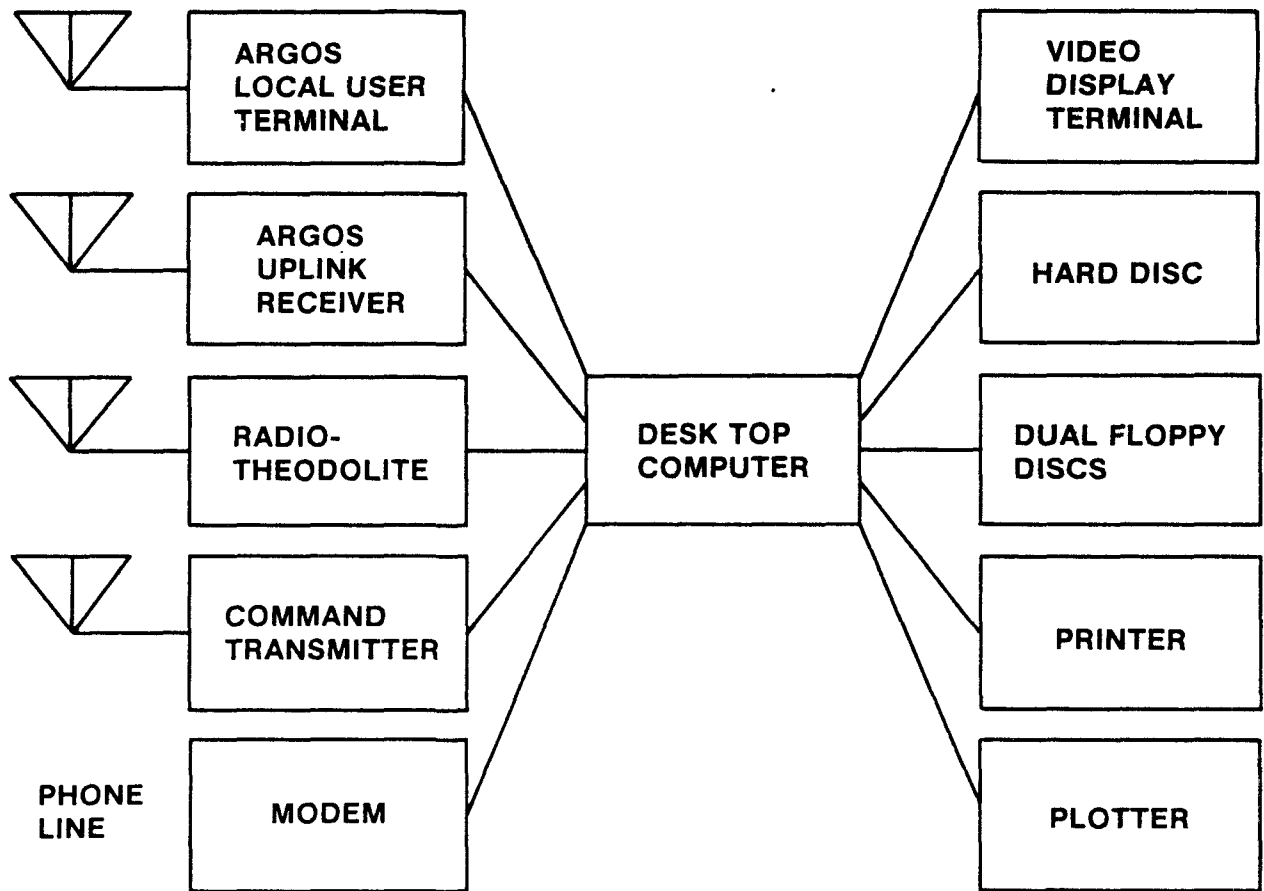


Figure 4-7. Block Diagram of Ground Support Station for an operational PLT system.

The elements of the GSS are shown in Figure 4-7. With the exception of the microcomputer and the standard peripherals, they have all been discussed in previous sections.

It should be noted that the problem of "skip" of HF radio signals which could affect the reliability of the command transmissions would be avoided by having another command transmitter at a remote location accessible by telephone modem, and also by having at least two different frequencies available in different bands. It is unlikely that a PLT would be in a "skip" zone relative to both command transmitters and both frequencies. This arrangement still allows world-wide command from a single fixed location.

In addition to accessing delayed ARGOS data from NOAA and real-time data from remote up-link receivers, the modem would also be used to retrieve any National Weather Service data relevant to the experiment via Weather Services, Incorporated, or some comparable supplier, to aid in conducting the experiment as meteorological conditions change.

The Ground Support Station would be a compact facility, easily accommodated in a small trailer or RV which could be moved to the area where experiments are planned, or to the home base of the institution responsible for a given set of experiments.

#### e. Control Algorithm

For the long range experiments currently envisioned, the main features of the control algorithm can now be discerned. It would very likely be of the hybrid type discussed in Section 3, making use of potential temperature and a measure of diabatic effects as control parameters during periods of

stability, and relative vertical motion or even barometric pressure during periods of instability. It should be recognized, however, that the PLT is a generic tool which can be put to many different uses. For each use, a somewhat different control algorithm would likely be optimal. Hence, control algorithm development is an open-ended task which will continue in parallel with research employing PLTs.

## 5. DEMONSTRATION OF TECHNICAL FEASIBILITY: THE TESTBED PROTOTYPE (TP)

### a. Approach

The theoretical analysis in Section 3 strongly suggests that the systems design presented in Section 4 will, in fact, work. To demonstrate feasibility, it remains to turn those essential elements of the design about which there could be doubt into functioning hardware.

There is no question of feasibility about most of the system. The ARGOS data collection and platform tracking system has been in operation for years, and has been used to track stratospheric balloons on flights which carried them around the world dozens of times (Lichfield, 1981). Likewise, microprocessor data acquisition and control systems for balloon application, as well as balloon radio command systems, are frequently used on other projects (see Morris, 1975; NCAR). The question that needed to be answered in Phase I concerned the buoyancy adjustment subsystem: Could that subsystem be built so that it performs as required within the weight and power constraints imposed by the balloon environment and FAR 101? The testbed prototype was designed to answer that question.

It was recognized early that a major task in the development of an operational PLT will be optimization of the control algorithm. This process will be facilitated if the control algorithm can be easily modified, especially if it can be modified in flight. The testbed prototype PLT accommodates that need. The microcomputer which contains the control algorithm is on the ground. All the necessary data are provided by telemetry, and all pump and valve commands are transmitted by radio back to the payload in flight. Modifications in the algorithm can be accomplished with a few keystrokes.

As the name implies, the testbed prototype is intended to be of continuing utility. In Phase II, as elements of the operational prototype emerge from the laboratory, they will be incorporated into this prototype for evaluation.

#### b. Balloon Envelope

The specifications for the seven TP balloons supplied by Raven were:

- 4.5 kg maximum payload
- 600 mb ceiling altitude
- 80 mb maximum superpressure
- 10,000 psi maximum skin stress
- Internal full volume ballonet
- Base fitting for required electrical and air feedthroughs
- Adequate load suspension harness
- Top-mounted inflation fitting
- Handling lines

The calculated parameters of the spherical balloon to meet these specifications were given in Section 3a. To get to 80

mb superpressure with skin stress limited to 10,000 psi would have required 3.3 mil polyester film. At Raven's suggestion, we relaxed that specification by 10% to take advantage of 3 mil bilaminated polyester film which Raven had in stock. This permitted us to avoid having the film manufactured on special order with attendant high cost and long delay. Estimated skin stress at failure is approximately a factor of two higher than the stress in the 3 mil material at 80 mb. The 10,000 psi spec would only have minimized balloon expansion at high superpressure.

Including fittings and control wires connecting the base with the crown, the balloons weigh  $4.568 \pm .018$  kg. This is about 0.5 kg above the weight calculated from the design parameters, and is entirely acceptable.

One of the balloons was earmarked to be tested to failure. However, after raising the pressure to 92 mb (12 mb above the design spec), Raven chose not to continue the test to failure because of the possibility of damage to windows at the site where the test was being conducted.

#### c. Payload

The decision to keep the buoyancy control microcomputer on the ground in Phase I permitted the testbed payload to be put together in a particularly convenient way. For the most part, commercially available components were used. Figure 5-1 gives a block diagram.

The airsonde printed circuit board used to measure pressure and temperature inside the balloon comes from a commercially-produced rawinsonde made by AIR (Atmospheric

Instrumentation Research), of Boulder, Colorado. Its specifications are given in Table 5-1.

---

TABLE 5-1  
AS-3A AIRSONDE SPECIFICATIONS

Temperature

Range: +50°C to -80°C  
Precision: 0.5°C for +40°C to -40°C  
Resolution: 0.01°C

Humidity

Range: 10% to 100% RH  
Precision: 5% RH 40°C to -40°C  
Resolution: 0.1% RH

Pressure (absolute barometric)

Range: 1050 mb to 5 mb  
Precision: 1 mb  
Resolution: 0.1 mb  
Temperature Compensation: Bead thermistor with automatic  
software correction

Telemetry Range: 100 km (nominal)

---

The tethersonde payload is also made by AIR. Its specifications are given in Table 5-2.

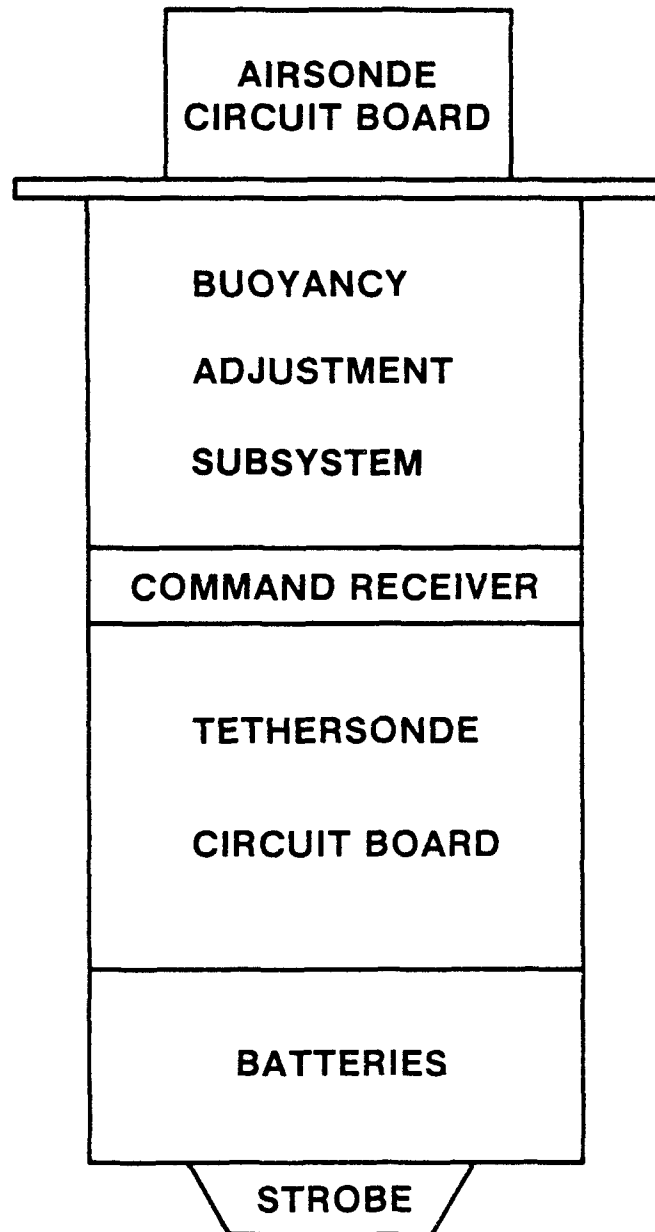


Figure 5-1. Block Diagram of the Testbed Prototype Payload.



---

TABLE 5-2

TS-3A-SP TETHERSONDE SPECIFICATIONS

Temperature

Range: +50°C to -70°C  
Precision: 0.5°C for +40°C to -40°C,  
typical accuracy 0.2°C  
Thermistor Match: 0.1°C for +35°C to -20°C  
Resolution: 0.01°C  
RMS Noise  
Equivalent: 0.04°C  
Response Time: 12 s

Humidity

Range: 3% to 100% RH  
Precision: 3% for 0°C to 50°C;  
5% for -10°C to 0°C;  
10% for -25°C to -10°C

Pressure (absolute barometric)

Range: 1050 mb to 600 mb  
Precision: 1 mb  
Resolution: 0.1 mb  
Temperature Compensation: Bead thermistor with automatic  
software correction

Wind Speed\*

Range: 0-20 m/s  
Precision: 0.25 m/s  
Resolution: 0.1 m/s

Wind Direction\*

Range: 2° - 358° (4° deadband)  
Precision: 5°  
Resolution: 1°

Spare Inputs (4)

Range: 0-100%  
Precision: 1%  
Resolution: 0.1%

---

---

TABLE 5-2 (Continued)

Weight: 225 g with alkaline battery  
Telemetry Range: 20 km (nominal)

\*In the TP, the wind speed sensor is not used; it is replaced by the high sensitivity vertical anemometer. The electronic compass associated with wind direction is used with the vertical anemometer to sense and correct for balloon rotation.

---

Figure 5-2 is a picture of the airsonde and tethersonde circuit boards.

Note that the specs on the temperature sensor for the tethersonde payload may be marginal for an operational PLT based on potential temperature. We are informed, however, that AIR can calibrate the sensors to the required accuracy.

In an operational PLT, the temperature, humidity, and vertical anemometer sensors will have to be located away from the body of the balloon itself to avoid errors caused by balloon-induced convection currents. There are two choices. One can suspend the sensors well below the balloon (ideally, ten diameters), or one can mount them laterally out beyond the balloon radius. The latter approach is more appealing. For the expected differences between the air temperature and the balloon skin temperature, the balloon boundary layer which would carry the convection currents would be quite thin. Using the results of Chiang et al (1964), we find that for a temperature difference of 5°K, the maximum convective velocity in the vicinity of the balloon equator is about 25 cm/s, and this occurs at a distance from the balloon skin of about 1 cm. At distances > 10 cm from the balloon skin, the effect is

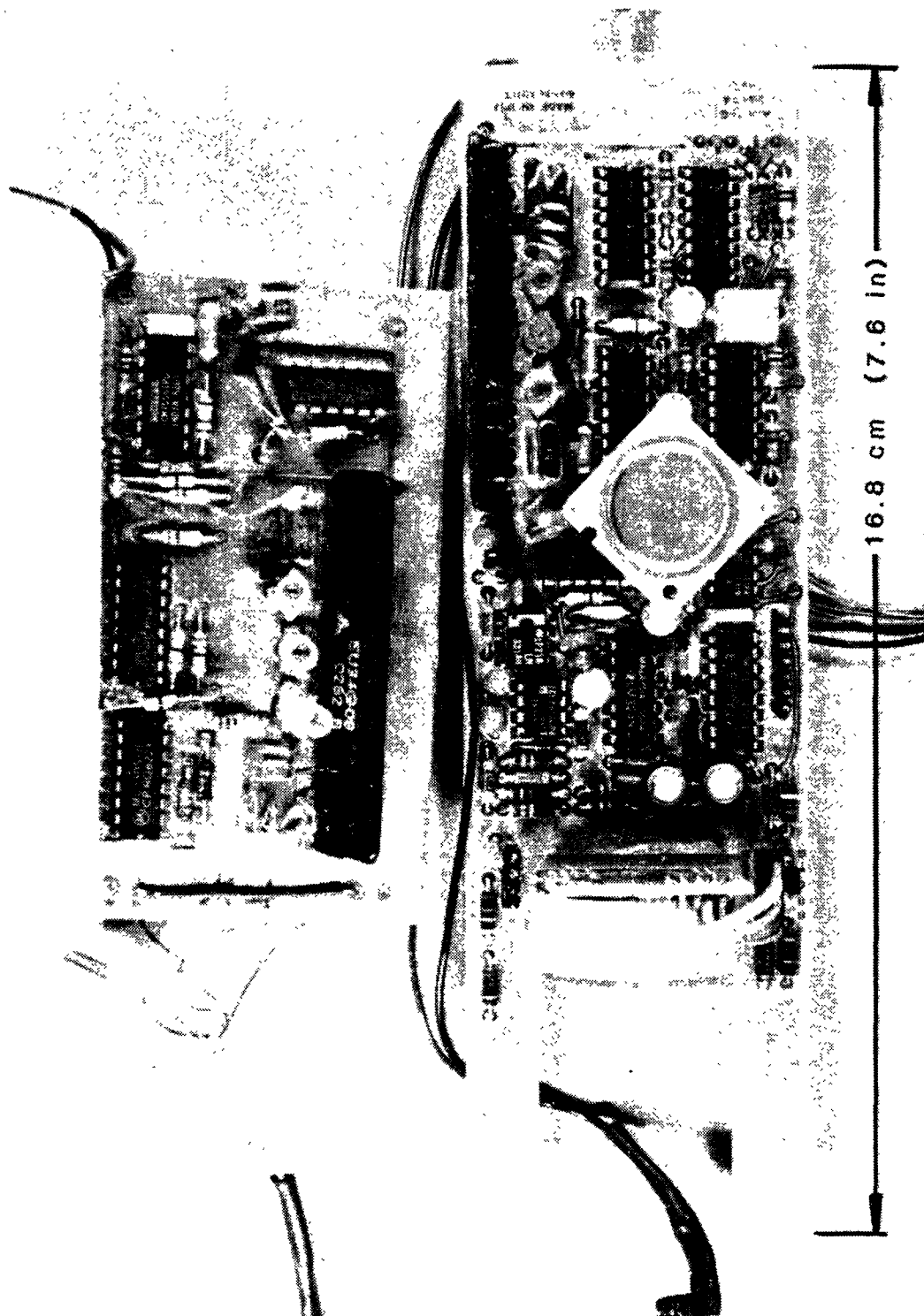


Figure 5-2. Airsonde and tethersonde circuit boards side by side. They weigh 37.3 g (1.3 oz) and 66.8 g (2.4 oz) respectively.

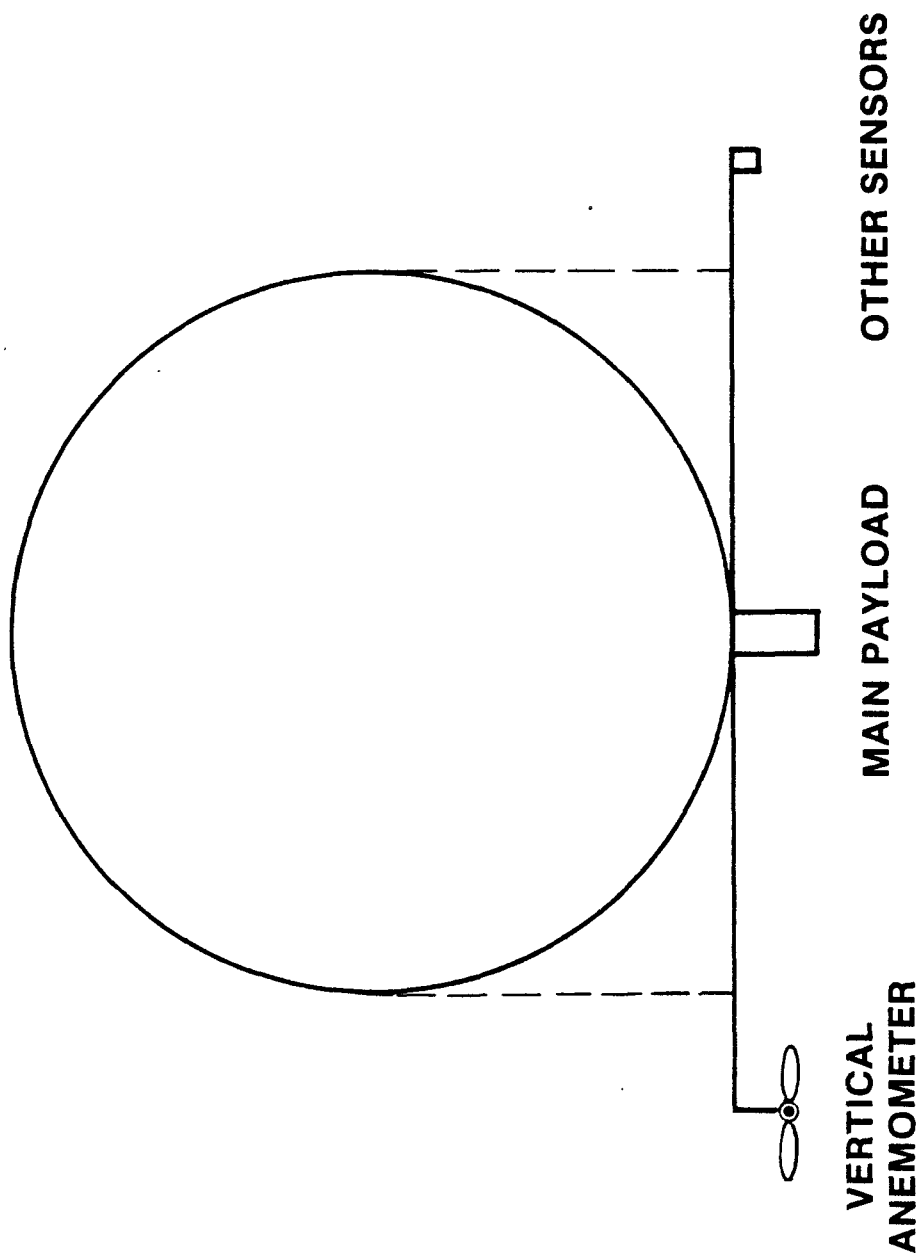


Figure 5-3. Preferred sensor placement relative to the balloon.

insignificant. The same is true of the effect on temperature. One comes to similar conclusions when one considers the flow patterns induced by motion of the balloon relative to the air, that is, forced convection (Schlichting, 1979). Thus, mounting the sensors out laterally would be feasible, and more convenient than suspending them far below the balloon (Figure 5-3). This sensor placement will be implemented in Phase II.

The testbed buoyancy adjustment system consists of two Gilian Model No. B22A06F48 pumps in parallel, two Klippard model No. MJV-2 mechanically-activated valves, and a Japan Remote Control servo. The servo actuates the valves. The servo is driven by an RC (radio control) receiver. Both are part of a Japan Remote Control N7C-4SM system. Figure 5-4 shows these components.

The Gilian pumps weigh 158 g each, and consist mostly of plastic. They are stock items which are satisfactory for an operational prototype as is, but effort will be devoted in Phase II to work with the manufacturer to see if their pumping speed can be increased.

The mechanically-activated valves, servo, and RC receiver will not be a part of the operational prototype. This set of components will be replaced by solenoid-operated valves, and will be driven by the onboard microprocessor or microcomputer.

In the TP, the batteries used are conventional lithium "D" cells, capable of operating the payload for approximately 72 hours. They will be replaced with paper lithium batteries in the operational prototype.

Figure 5-5 shows the assembled testbed prototype payload. It weighs 2.36 kg, including 0.99 kg of batteries. The main

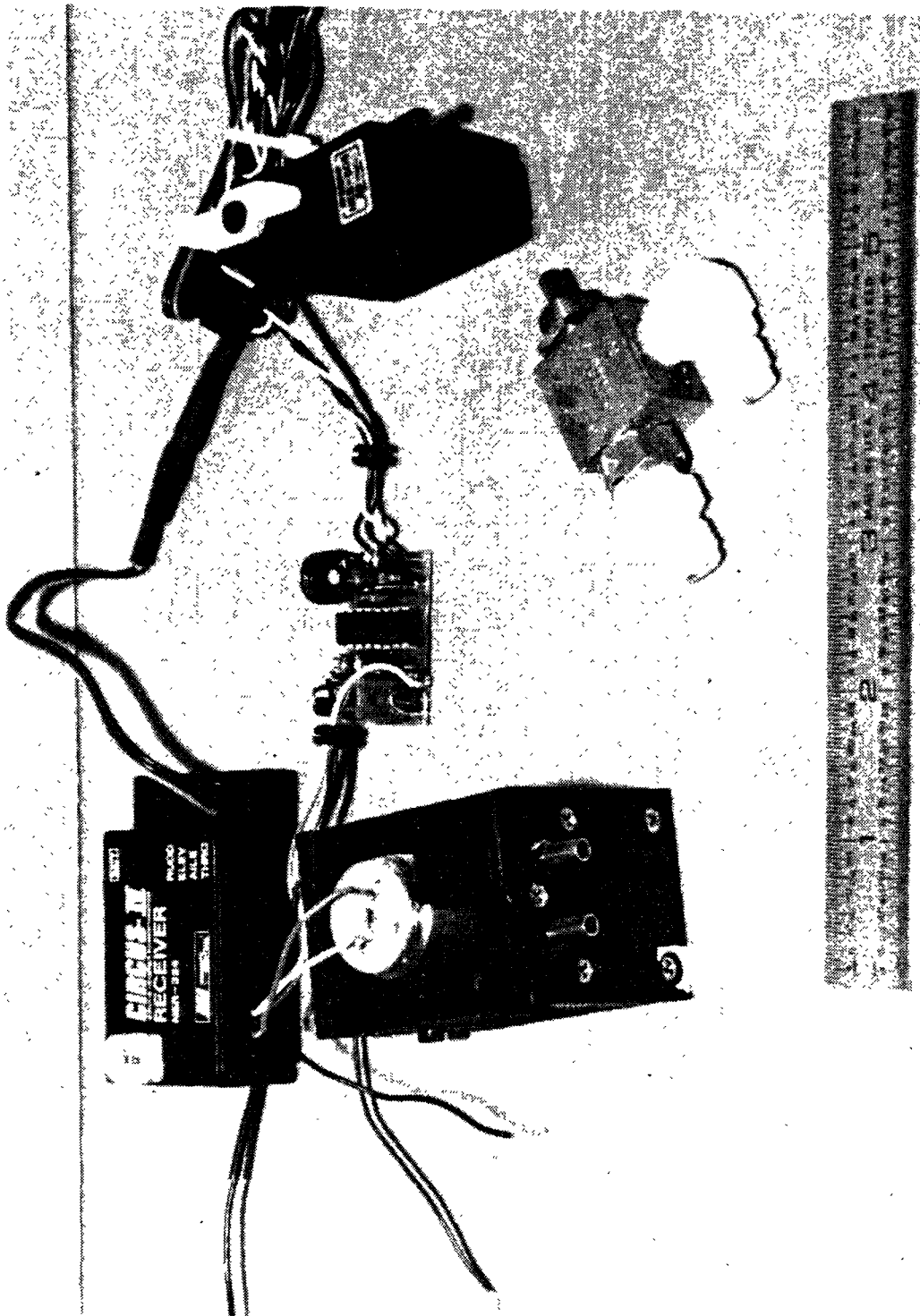


Figure 5-4. Gilian pump, Klippard valve, and Japan Remote Control receiver and servo. The valve will be replaced by a solenoid-operated unit in the operational prototype, and the RC unit will be replaced by an HF command receiver. Shown nearly actual size.

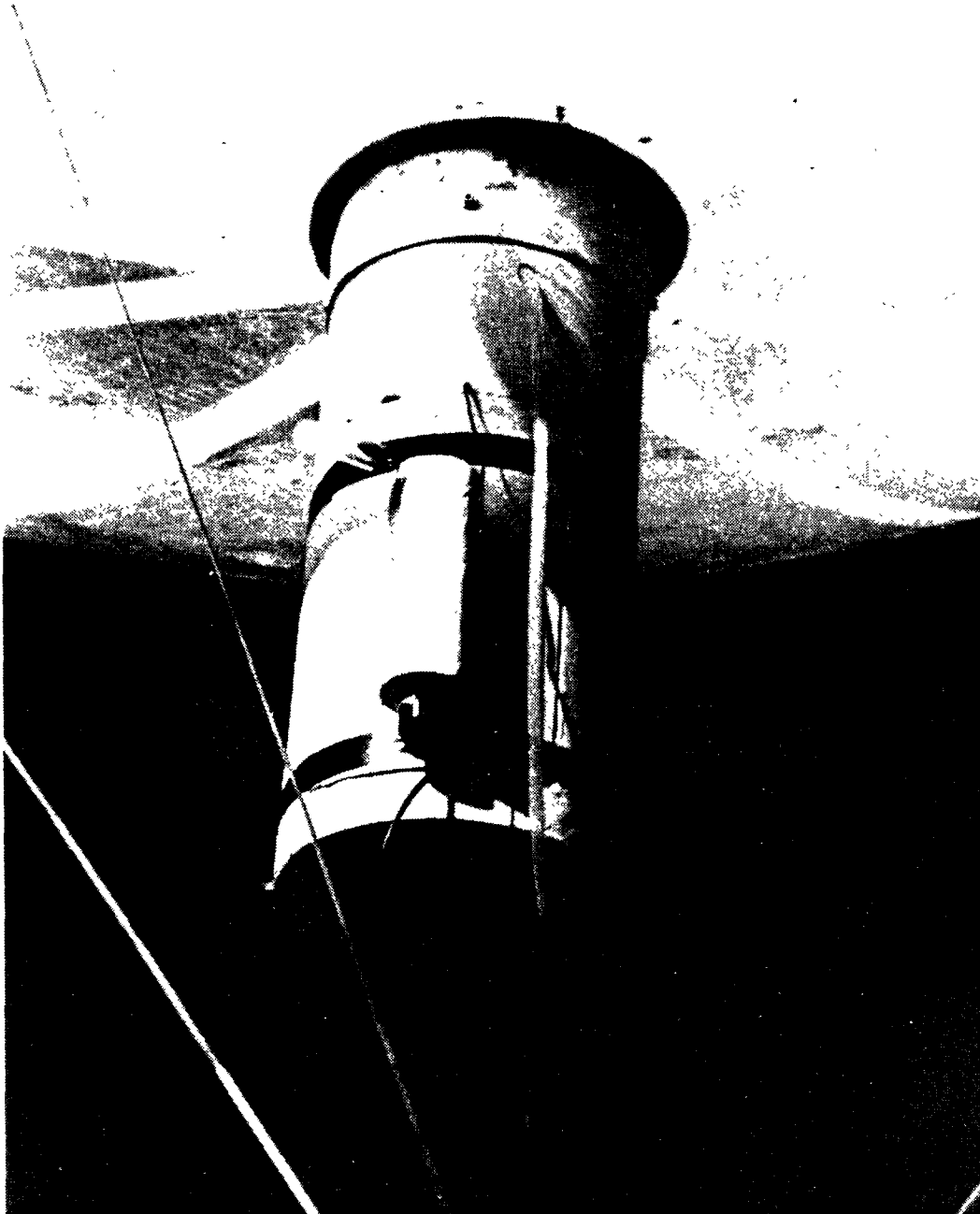


Figure 5-5. Assembled Testbed Prototype Payload. Tubing is air ballast vent line. Wires are airsonde and tethersonde antennae. Smaller diameter cylinder contains the aspirated temperature and humidity probes. Payload housing is styrofoam covered with 0.6 oz fiberglass. The payload meets the exemption conditions of FAR 101.

cylinder is 31.5 cm (12.5 in) long, and 16.5 cm (6.5 in) in diameter. The weight/size ratio satisfies the exemption clauses of FAR 101. The payload structure is made of expanded styrofoam covered with 0.6 oz fiberglass. The combination yields a strong but light structure.

#### d. Vertical Anemometer

The sensor for the vertical anemometer being developed and tested makes use of a stock 22.9 cm (9 in) diameter expanded styrofoam Gill propeller from R. M. Young, and a slightly-modified Spaulding Instruments C1 rotation sensor (Figure 5-6). The Spaulding sensor is a photoelectric type which gives both rate and direction of rotation. It makes use of the highest quality low-friction instrument bearings available without special order. It is modified only in that dust seals normally supplied were removed to minimize friction.

This wind sensor has a starting air speed of under 2 cm/s, and a measurement threshold of under 3 cm/s (MacCready, 1981) -- that is, at 3 cm/s, a reproducible air speed measurement can be made. This appears to be just about as well as Gill (1979) did with a special laboratory-produced 50 cm propeller and sensor.

It is unlikely that starting speed or very low velocity performance will determine whether or not relative vertical air motion measurements averaged over 1-5 minutes can be made satisfactorily. Even at a low intensity of turbulence, the instantaneous vertical air velocities are likely to be considerably higher. The point is illustrated by the data from one of the experiments in which MacCready's anemometer was used, DaVinci II (Figure 5-7). The figure presents five minute averages of data taken once per second. Only very



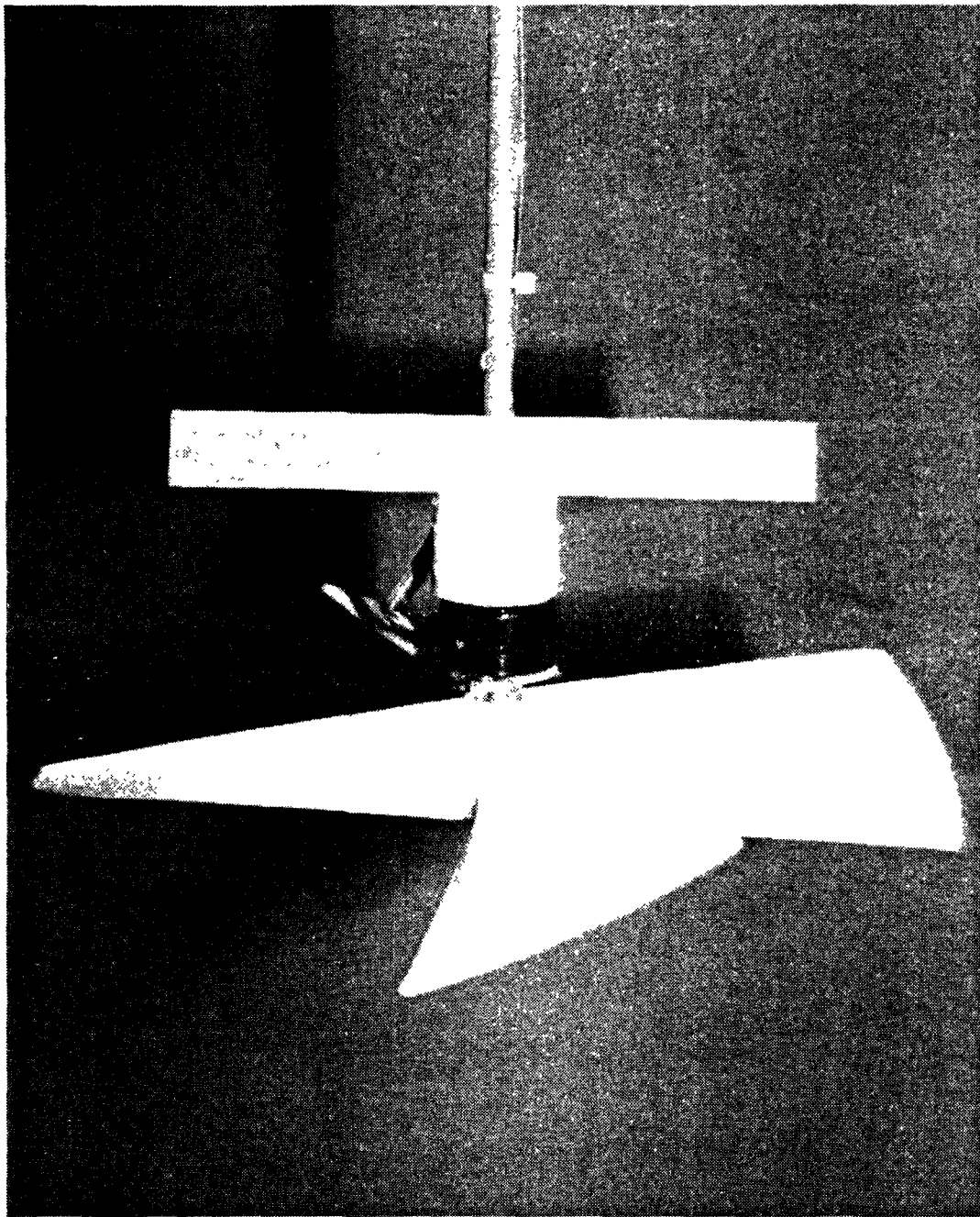


Figure 5-6. High sensitivity vertical anemometer for relative vertical air motion measurement.

# DA VINCI II - FIVE MINUTE AVERAGED DATA

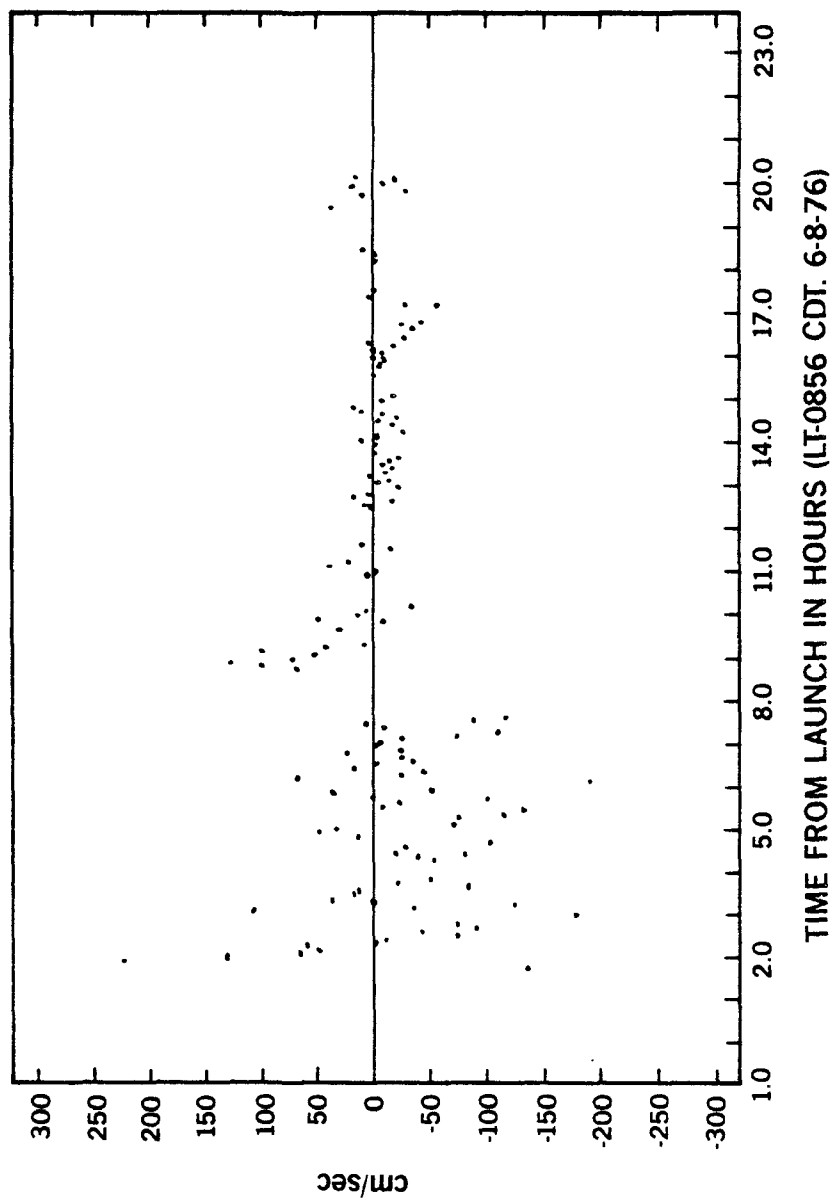


Figure 5-7. Vertical air motion observed with MacCreedy anemometer on DaVinci II balloon flight. Placement of the anemometer too close below the balloon biased the data with wake effects, but the values of the observed velocities were not seriously affected.

rarely were one second values of velocities as low as 2.5 cm/s. MacCready remarks that for certain nighttime portions of the DaVinci flight, the intensities of turbulence were among the lowest ever measured.

Because of these encouraging results, supporting electronics were built for the MacCready sensor to enable the tethersonde telemetry to handle the vertical anemometer data for the testbed prototype. Currently, the range of the resulting anemometer is 0.3 - 300 cm/s. It makes a measurement to better than 1 cm/s in one cycle of the tethersonde data system, about 10 s. Taking into account random error alone, in one minute, the estimated uncertainty on average velocity is less than  $\pm 0.4$  cm/s, and in 5 minutes,  $\pm 0.2$  cm/s.

#### e. Prototype Ground Station

The choices made for the testbed prototype payload largely dictated the choices for the prototype ground station (PGS). The block diagram of the PGS is given in Figure 5-8.

Data from both the airsonde within the balloon and the tethersonde in the ambient air are telemetered to the AIR ground unit, the ADAS (Atmospheric Data Acquisition System). The ADAS contains a Z-80 microprocessor which calculates the values of the selected variables from the raw data coming from the sondes, and from either an optical theodolite or radiotheodolite equipped with AIR shaft encoders. It does this by applying calibration factors for each sonde which are read into the ADAS from calibration punched paper tapes at the time the program is started. Upon completing the calculations for each sonde, the ADAS dumps a line of data to an external

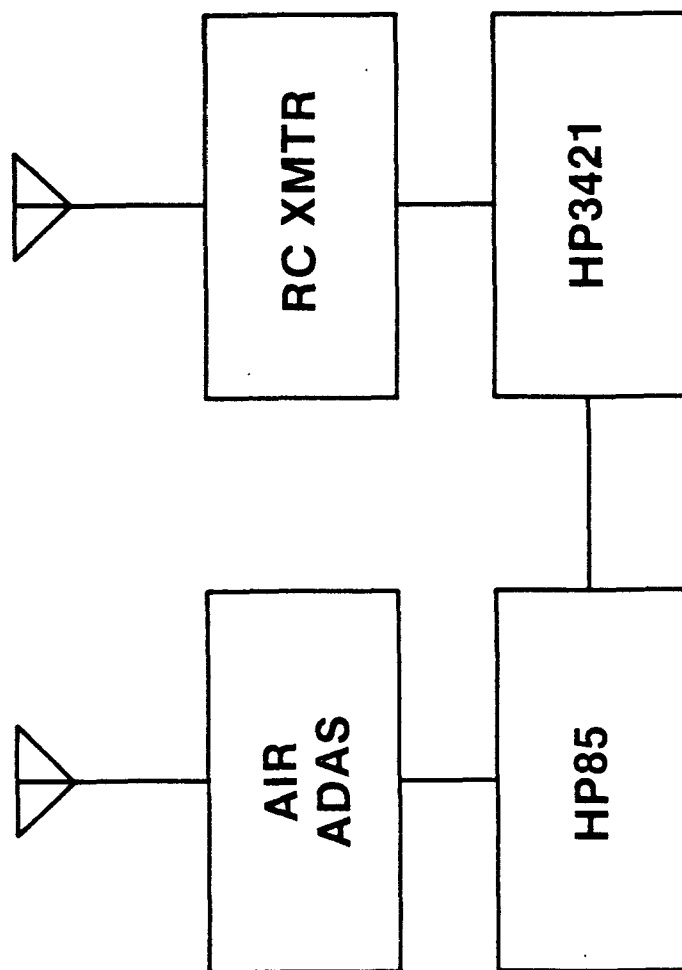


Figure 5-8. Block Diagram of Prototype Ground Station. The AIR ADAS (Atmospheric Data Acquisition System) receives and decodes the airsonde and tethersonde signals, and passes the data to the HP85, which contains the control algorithm. The HP85 activates the HP3421, which gives switch closures as appropriate to activate the pumps or valves through the RC transmitter.

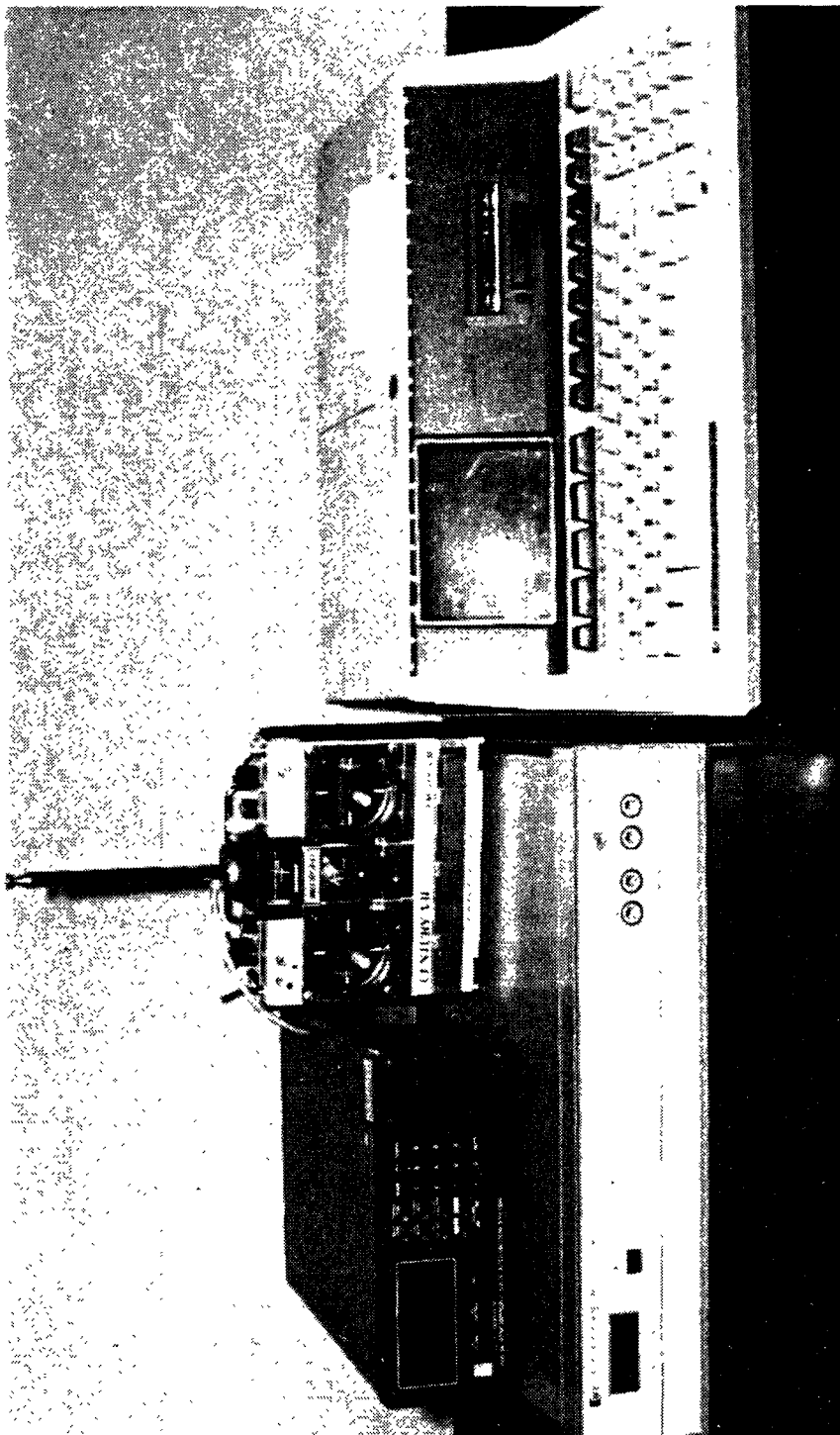


Figure 5-9. Prototype Ground Station. The ADAS is at upper left, the HP85 on the right, the HP3421 on the lower left, and the RC command transmitter at the center.

printer and to the HP85 desktop computer. Tracking information is included.

The HP85 applies the control algorithm, displays, prints, and writes to cassette tape selected calculated variables, and transmits appropriate instructions to the HP3421 interface unit to actuate the pumps and valves. The HP3421 effects switch closures which cause the attached RC unit to transmit the radio commands to the RC receiver in the payload to operate the pumps, operate the valves, or do nothing, whichever the control algorithm dictates. The PGS is shown in Figure 5-9.

## 6. EXPERIMENTAL RESULTS

In Phase I, time and resources limited the experimental program to the minimum necessary to demonstrate that the concept for the PLT is viable. Initially, measurements were made on individual components in the laboratory to determine if their performance was acceptable. Next, the testbed prototype system underwent tests in a tower. Finally, testing began in the ambient atmosphere. Phase I did not include true "free flight" testing. Such tests are manpower intensive and, for flights of any duration, require a tracking capability which will not be available until Phase II. Thus, the focus was on testing in the controlled atmosphere of the tower.

### a. Laboratory

It has already been mentioned that Raven conducted a superpressure test on one of the balloons to assure that they are capable of withstanding the 80 mb specified maximum superpressure. SNL will carry out a test during Phase II to

determine the superpressure at which balloon failure occurs. It is important to establish the margin of safety between operational superpressure levels, and superpressure at failure. For the operational system, a device will be incorporated which would initiate a controlled shutdown if the superpressure should exceed safe levels.

Superpressure balloons, or CVBs, have only approximately constant volume. The material from which they are constructed, polyester film (mylar), has high but finite modulus of elasticity. Consequently, the balloon will expand to some degree as the superpressure rises.

A test was conducted to measure the change in volume of the balloon with superpressure. The volume was determined by measuring the polar and equatorial circumferences of the balloon. This was necessary because the balloon is slightly ellipsoidal. A 30 mb change in superpressure (from 20 to 50 mb), such as one might expect during the day-night transition, results in a 1.3% change in volume. In the absence of a corrective response by the control system, this would result in a 135 m change in altitude at 1000 m in a standard atmosphere.

After the balloon itself, the element which involved the most uncertainty was the pump. At the outset, it was not certain that a pump could be found which met our requirements for flow at high backpressure, low weight, and high efficiency. Four different pumps were examined. They were each weighed, and then operated at their rated voltages against backpressures of 34.5 and 69 mb (0.5 and 1 psi). The pumping speeds and power consumptions were measured at these backpressures. The results are given in Table 6-1.

TABLE 6-1. PUMP CHARACTERISTICS

<u>Make &amp; Model</u>	<u>Weight (g)</u>	<u>Backpressure (mb)</u>	<u>Voltage (V)</u>	<u>Current (A)</u>	<u>Power (W)</u>	<u>Speed (1/min)</u>	<u>SxP/W</u>	<u>SxP/Wt</u>
Brey 290 G-12-07	381	69	12	2.1	25	14.3	39.5	2.6
		34.5	12	2.0	24	14.3	20.5	1.3
Brey 290 G-12-04	86.5	63*	12	.42	5.0	1.02	13	.74
		34.5	12	.40	4.8	3.04	22	1.2
Gilian B22A06F48	158	69	5	.25	1.25	2.55	141	1.11
		34.5	5	.21	1.05	3.1	102	.68
Brailsford T0-2A (Single head)	234.5	69	14	.070	.98	1.15	81	0.34
		34.5	14	.070	.98	2.4	84.5	0.35

\*No flow at 69.5 mb.



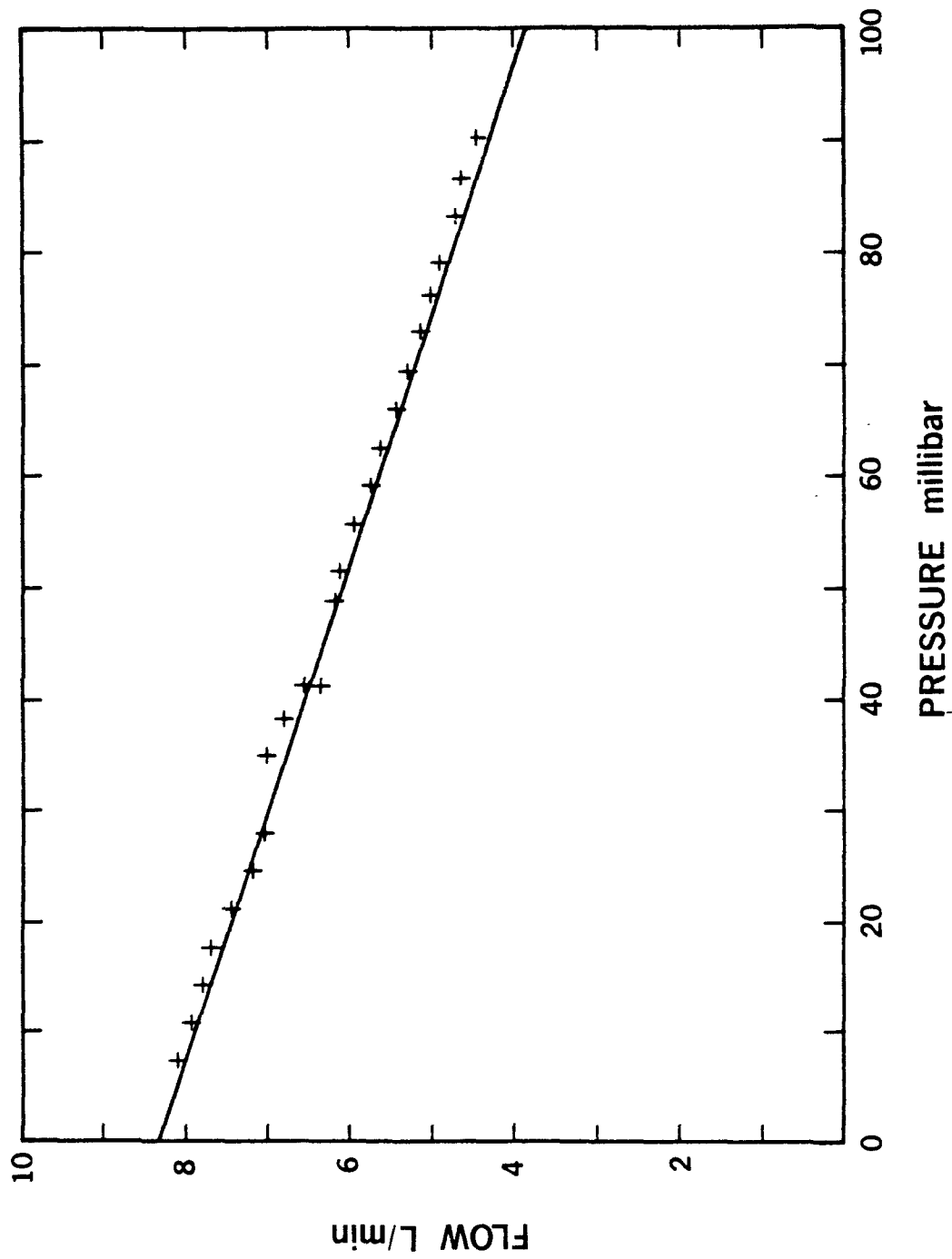


Figure 6-1. Combined speed of two Gilian pumps versus backpressure.

The second to the last column in the table gives pumping speed times backpressure divided by power consumption. This is a figure of merit related to efficiency (multiply by .167 to get % efficiency). The last column gives speed times backpressure divided by weight. This is also a figure of merit, but it is less important because the batteries to run the pump are likely to outweigh the pump in any case.

On the basis of published data, the larger Brey pump had been procured for the testbed prototype. However, on the basis of the test data, it became clear that the Gilian is several times more efficient. Hence, Gilian pumps were selected.

To get the required flow from the TP system, two Gilians were operated in parallel. For the actual pumps used, pumping speed and current measurements were made as a function of backpressure. The results are given in Figures 6-1 and 6-2. Similarly, flow vs superpressure measurements were made through the Klippard valves and associated plumbing. The results are given in Figure 6-3.

From these results, the tradeoffs influencing choice of initial superpressure become apparent. At high superpressure, pump speed decreases, and power consumption goes up, but so does the rate at which air can be valved off. Hence the pumpdown speed decreases, but the valve-up speed increases. The reverse is true at low superpressure. If inadequate superpressure is available to counteract condensation on the balloon, then when all the available superpressure has been valved off, the balloon will go slack while still negatively buoyant. It will then begin descending, and will continue to descend until it reaches the ground. On the other hand, if the superpressure is too high, the maximum safe superpressure

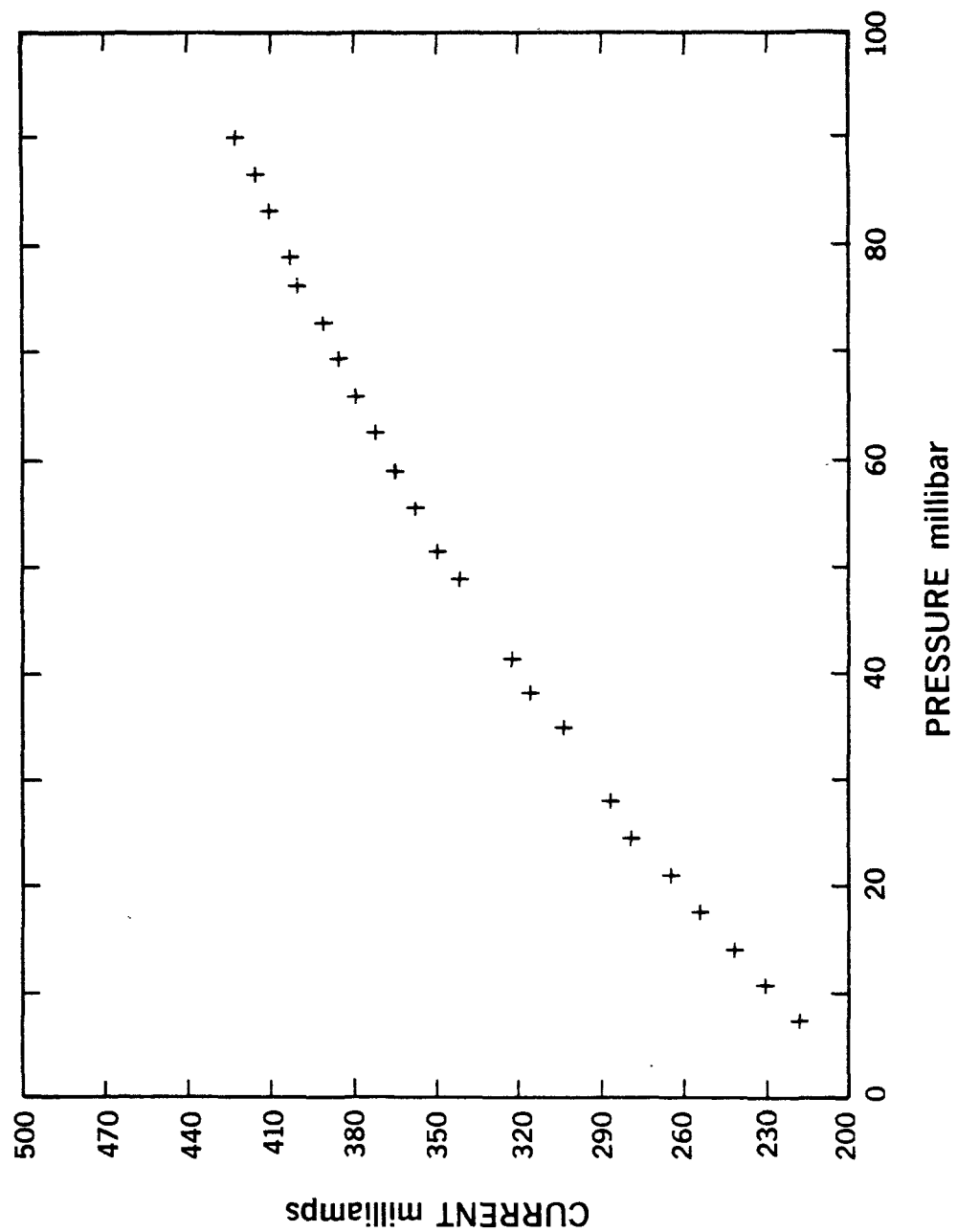


Figure 6-2. Combined current consumption of two Gilian pumps at 6 VDC versus backpressure.

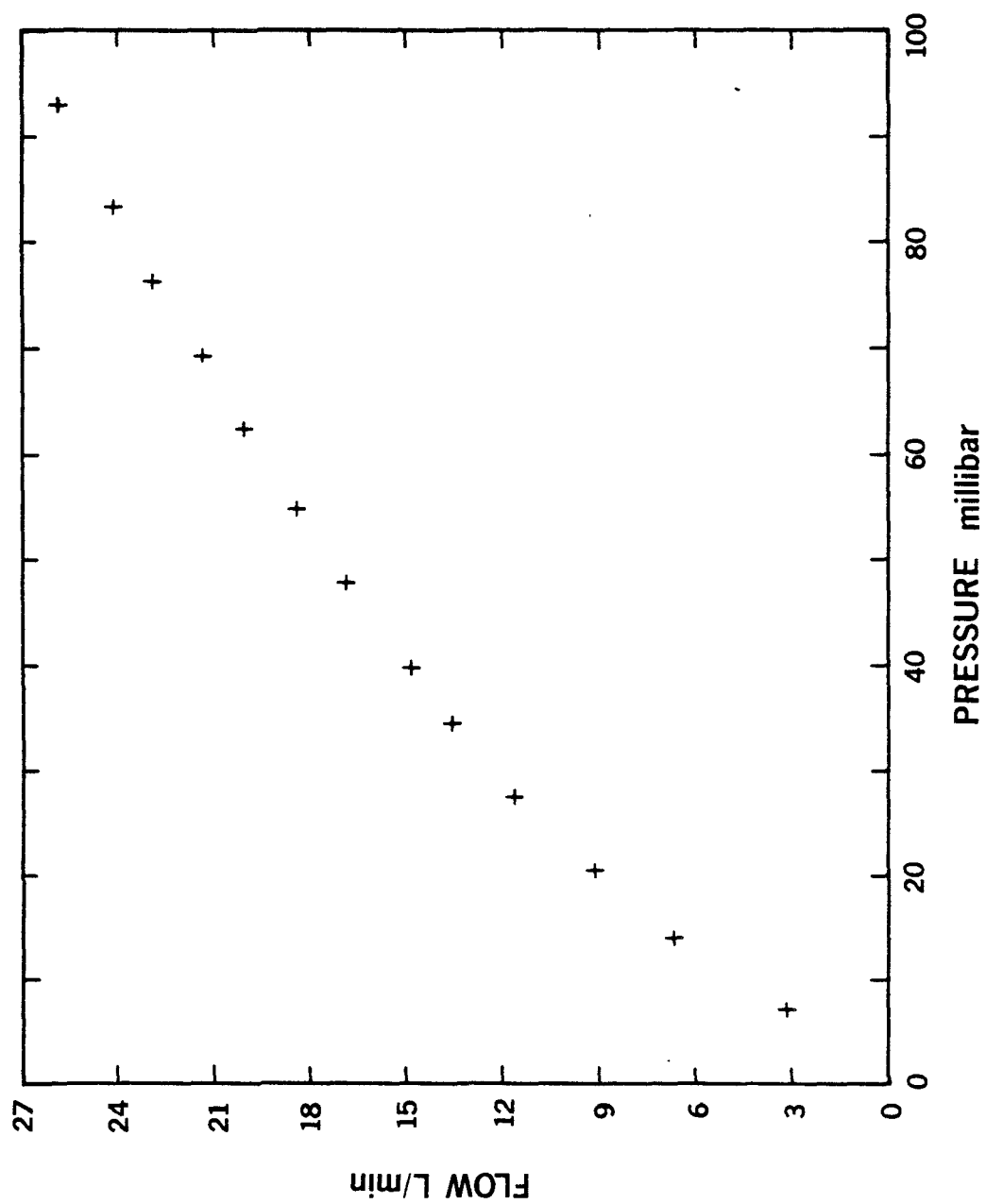


Figure 6-3. Vent valve flow as a function of superpressure.

may be exceeded when the PLT is swept up in a thermal, causing the automatic shutdown system to activate to prevent the balloon from failing in an uncontrolled manner. The auto-shutdown provides a controlled descent, but also decisively terminates the experiment.

#### b. Tower

In order to check the actual behavior of the testbed prototype under pumping and valving against the equations which describe its behavior, tests were conducted inside a tower. The tower is part of the Solar Central Receiver Test Facility at Sandia National Laboratories, Albuquerque (Figure 6-4). The tower offers an enclosed volume roughly 10 m square by 52 m high. Since the tower is enclosed, it offers a more controlled environment than does the ambient atmosphere, making it easier to interpret test results.

Figure 6-5 is a diagram of the interior of the tower and the various levels to which one has access. A monofilament fishing line was run from the top to the bottom of the tower at about the center of the shaft to act as a guide for the balloon. The balloon was attached to the guideline by a miniature carabiner which was free to move up and down the line with very little friction. On one side of the tower, a high door extends from ground level up to about 23 m. The door is the width of the interior of the elevator shaft. A significant air leak exists around the periphery of the door, and the door itself acts as a thermal leak.

Figure 6-6 gives the approximate dimensions and reference levels of the testbed prototype as used in these tests. Initially, the ballonet was nearly completely filled with helium. The mass of the payload was then increased with

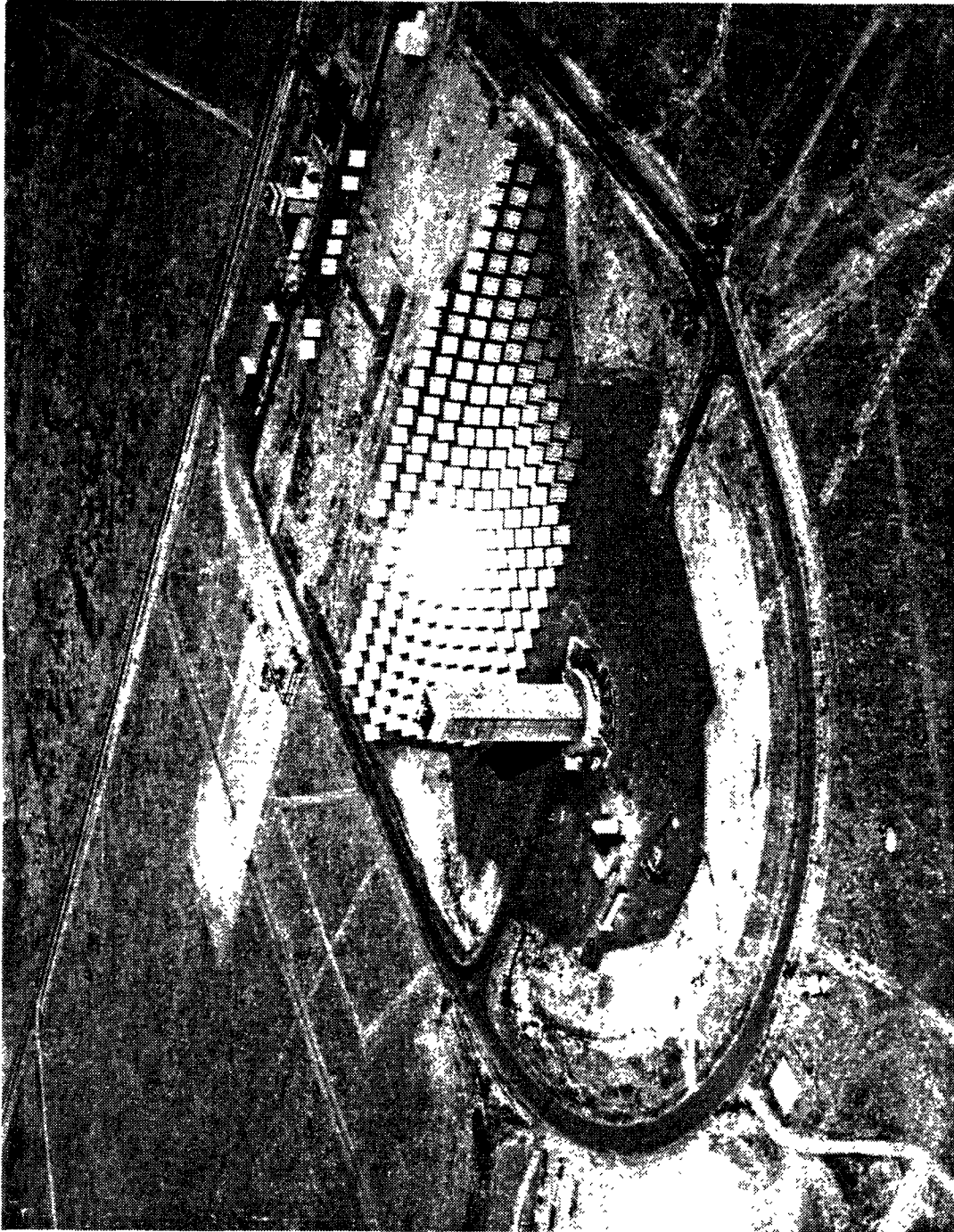


Figure 6-4. Two-hundred-foot tall tower of Solar Central Receiver Facility, the interior of which was used to test the testbed prototype PLT.

# SOLAR TOWER INTERIOR

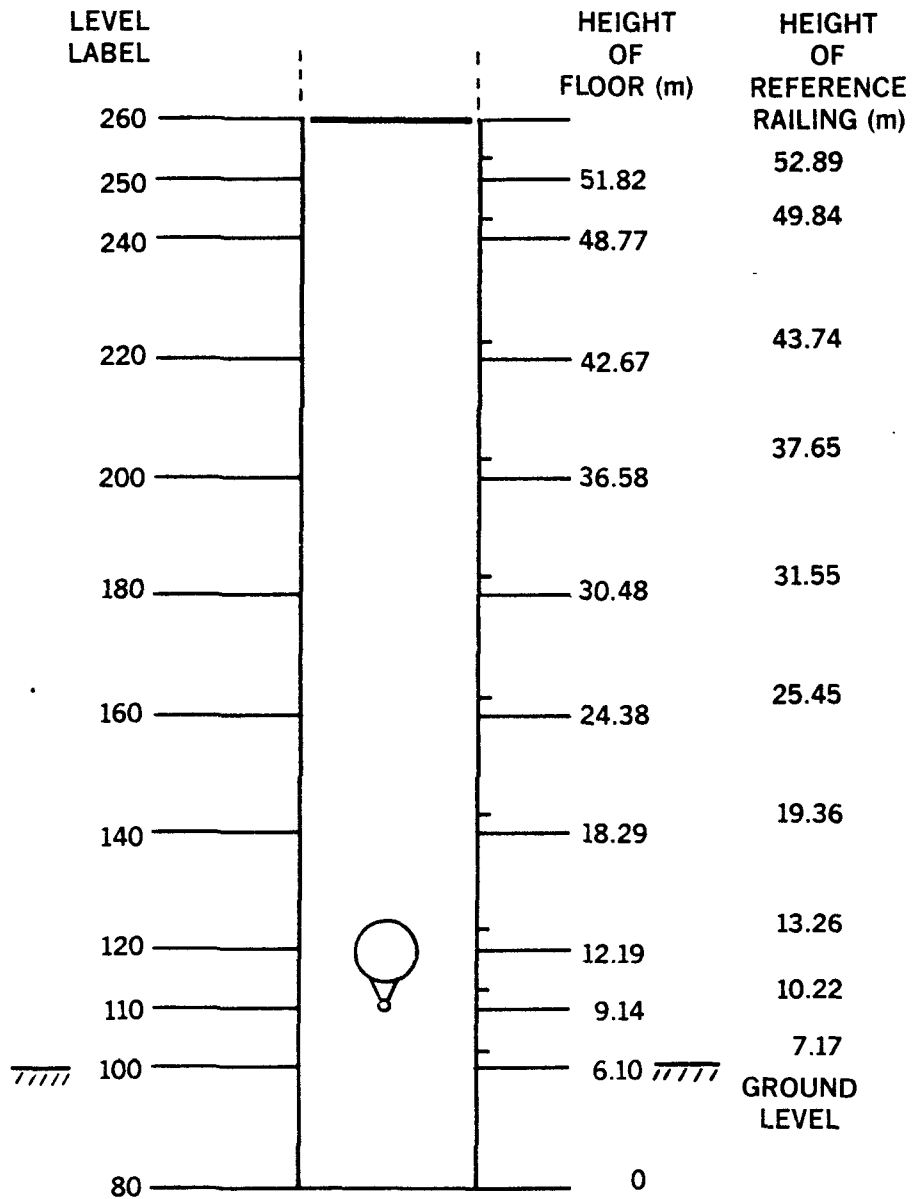


Figure 6-5. Interior of the Solar Tower with reference levels indicated.

## REFERENCE POINTS:

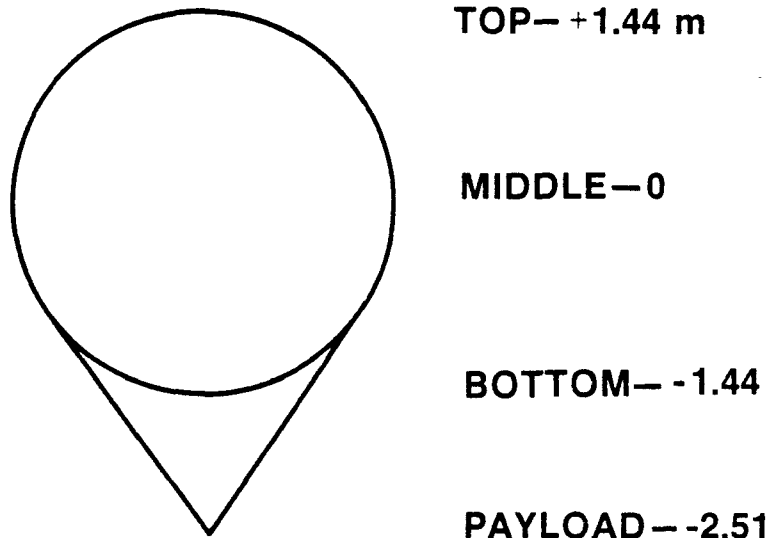


Figure 6-6. Dimensions and Reference Levels on testbed prototype PLT for Tower tests.



ballast to the point that pressurizing the constant volume balloon with air to about 40 mb yielded neutral buoyancy at the floor level of the tower.

Subsequently, two valve-up and pumpdown cycles were executed. Vertical position as a function of time was recorded by recording the time when reference points on the balloon passed reference levels in the tower. When the marker balloon was moving slowly, it was possible to keep up with it, moving from level to level, recording its passage. When it was moving rapidly, it was not possible to record its passage at every reference level. Hence the data points are unevenly distributed. The time standard was a high-quality stopwatch.

Figure 6-7 shows valve-up number one. Note the much more rapid rise in the upper portion of the tower than in the lower. The balloon hit the top of the tower with considerable excess buoyancy.

Figure 6-8 shows the results of pumpdown number one. Note that it took nearly 500 seconds of pumping to overcome the excess buoyancy generated during the preceding valve-up. After the excess buoyancy had been overcome, the balloon began to descend, slowly at first, and then more rapidly. The apparent variations in descent rate are real. As noted on the figure, the uncertainties are smaller than the data points.

During the pumpdown, the tethersonde system was taking temperature data. Those data are given in Figure 6-10. Here the altitude shown is from the tethersonde system itself, which gets altitude by integrating the hydrostatic equation. Note the grossly different thermal structure in the upper and lower portions of the tower. The existence of the door which provides a leak path for both air and heat undoubtedly

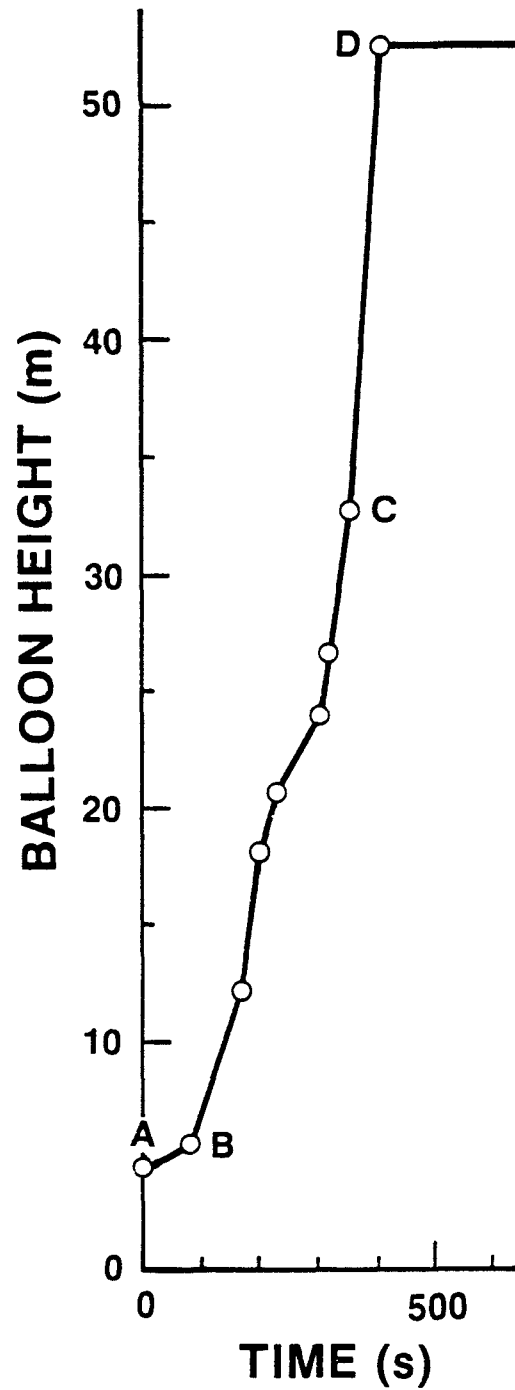


Figure 6-7. Valve-up number one. Uncertainties are smaller than the data points. Valve was opened at A. From B to C, the mean vertical velocity was 8.1 cm/s; from C to D, 24.9 cm/s.

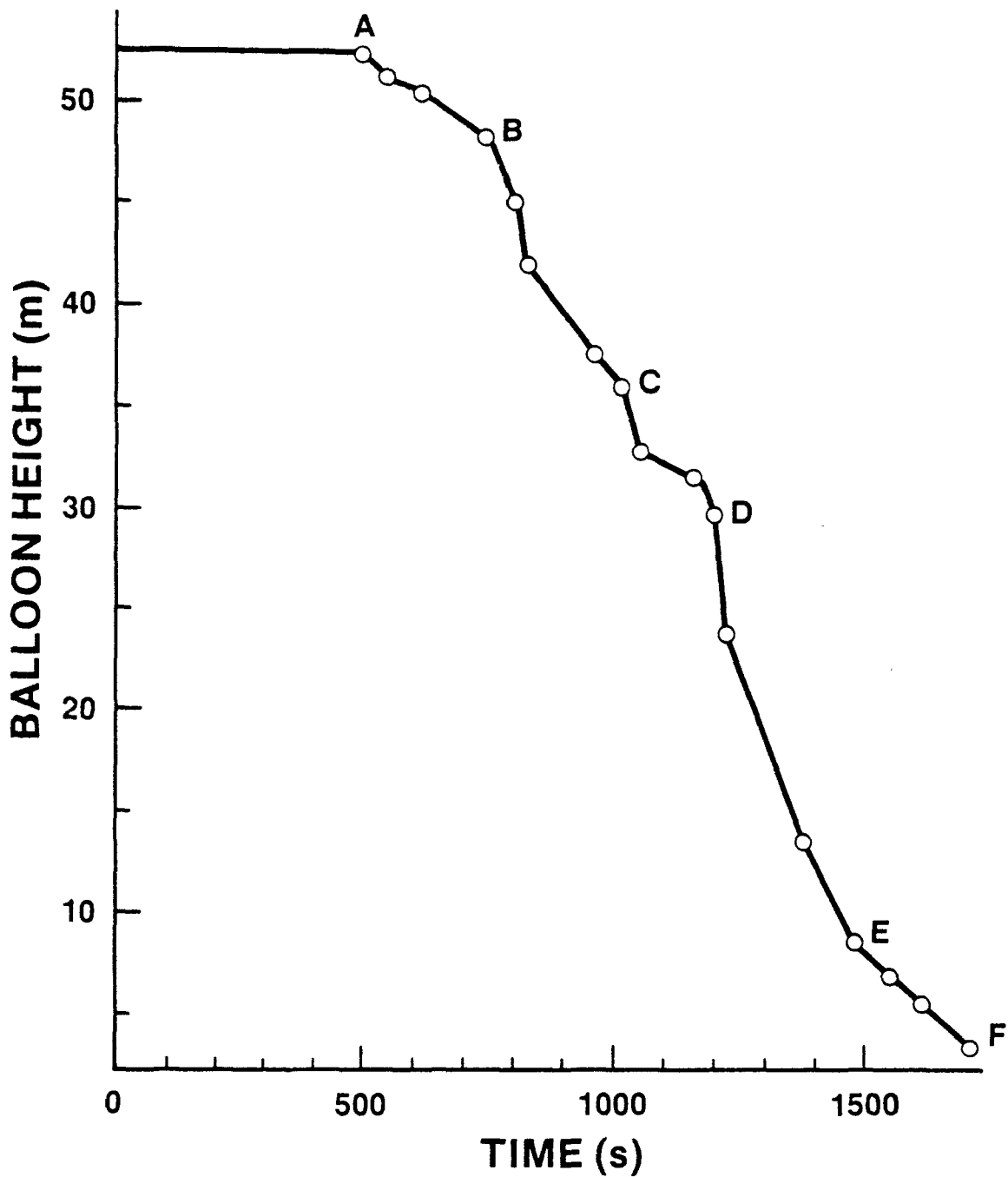


Figure 6-8. Pumpdown number one. Pumps were turned on at time zero. It took the balloon system approximately 500 s to overcome excess buoyancy, and to begin to descend (point A). From A to B, the mean vertical velocity was  $-1.6$  cm/s; from B to C,  $-4.6$  cm/s; from C to D,  $-2.9$  cm/s; from D to E,  $-5.8$  cm/s; and from E to F,  $-2.2$  cm/s.

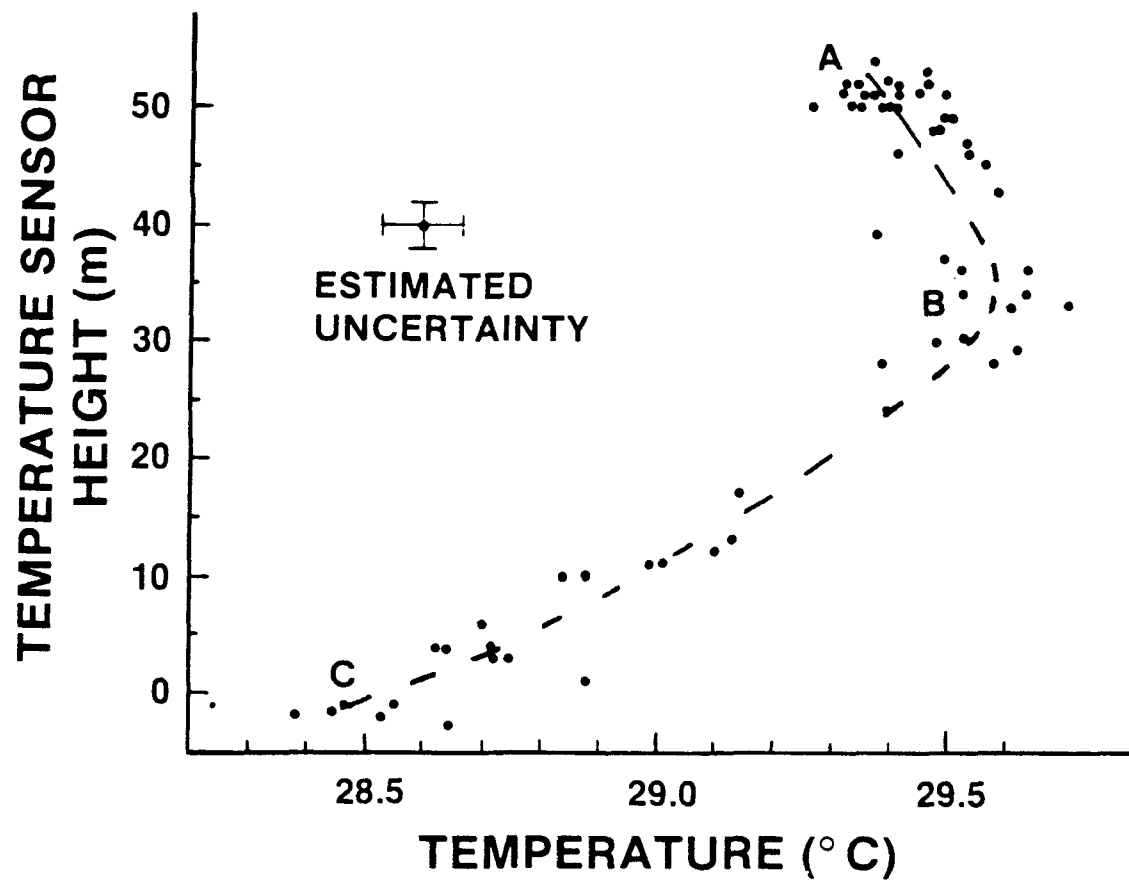


Figure 6-9. Temperature vs Altitude on pumpdown number one. The temperature lapse rate is approximately  $+15^{\circ}\text{K/km}$  from A to B, and  $-34^{\circ}\text{K/km}$  from B to C.

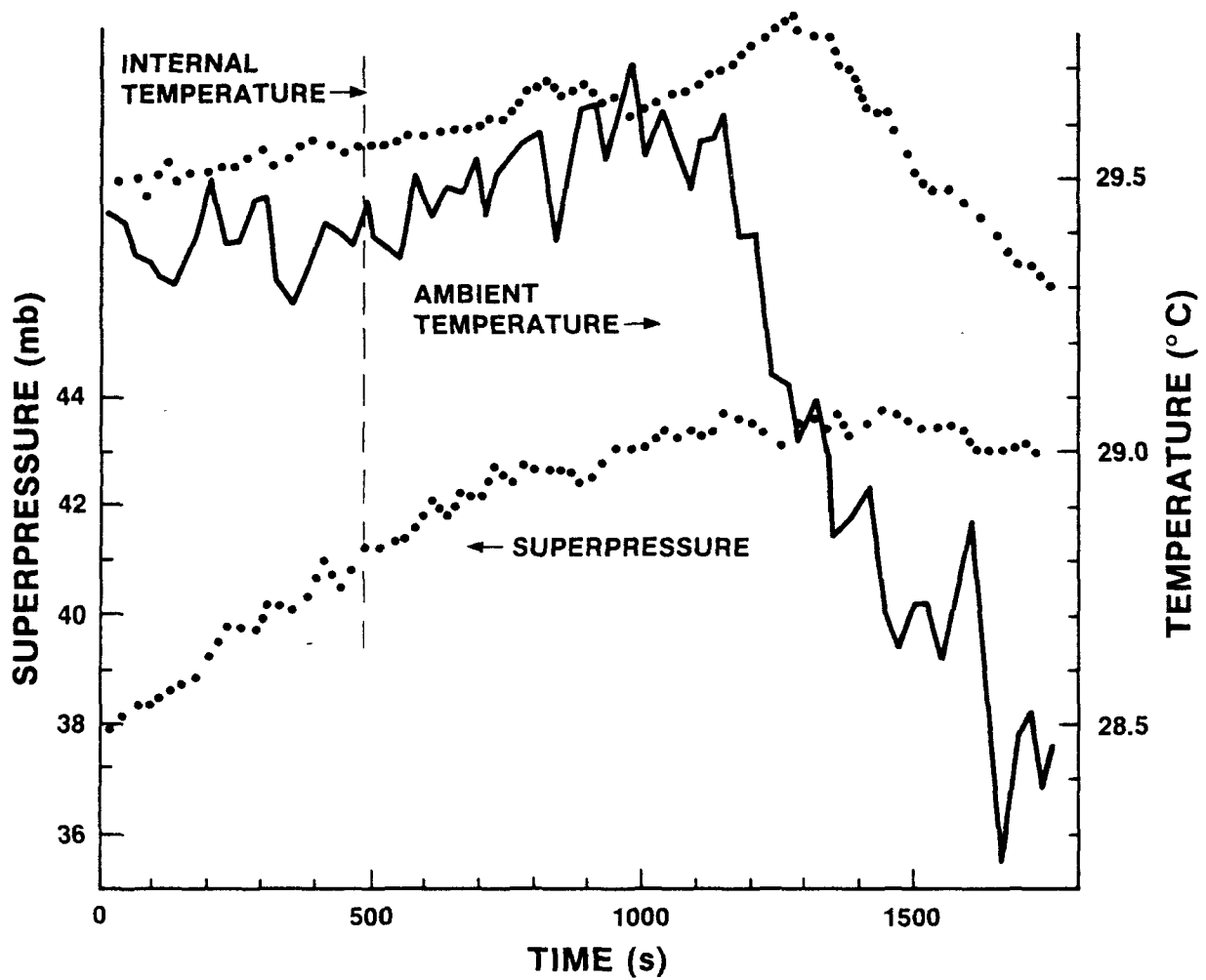


Figure 6-10. Internal temperature, ambient temperature, and superpressure as a function of time on pumpdown number one. Pumping began at  $t=0$ ; descent at about 500 s.

influences the thermal structure in the lower part of the tower.

The internal balloon temperature, the external temperature at the payload, and the superpressure -- the difference between the internal and external pressures -- were plotted for pumpdown number one as a function of time. Those results are given in Figure 6-10.

Note that when the balloon reached neutral buoyancy at the top of the tower (came off the ceiling) the superpressure was about 41 mb. When it reached the bottom of the tower, the superpressure was about 43 mb. At the top of the tower, the balloon was only  $0.15^{\circ}$  above ambient temperature, whereas at the bottom, it was  $0.9^{\circ}$  above ambient. If the balloon were brought to thermal equilibrium with its surroundings at the base of the tower, the superpressure would have been very nearly the same at the base as at the top of the tower, as expected. The ambient pressure varies by about 5 mb over this altitude range.

Next, valve-up number two was carried out. The results are shown in Figure 6-11. This run was marred by the balloon straying to one side of the tower and hitting the underside of a gallery, in spite of the guideline (which had only minimal tension on it, since it was a 10-pound test line). The gallery it hit is immediately above the high door. It is probable that a gentle flow caused by a convection cell involving the door drew the balloon towards the door. The tests were done at night when the external temperature on the other side of the door was substantially cooler than the interior temperature.

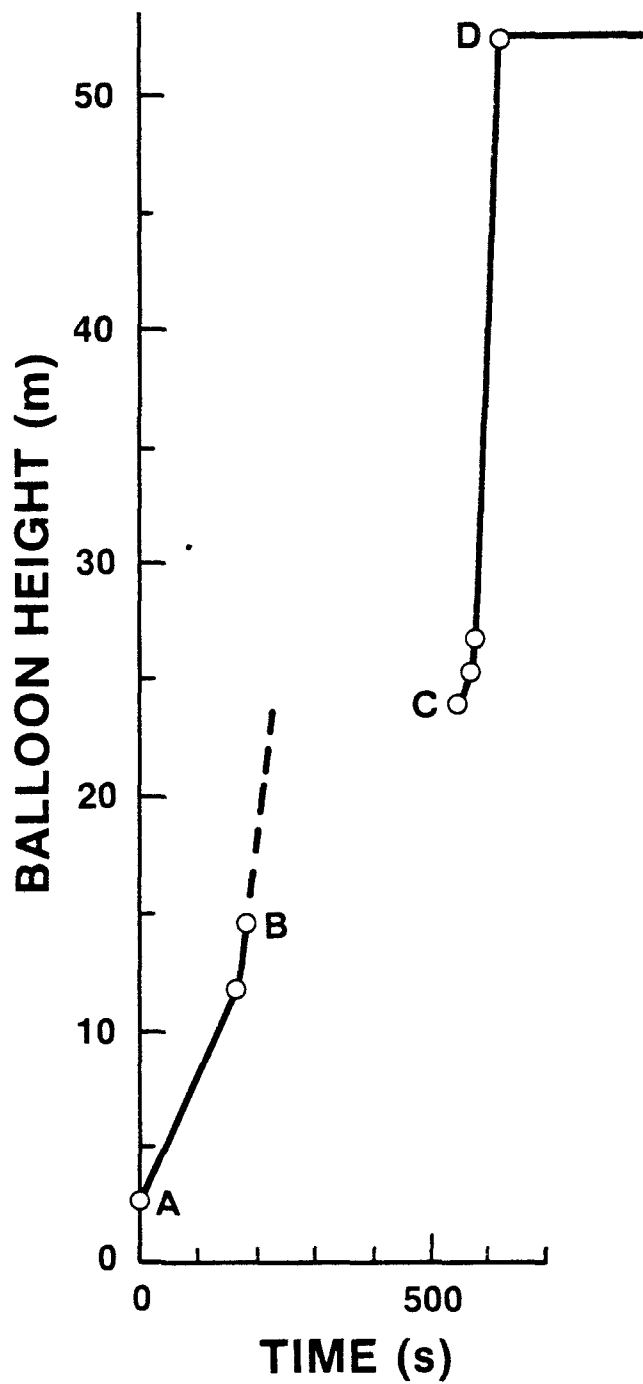


Figure 6-11. Valve-up number two. Valve was opened at A. From A to B, the mean vertical velocity was 6.4 cm/s. At B, the balloon hit an overhang and bounced down. It tarried in the vicinity of the overhang from B to C. From C to D, the mean vertical velocity was 41.5 cm/s.

The results from pumpdown number two are shown in Figure 6-12. Again, considerable excess buoyancy had been generated on the way up, plastering the balloon against the ceiling of the tower. It took nearly 700 seconds of pumping to overcome that and start the balloon down. Again, the first few metres were traversed rather slowly, followed by a much more rapid descent to the vicinity of 20-22 m. Here the balloon literally stopped. It didn't hit a solid obstruction -- it hit a thermal barrier. Once that barrier was overcome, it dropped rapidly to the base of the shaft.

Figure 6-13 shows the results from the temperature measurements made on the way down. The thermal barrier in the 20-22 m region is very clear.

One starts on the interpretation of the data with an expression for the pumpdown speed in terms of the lapse rate  $\gamma$  (Appendix I):

$$v_p = - S T / [ V (Mg/R - \gamma) ] \quad (6-1)$$

Here  $S$  is pumping speed in  $\text{m}^3$ ;  $T$  is ambient temperature at the balloon;  $V$  is the volume of the balloon;  $R$  is the universal gas constant;  $M$  is the molecular weight of air;  $g$  is the acceleration due to gravity; and  $\gamma$  is the lapse rate defined as  $\gamma = - dT/dz$  (here taken as positive if  $T$  decreases with altitude). We take  $S = 1.17 \times 10^{-4} \text{ m}^3/\text{s}$  (7.0 l/min);  $V = 12.5 \text{ m}^3$ ;  $g = 9.8 \text{ m/s}^2$ ,  $R = 8314 \text{ J/(kg-mol}^\circ\text{K)}$ . For a standard atmosphere, this expression agrees with that given in Equation (3-1). At  $T = 293^\circ\text{K}$ , this expression gives



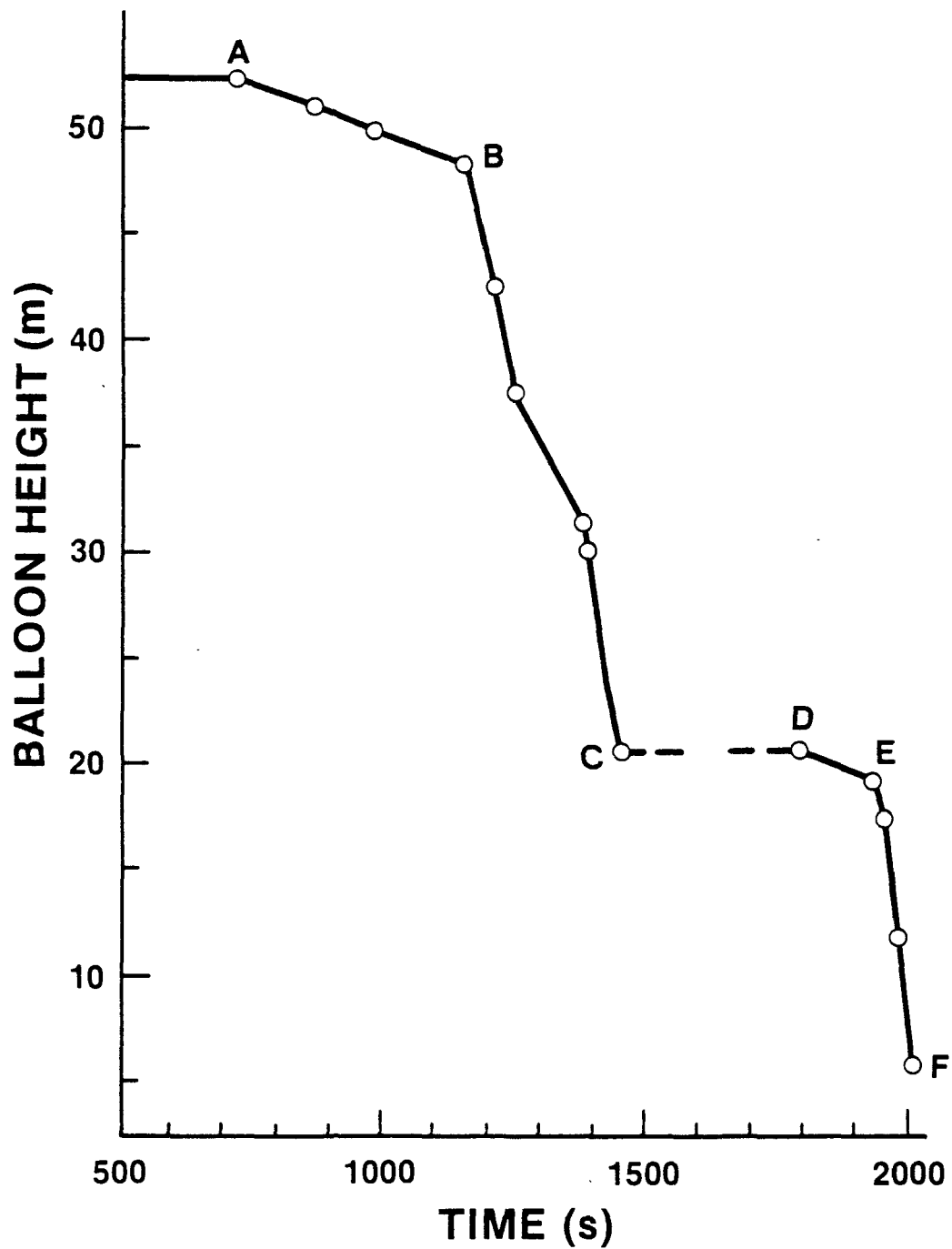


Figure 6-12. Pumpdown number two. Pumps were turned on at time zero. It took the balloon system approximately 700 s to overcome excess buoyancy and to begin to descend. From A to B, the mean vertical velocity was  $-0.9$  cm/s; from B to C,  $-9.2$  cm/s; from C to D,  $0$  cm/s; from D to E,  $-1.1$  cm/s; and from E to F,  $-16.8$  cm/s.

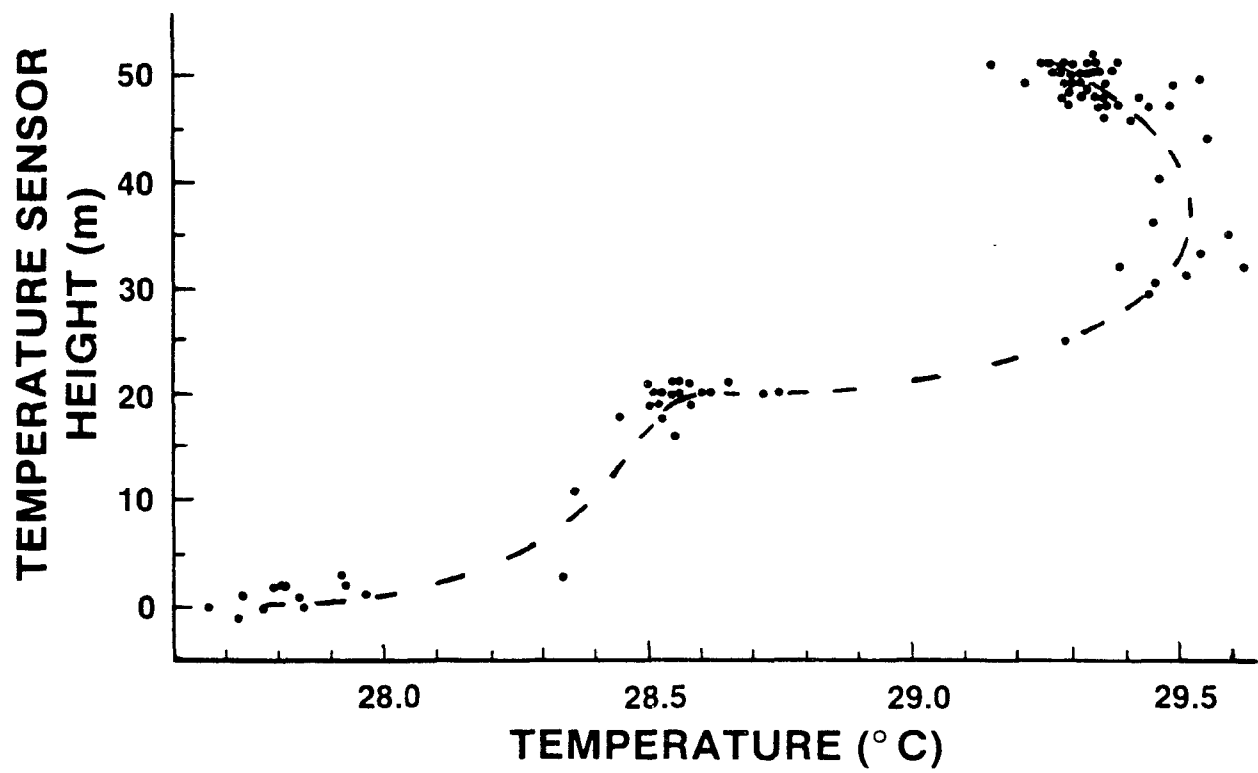


Figure 6-13. Temperature versus Altitude on pumpdown number two.

	$\gamma$ (K/km)	$v_p$ (cm/s)
	14	13.5
(adiabatic)	10	11.3
(standard)	6.5	9.9
(isothermal)	0	8.0
	-10	6.2
	-20	5.0
(observed in lower part of tower on run #1)	-34	4.0

It is important to emphasize that the pumpdown speed given by the expression above is the speed with which the equilibrium altitude changes, which is not necessarily the speed with which the balloon actually moves. It would be the actual vertical speed of the balloon in the absence of drag and dynamic effects -- if the balloon system were massless, and if the air had zero viscosity. In the presence of dynamic effects, the balloon will not always be in equilibrium, and Newton's second law must be used to determine its motion.

During both pumpdowns, initially the balloon falls very slowly. This may be due in part to a dynamic effect -- it requires some time to approach "terminal velocity" -- but it might also be possible that at the very top of the tower, above the region accessible to the tether sonde payload, there is a strong inversion that accounts for the slow pumpdown.

Below the first few metres, there is a region with a positive lapse rate during both pumpdowns. In the first pumpdown, this region is traversed at about 4.6 cm/s, whereas in the second, the speed is 9.2 cm/s. Both are slower than the 10-20 K/km lapse rate would lead one to expect on the basis of the pumpdown speed expression. The thermal structure does not seem to be able to account for the difference, although

differences in thermal structure smaller than can be detected by the tether sonde can make a significant difference in pumpdown speed. Another possibility is that vertical air flows of a few cm/s are present and are complicating the dynamics.

In the lower part of the tower, during pumpdown number one, the vertical velocity observed is in reasonable agreement with the predicted pumpdown velocity. In pumpdown number two, however, the thermal barrier introduces a delay, followed by an accelerated fall rate -- a dynamic effect.

The dynamic effects were examined in a simplified fashion. Ultimately, a computer model will be needed, but an approximate analytical treatment yields considerable insight.

Newton's second law can be written:

$$\vec{F} = m \frac{d\vec{v}}{dt} \quad (6-2)$$

where  $\vec{F}$  is the force on a system,  $m$  is the mass of the system, and  $\vec{v}$  is its velocity. For the balloon system, we may write

$$\begin{aligned} -g [V (\rho_b - \rho_a) + m] \vec{k} - \frac{1}{2} \rho_a C_D A_D |\vec{v}_b - \vec{v}_a| (\vec{v}_b - \vec{v}_a) \\ = [\rho_b V + m + \frac{1}{2} \rho_a V] \frac{d\vec{v}}{dt} \end{aligned} \quad (6-3)$$

Here the first term is the buoyant force, the second the drag force, and the quantity in brackets on the right side of the equation is the "virtual mass" of the balloon system. Here  $\rho_b$  is the mean density of the gas in the balloon,  $\rho_a$  is the density of the ambient air,  $m$  is the mass of the balloon system excluding the mass of the gas in the balloon,  $\vec{k}$

is a vertical unit vector,  $C_D$  is the drag coefficient (taken as 0.47 for low Reynolds number);  $A_D$  is the cross-sectional area of the balloon,  $\vec{v}_b$  is the velocity of the balloon,  $\vec{v}_a$  is the velocity of the air, and the term  $(1/2)\rho_a V$  on the right side of the equation accounts for an increase in effective mass of the system due to entrainment of air.

If we choose to make the equation specific for the system heading downwards, we can drop the vector notation:

$$-m_L g + b v^2 = m_v \frac{dv}{dt} \quad (6-4)$$

where here  $m_L$  is the net (buoyant) mass of the system

$$m_L \equiv V (\rho_b - \rho_a) + m \quad (6-5)$$

(here presumed constant),  $b$  is a redefined drag coefficient, and  $m_v$  is the virtual (inertial) mass of the system. Now  $v$  is the velocity relative to the air, which is presumed to be either quiescent or in uniform (non-accelerated) motion.

The solution to this equation, starting from rest relative to the air, is

$$v = -\alpha \tanh \beta t \quad (6-6)$$

where  $\alpha$  can be shown to be the terminal velocity, and is given by:

$$\alpha = \sqrt{\frac{m_L g}{b}} \quad (6-7)$$

and

$$\beta = \frac{m_L g}{m_v \alpha} = \frac{1}{m_v} \sqrt{b m_L g} \quad (6-8)$$

This solution implies a characteristic relaxation time  $\tau$  to reach  $(1 - 1/e)$  of terminal velocity  $\alpha$ :

$$\tau \approx .75 \frac{m_v \alpha}{m_L g} \quad (6-9)$$

For our system,

$$\tau \approx \frac{2.3}{\sqrt{m_L}} \approx \frac{5.6}{\alpha} \quad (6-10)$$

The relaxation times can be quite significant. For  $\alpha = 0.1$  m/s (10 cm/s),  $\tau \approx 56$  s. For smaller terminal velocities, the relaxation times can be very long indeed. When the pump or valve is operated with the system neutrally buoyant, initially  $m_L = 0$ , so  $\tau$  is infinite. As  $m_L$  departs from zero,  $\tau$  becomes shorter.

The complexities of the dynamics and of the tower environment make it difficult to confirm our understanding of the system in detail, but the observations are consistent with the analysis to within the uncertainties induced by the system dynamics. A better model, taking the dynamics into account more accurately, is clearly in order. Nonetheless, the tower tests confirm the ability to adjust the equilibrium altitude of the system at the required rate -- 10 cm/s -- in a standard atmosphere.

### c. Ambient Atmosphere

In Phase I, the ambient atmosphere tests were of two types. The first is closely analogous to the tower tests, in that the testbed prototype was constrained by a guideline, only now the guideline is the tetherline of an aerodynamically-shaped tethered balloon (Figure 6-14). We

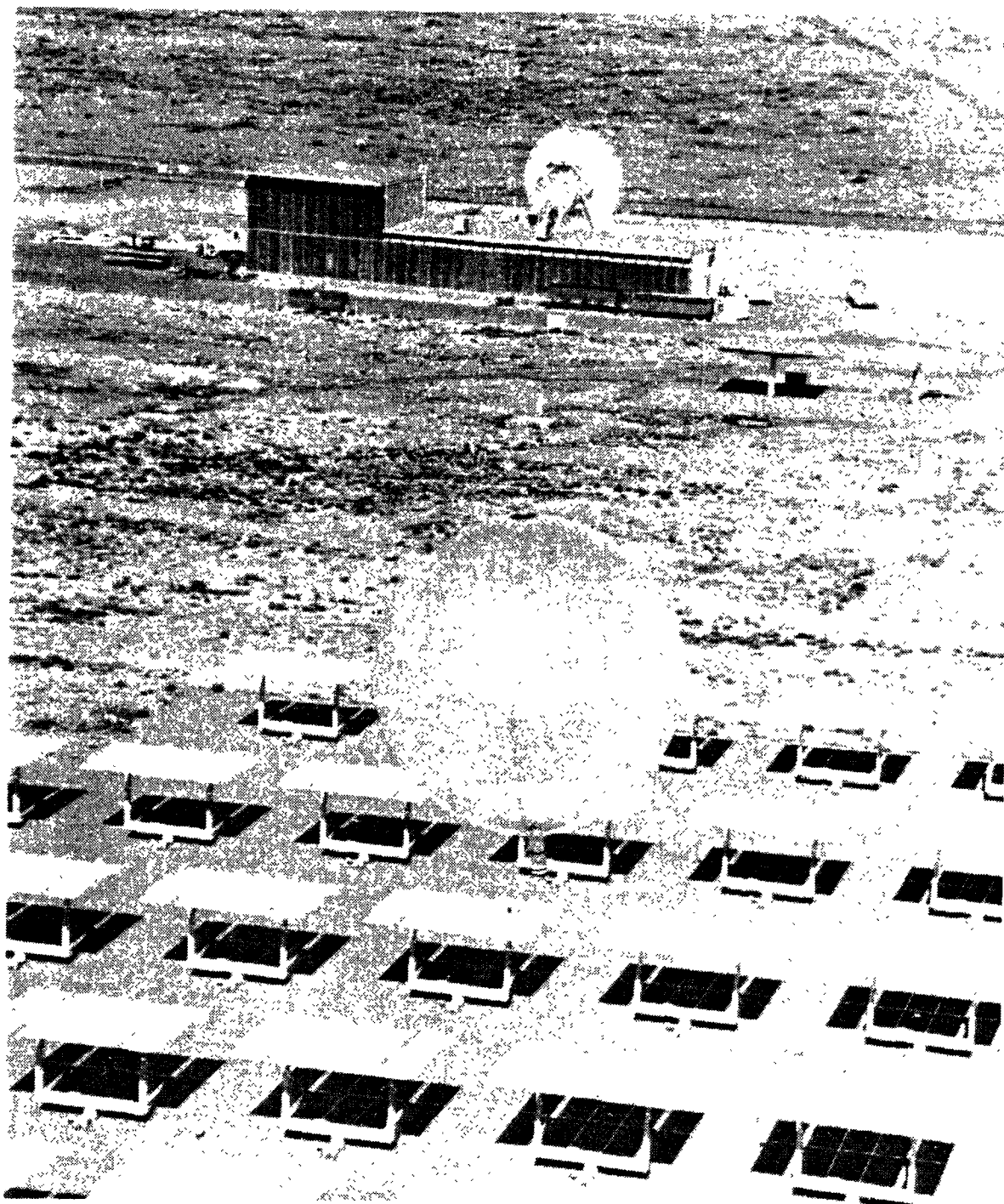


Figure 6-14. Testbed Prototype PLT during "open air tower" tests, viewed from the solar tower. Here the TP rides up and down on the tetherline of a tethered balloon out of the field of view above.

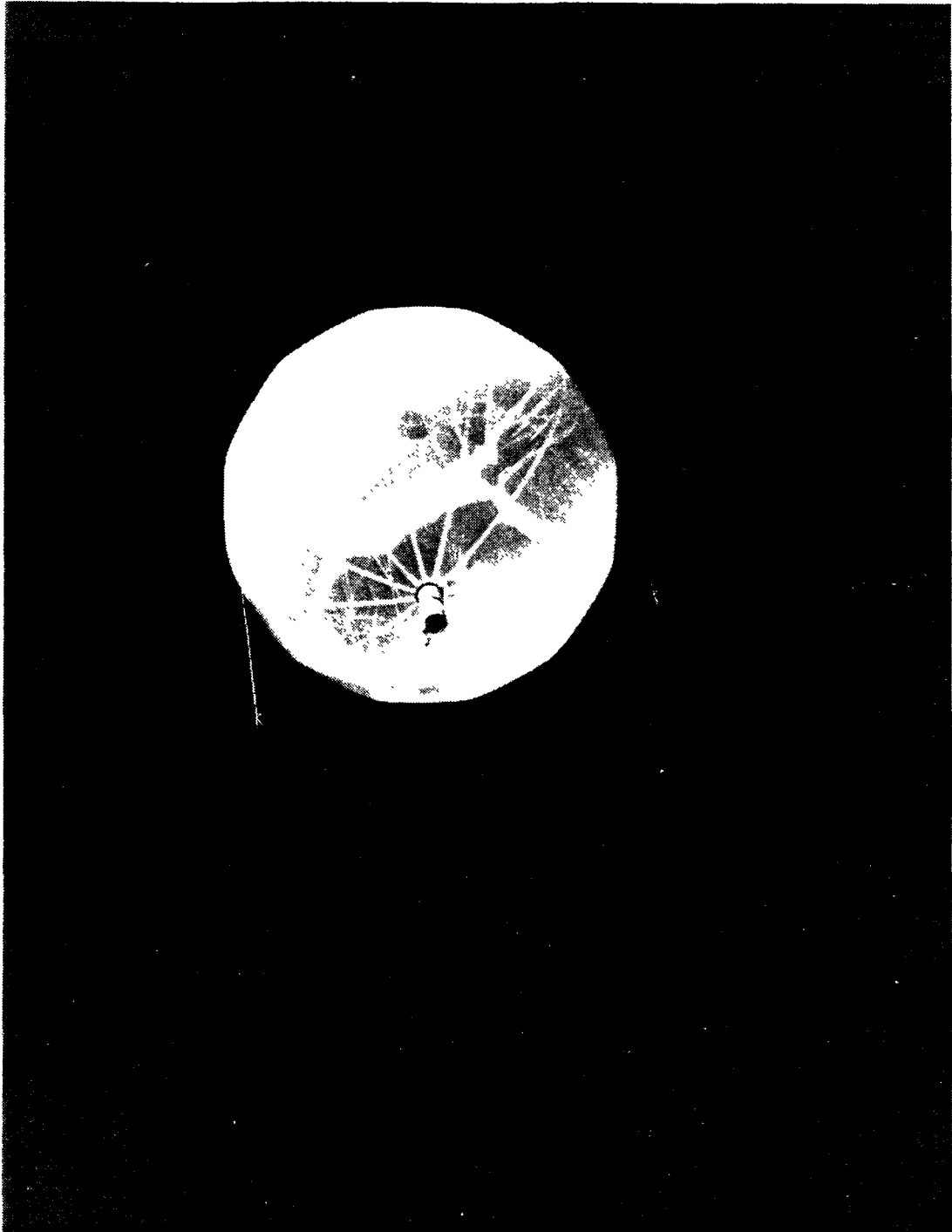


Figure 6-15. Testbed prototype PLT during a slack-tether flight test.



call these "open air tower" tests. This permits greater vertical excursions, and exposure to the outdoor environment.

At very low wind speed, this arrangement approximates a free-flight test. The balloon is free to respond to relative vertical air motions, and to heating or cooling caused by clouds and night sky. The great advantage is that the balloon remains in place laterally, and testing can go on for hours without having to chase the balloon. However, horizontal air motion exerts forces on the balloon which are not present in free flight. Consequently, the results of these tests need to be interpreted with this in mind.

In the second type of test, the balloon is prevented from floating away by a lightweight tether. The tether is kept slack during a flight by keeping a chase vehicle under the balloon, and by reeling out or reeling in tether as appropriate (Figure 6-15). This is still not a perfect approximation to free flight, but it is an improvement. Unfortunately, the duration of the flights obtainable in this manner are limited by where the chase vehicle can go to follow the balloon. In Phase II, true free-flight testing will begin.

The outdoor tests further qualitatively confirmed that the system behaves as expected. The outdoor environment is so complex, however, that it became clear that in the absence of long free-flight tests, quantitative understanding of system behavior could only come from the tower.

## 7. FUTURE WORK

There are two major thrusts in Phase II. The first is to turn the design for the operational prototype flight system

into functional hardware. The second is to continue development and refinement of the hybrid control algorithm through a continuing test program, at first with the testbed prototype, but later with the operational prototype. This involves modifying the prototype ground station to accommodate a radiotheodolite or LORAN tracking system, an ARGOS uplink receiver, and telephone reception of ARGOS data from NOAA. It does not involve significantly upgrading the ground station computer facility, or the incorporation of a Local User Terminal to permit reception of real time data from the PLT via satellite. In Phase II, ARGOS data can either be directly received from a nearby PLT via the uplink receiver, or it can be received via Service ARGOS/NOAA with a 4-6 hour delay. Because of resource constraints, the GSS described in Section 4 will not be built during Phase II. Nonetheless, at the end of Phase II, an operational prototype system will exist which can be used in both long and short range field studies.

For applications of the PLT involving more than a few single-balloon experiments, it would be cost-effective to proceed to Phase III: Building the Ground Support Station as described in Section 4, and carrying out systems tests with commercially-produced PLT payloads. Routine or major use of the PLT system will require a commercial source for PLT payloads, and the capabilities represented by the GSS.

Parallel to the systems development work described above, we are also tasked to conceive, develop, and propose appropriate applications for the balloon tracer system. Only one will be discussed here.

To date, most thought has been given to using the tracer to investigate long range transport -- specifically, source-receptor relationships, intrinsic limits on predictability,

and transport model verification. These applications are indeed important, but less thought has been given to use of the system in the investigation of the chemical and physical transformations relevant to long range air pollution. In such studies, it would be extremely helpful to be able to follow the processes in a Lagrangian frame. It has long been recognized that such a frame is a natural choice for investigation of pollutant behavior (Seinfeld et al, 1973), but only a few such studies have in fact been done (Zak, 1983). This is the case because the technology has not been available to support Lagrangian studies. By the end of Phase II, it will be.

For example, once the operational PLT exists, it would be quite simple to put a transponder on board which would permit an aircraft in the area to range on the balloon -- perhaps using an inexpensive distance-finding system such as that manufactured by Meeda Instrumentation (Meeda, no date) for use as a balloon radio altimeter, or alternately, using an airborne radar.

Once having a means of measuring the distance to the balloon, an aircraft instrumented to investigate homogenous and heterogenous processes could execute a standard circular path relative to it, perhaps at more than one altitude, every few hours for up to three days (Figure 7-1).

If the balloon had been injected into the plume from a major source -- urban or industrial -- this would provide a means of observing the time-dependent behavior of the source effluents over an extended period of time. Alternately, studies could be done in areas with low background contamination, but with an intentional release of a selected

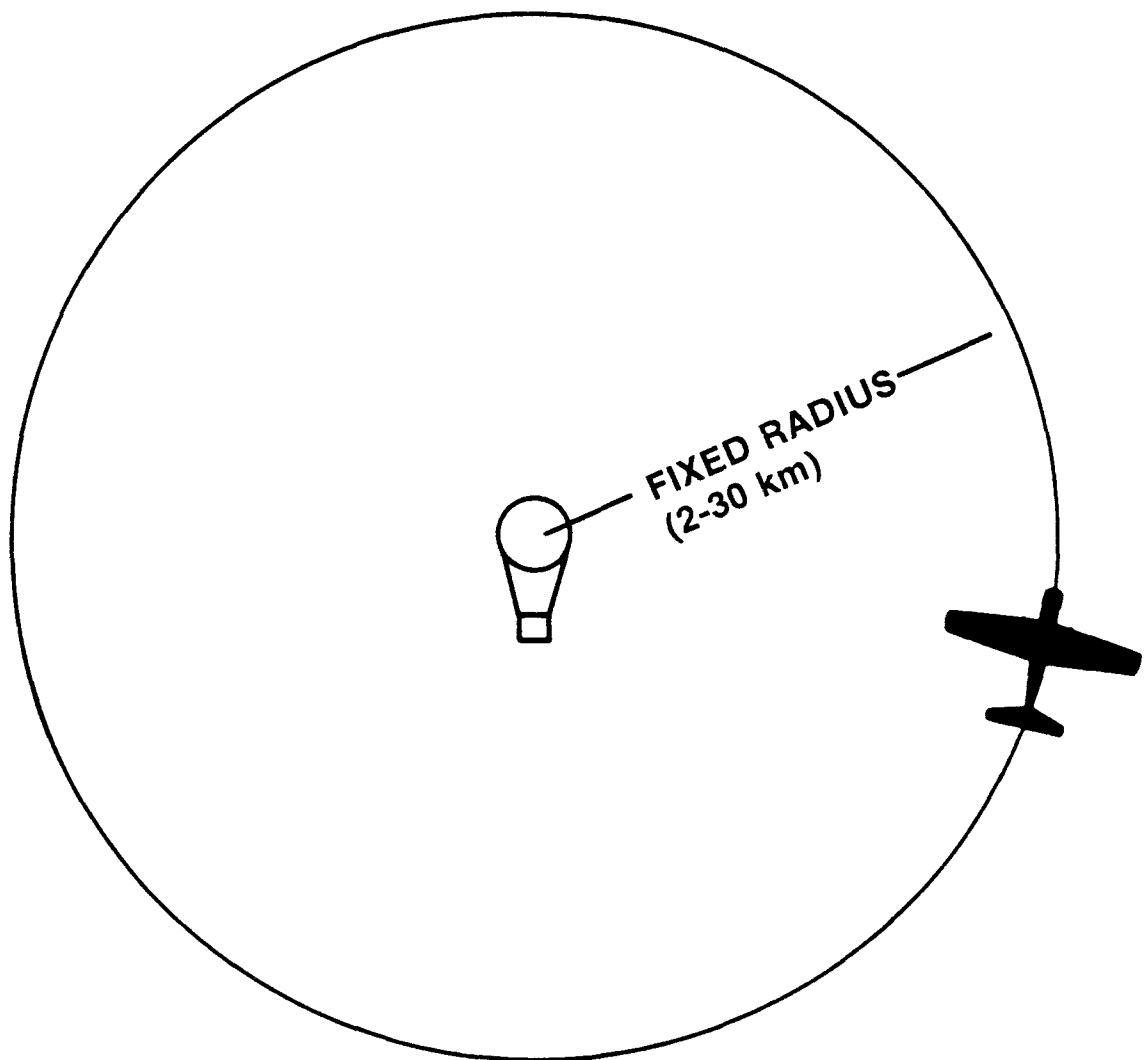


Figure 7-1. Lagrangian experiment instrumented-aircraft measurement pattern. PLT marks mean flow; measurement aircraft periodically executes pattern relative to marker at 2-4 altitudes.

mix of pollutants around the balloon. The subsequent behavior of those effluents could be observed with instrumented aircraft as well, albeit for a shorter period. The PLT would permit either type of experiment to be done in cloud, perhaps even in rain, as well as in clear air. To some of us concerned with acid deposition, this is an exciting prospect.

## 8. CONCLUSIONS AND DISCUSSION

Now, in light of our theoretical analysis, the experience we have gained in designing and building the testbed prototype PLT, and the experimental results we have obtained with it, we go back and examine the design goals set forth in Section 2.

- Operates under the exemption clauses of FAR 101.

FAR 101 permits up to 12 lbs (5.45 kg) of payload, as long as the payload is distributed in packages weighing no more than 6 lbs (2.73 kg) each, which meet the 3 oz/in<sup>2</sup> areal density limit. The current testbed prototype payload weighs about 2.36 kg including batteries, and meets the areal density limits. The operational PLT payload could be twice as large, and as long as care were exercised in its design, it would still satisfy the exemption provisions of FAR 101.

- Lifetime  $\geq$  3 days.

The pair of Gilian pumps which yield adequate pumpdown speed consume 2-2.5 watts total power when pumping. If the pumps operated 50% of the time during a 72-hour experiment, they would consume 90 watt hours of energy. At lithium battery energy densities of 100-200 watt hrs/lb, this would take less than one pound of batteries. Even with three pumps operating

more than 50% of the time, the battery weight required would likely be acceptable. Thus, as long as the remainder of the payload is designed so that it uses no more than the pumps, power should not be a problem for 3 day experiments.

- Tracking range > 1000 km in the northeast quadrant of the United States.

ARGOS tracks worldwide.

- Telemetry of relative vertical air motion, pressure, temperature, and humidity.

ARGOS data handling can easily accommodate these and the several other parameters it would be desirable to transmit. If continuous data are needed, a regional/hybrid system can provide it at additional cost for a network of ground stations equipped with ARGOS uplink receivers.

- Ground system capable of handling several PLTs at a time.

ARGOS can handle 200 PTTs in its field of view simultaneously.

- Capable of establishing specified ascent and descent rates under radio command.

A 2-site, 2-band HF radio command system should offer reliable command capability. Command technology is well developed.

- Capable of reaching altitudes up to 500 mb (5.5 km).

Our calculations indicate that would not be a problem for the testbed prototype PLT. As long as the balloon is properly

designed and filled for the desired ceiling altitude, and the operational PLT payload weight, it should not be a problem.

- Capable of following mean vertical flows as low as 1 cm/s with "acceptable" fidelity.

Under standard atmosphere conditions, we've shown theoretically that a trajectory based on potential temperature meets that specification (Appendix G). We've shown that the testbed prototype buoyancy control system is capable of handling mean vertical flows as high as 10 cm/s on average, which equals or exceeds expected long-term average vertical air speeds, and that higher speeds can be accommodated. However, in the mixed layer, potential temperature is not a good control parameter. During convective mixing, it would be necessary to go to some other control strategy. We also put forward an argument that in a mixed layer, because of the rapid spread of effluents throughout the layer, the exact position of the balloon tracer within the layer is not important. The conclusion is that this design goal can be met most of the time, and when it cannot with the potential temperature control strategy because of mixing, it doesn't matter. This point, and the meaning of "acceptable" fidelity, are discussed in detail in Appendix J.

- Sufficiently inexpensive to permit use in significant numbers on an expendable basis.

This goal is somewhat elastic, in that it depends upon the budgetary constraints in existence at a given time. We choose to address it by considering the likely cost of the elements of the operational PLT in small numbers (1-10) and in large (>50).

<u>Cost Elements</u>	<u>1-10 (ea)</u>	<u>Cost (\$K)*</u>	<u>&gt;50 (ea)</u>
CVB with Ballonet	1.5		1.0
Buoyancy Adjustment Subsystem	0.5		0.3
Sensors	1.2		0.7
Microcomputer	1.0		0.7
ARGOS Telemetry	1.3		0.8
Command Receiver and Decoder	0.7		0.5
Tracking Aids, including FAA Transponder	1.3		0.9
Batteries	0.1		0.1
Assembly Labor	<u>1.0</u>		<u>0.5</u>
	\$8.6K		\$5.5K

\*CY84 dollars.

The costs in quantity are approximate and merely project typical quantity procurement savings. Assuming these for the near future, one can make a reasonable estimate of the cost per use. V. E. Lally indicates that balloon payloads carrying a simple message to return to a stated address have better than a 50% return rate in the Continental U.S. If a reward is offered for return, an even higher return rate could be obtained. We ignore that to allow for damage on the returned payloads. On the other hand, the balloon itself must be considered expended on each use. With these assumptions, in quantity, the PLTs would cost approximately \$3.2 K per use. This cost does not seem to prohibit use in significant numbers on an "expendable" basis. For the longer term, more dramatic cost savings are likely to come about if continual use occurs, much as they have for tethersonde payloads, which underwent a factor of three reduction in cost over several years.

In summary, the authors are confident in concluding that an adjustable buoyancy physical Lagrangian tracer meeting the



stated design goals is both technically and economically feasible. We are proceeding in Phase II to turn that conviction into operational hardware.

## REFERENCES

- Barat, J. (1982). "Initial Results from the Use of Ionic Anemometers Under Stratospheric Balloons: Applications to the High-Resolution Analysis of Stratospheric Motions," J. Appl. Meteor. 21, 1489.
- Blamont, J., Heinsheimer, T., and Pommereau, J. (1974). "New Method of Study of the Dynamics of the Stratosphere - Principle and First Results," Academie des Sciences (Paris), Comptes Rendus (B) 228, 249.
- Boas, M. L. (1966). Mathematical Methods in the Physical Sciences, John Wiley and Sons, New York.
- Chiang, T., Ossin, A., Tien, C. L. (1964). "Laminar Free Convection from a Sphere," J. Heat Transfer, 537.
- Danielson, E.F. (1961). "Trajectories: Isobaric, Isentropic, and Actual," J. Meteor. 18, 479.
- Gay, G.T., Zak, B.D., Barker, B., Holland, R.M., and Homann, P.S. (1981). Lagrangian Measurement Platform Flights in Support of the Tennessee Plume Study: Field Effort and Data, Sandia National Laboratories Report SAND79-1336, Albuquerque, NM.
- Gill, G.C. (1979). Personal communication with V.E. Lally.
- Holton, J.R. (1979). An Introduction to Dynamic Meteorology, Second Edition, Academic Press, New York, NY.
- Lally, V.E. (1967). "Superpressure Balloons," in Scientific Ballooning Handbook, A. L. Morris, Ed., National Center for Atmospheric Research Technical Note NCAR-TN/IA-99, Boulder, CO.
- Lally, V.E. (1975). Superpressure Balloons for Horizontal Soundings of the Atmosphere, National Center for Atmospheric Research Technical Note NCAR-TN-28, Boulder, CO.
- Lally, V. E. (1985). Personal communication.
- Lamb, R. G. (1984). "Air Pollution Models as Descriptors of Cause-Effect Relationships," Atmos. Environ. 18, 591.
- Lichfield, E. (1981) "Tracking and Communication in Long Duration Flights," COSPAR Session on Scientific Ballooning.

MacCready, P. B., Baboolal, L. A., Lissamen, P.B.S. (1974). "Diffusion and Turbulence Aloft over Complex Terrain," in preprint volume, Symposium on Atmospheric Diffusion and Air Pollution, Santa Barbara, CA, Sept. 9-13. Amer. Meteor. Soc. 218-225.

MacCready, P.B., and Mullen, J.B. (1977). Turbulence Investigation on DaVinci II, AeroVironment Report No. AVFR 7141, Pasadena, CA.

MacCready, P.B. (1981). "Turbulence and the Local Flow Field. The AV Experiment on DaVinci I", in Final Report on Project DaVinci: A Study of Long Range Air Pollution Using A Balloon-Borne Lagrangian Measurement Platform, Vol. 2: Reports of Participants in DaVinci I, Sandia National Laboratories Report SAND78-0403/2, Albuquerque, NM.

Margolin, B. (1982). "Paper Thin Lithium Battery Powers Handheld Electronics," Electronic Products, March 26, 1982.

Meeda Scientific Instrumentation (no date). "Series 200 Balloon-Borne Radio Altimeter," Romat-Gan, Israel.

Morris, A.L. (1975). Scientific Ballooning Handbook, National Center for Atmospheric Research Technical Note NCAR-TN/IA-99, Boulder, CO.

Morris, A.L. and Solot, S.B. (1975). "The Atmosphere," in Scientific Ballooning Handbook, A. L. Morris, Ed., National Center for Atmospheric Research Technical Note NCAR-TN/IA-99, Boulder, CO.

NCAR, Atmospheric Technology, periodical published by the National Center for Atmospheric Research, Boulder, CO.

Reif, F. (1965). Fundamentals of Statistical and Thermal Physics, McGraw-Hill, New York.

Schlichting, H. (1979). Boundary Layer Theory, Seventh Edition, Translated by J. Kestin, McGraw-Hill, New York, p. 238.

Seinfeld, J.H., Hecht, T.A., and Roth, P.M. (1973). Existing Needs in the Observational Study of Atmospheric Chemical Reactions, U.S.E.P.A. Report EPA-R4-73-031.

Tatom, F.B. and King, R.L. (1977). Constant Volume Balloon Capabilities for Aeronautical Research, NASA Contractor Report NASA CR-2805, Huntsville, AL.

Wallace, J.M. and Hobbs, P.V. (1977). Atmospheric Science, an Introductory Survey, Academic Press, New York, NY.

Zak, B.D. (1981a). Final Report on Project DaVinci: A Study of Long Range Air Pollution Using A Balloon-Borne Lagrangian Measurement Platform, Vol. 1: Overview and Data Analysis, Sandia National Laboratories Report SAND78-0403/1, Albuquerque, NM.

Zak, B.D. (1981b). "Lagrangian Measurements of Sulfur Dioxide to Sulfate Conversion Rates," Atmos. Environ. 15, 2583.

Zak, B.D. (1983). "Lagrangian Studies of Atmospheric Pollutant Transformations," in Trace Atmospheric Constituents: Properties, Transformations, and Fates, Volume 12 in series, Advances in Environmental Science and Technology. S.E. Schwartz, Ed., John Wiley and Sons, New York, NY.

## APPENDIX A

### FEDERAL AVIATION REGULATIONS PART 101: MOORED BALLOONS, KITES, UNMANNED ROCKETS, AND UNMANNED FREE BALLOONS

The following is a reprint of the FAA regulation most relevant to the adjustable buoyancy balloon.

## **Part 101—Moored Balloons, Kites, Unmanned Rockets, and Unmanned Free Balloons**

### **Subpart A—General**

#### **§101.1 Applicability.**

(a) This Part prescribes rules governing the operation, in the United States, of the following:

(1) Except as provided for in § 101.7 of this Part, any balloon that is moored to the surface of the earth or an object thereon and that has a diameter of more than 6 feet or a gas capacity of more than 115 cubic feet.

(2) Except as provided for in § 101.7 of this Part, any kite that weighs more than 5 pounds and is intended to be flown at the end of a rope or cable.

(3) Any unmanned rocket except—

- (i) Aerial firework displays; and
- (ii) Model rockets—

(a) Using not more than 4 ounces of propellant;

(b) Using a slow-burning propellant;

(c) Made of paper, wood, or breakable plastic, containing no substantial metal parts and weighing not more than 16 ounces, including the propellant; and

(d) Operated in a manner that does not create a hazard to persons, property, or other aircraft.

(4) Except as provided for in § 101.7 of this Part, any unmanned free balloon that—

(i) Carries a payload package that weighs more than four pounds and has a weight/size ratio of more than three ounces per square inch on any surface of the package, determined by dividing the total weight in ounces of the payload package by the area in square inches of its smallest surface;

(ii) Carries a payload package that weighs more than 6 pounds;

(iii) Carries a payload of two or more packages, that weighs more than 12 pounds; or

(iv) Uses a rope or other device for suspension of the payload that requires an impact force of more than 50 pounds to separate the suspended payload from the balloon.

(b) For the purposes of this Part, a “gyroglider” attached to a vehicle on the surface of the earth is considered to be a kite.

#### **§101.3 Waivers.**

No person may conduct operations that require a deviation from this Part except under a certificate of waiver issued by the Administrator.

#### **§101.5 Operations in prohibited or restricted areas.**

No person may operate a moored balloon, kite, unmanned rocket, or unmanned free balloon in a prohibited or restricted area unless he has permission from the using or controlling agency, as appropriate.

#### **§ 101.7 Hazardous operations.**

[(a) No person may operate any moored balloon, kite, unmanned rocket, or unmanned free balloon in a manner that creates a hazard to other persons, or their property.

[(b) No person operating any moored balloon, kite, unmanned rocket, or unmanned free balloon may allow an object to be dropped therefrom, if such action creates a hazard to other persons or their property.]

### **Subpart B—Moored Balloons and Kites**

#### **§101.11 Applicability.**

This subpart applies to the operation of moored balloons and kites. However, a person

operating a moored balloon or kite within a restricted area must comply only with §101.19 and with additional limitations imposed by the using or controlling agency, as appropriate.

#### **§101.13 Operating limitations.**

(a) Except as provided in paragraph (b) of this section, no person may operate a moored balloon or kite—

- (1) Less than 500 feet from the base of any cloud;
- (2) More than 500 feet above the surface of the earth;
- (3) From an area where the ground visibility is less than three miles; or
- (4) Within five miles of the boundary of any airport.

(b) Paragraph (a) of this section does not apply to the operation of a balloon or kite below the top of any structure and within 250 feet of it, if that shielded operation does not obscure any lighting on the structure.

#### **§101.15 Notice requirements.**

No person may operate an unshielded moored balloon or kite more than 150 feet above the surface of the earth unless, at least 24 hours before beginning the operation, he gives the following information to the FAA ATC facility that is nearest to the place of intended operation:

- (a) The names and addresses of the owners and operators.
- (b) The size of the balloon or the size and weight of the kite.
- (c) The location of the operation.
- (d) The height above the surface of the earth at which the balloon or kite is to be operated.
- (e) The date, time, and duration of the operation.

#### **§101.17 Lighting and marking requirements.**

(a) No person may operate a moored balloon or kite [between sunset and sunrise] unless the balloon or kite, and its mooring lines, are lighted so as to give a visual warning equal to that required for obstructions to air navigation in the FAA publication "Obstruction Marking and Lighting".

(b) No person may operate a moored balloon or kite [between sunrise and sunset] unless its mooring lines have colored pennants or streamers attached at not more than 50-foot intervals beginning at 150 feet above the surface of the earth and visible for at least one mile.

#### **§101.19 Rapid deflation device.**

No person may operate a moored balloon unless it has a device that will automatically and rapidly deflate the balloon if it escapes from its moorings. If the device does not function properly, the operator shall immediately notify the nearest ATC facility of the location and time of the escape and the estimated flight path of the balloon.

### **Subpart C—Unmanned Rockets**

#### **§101.21 Applicability.**

This subpart applies to the operation of unmanned rockets. However, a person operating an unmanned rocket within a restricted area must comply only with subparagraph 101.23 (g) and with additional limitations imposed by the using or controlling agency, as appropriate.

#### **§101.23 Operating limitations.**

No person may operate an unmanned rocket—

- (a) In a manner that creates a collision hazard with other aircraft;
- (b) In controlled airspace;
- (c) Within five miles of the boundary of any airport;
- (d) At any altitude where clouds or obscuring phenomena of more than five-tenths coverage prevails;
- (e) At any altitude where the horizontal visibility is less than five miles;
- (f) Into any cloud;
- (g) Within 1,500 feet of any person or property that is not associated with the operations; or
- (h) [Between sunset and sunrise.]

#### **§101.25 Notice requirements.**

No person may operate an unmanned rocket unless, within 24 to 48 hours before beginning the operation, he gives the following info.ma-

tion to the FAA ATC facility that is nearest to the place of intended operation:

- (a) The names and addresses of the operators.
- (b) The number of rockets to be operated.
- (c) The size and weight of each rocket.
- (d) The maximum altitude to which each rocket will be operated.
- (e) The location of the operation.
- (f) The date, time, and duration of the operation.
- (g) Any other pertinent information requested by the ATC facility.

#### **Subpart D—Unmanned Free Balloons**

##### **§ 101.31 Applicability.**

This subpart applies to the operation of unmanned free balloons. However, a person operating an unmanned free balloon within a restricted area must comply only with § 101.33 (d) and (e) and with any additional limitations that are imposed by the using or controlling agency, as appropriate.

##### **§ 101.33 Operating limitations.**

No person may operate an unmanned free balloon—

- (a) Unless otherwise authorized by ATC, in a control zone below 2,000 feet above the surface, or in an airport traffic area;
- (b) At any altitude where there are clouds or obscuring phenomena of more than five-tenths coverage,
- (c) At any altitude below 60,000 feet standard pressure altitude where the horizontal visibility is less than five miles;
- (d) During the first 1,000 feet of ascent, over a congested area of a city, town or settlement or an open-air assembly of persons not associated with the operation; or
- (e) In such a manner that impact of the balloon, or part thereof including its payload, with the surface creates a hazard to persons or property not associated with the operation.

##### **§ 101.35 Equipment and marking requirements.**

(a) No person may operate an unmanned free balloon unless—

- (1) It is equipped with at least two payload cut-down systems or devices that operate independently of each other;
- (2) At least two methods, systems, devices, or combinations thereof, that function independently of each other are employed for terminating the flight of the balloon envelope; and
- (3) The balloon envelope is equipped with a radar reflective device(s) or material that will present an echo to surface radar operating in the 200 MHz to 2700 MHz frequency range.

The operator shall activate the appropriate devices required by subparagraphs (1) and (2) of this paragraph when weather conditions are less than those prescribed for operation under this subpart, or if a malfunction or any other reason makes the further operation hazardous to other air traffic or to persons and property on the surface.

[(b) No person may operate an unmanned free balloon below 60,000 feet standard pressure altitude between sunset and sunrise (as corrected to the altitude of operation) unless the balloon and its attachments and payload, whether or not they become separated during the operation, are equipped with lights that are visible for at least 5 miles and have a flash frequency of at least 40, and not more than 100, cycles per minute.]

(c) No person may operate an unmanned free balloon that is equipped with a trailing antenna that requires an impact force of more than 50 pounds to break it at any point, unless the antenna has colored pennants or streamers that are attached at not more than 50-foot intervals and that are visible for at least one mile.

(d) No person may operate [between sunrise and sunset] an unmanned free balloon that is equipped with a suspension device (other than a highly conspicuously colored open parachute) more than 50 feet long, unless the



suspension device is colored in alternate bands of high conspicuity colors or has colored pennants or streamers attached which are visible for at least one mile.

#### § 101.37 Notice requirements.

(a) *Prelaunch notice.* Except as provided in paragraph (b) of this section, no person may operate an unmanned free balloon unless, within 6 to 24 hours before beginning the operation, he gives the following information to the FAA ATC facility that is nearest to the place of intended operation:

- (1) The balloon identification.
- (2) The estimated date and time of launching, amended as necessary to remain within plus or minus 30 minutes.
- (3) The location of the launching site.
- (4) The cruising altitude.
- (5) The forecast trajectory and estimated time to cruising altitude or 60,000 feet standard pressure altitude, whichever is lower.
- (6) The length and diameter of the balloon, length of the suspension device, weight of the payload, and length of the trailing antenna.
- (7) The duration of flight.
- (8) The forecast time and location of impact with the surface of the earth.

(b) For solar or cosmic disturbance investigations involving a critical time element, the information in paragraph (a) of this section shall be given within 30 minutes to 24 hours before beginning the operation.

(c) *Cancellation notice.* If the operation is canceled, the person who intended to conduct the operation shall immediately notify the nearest FAA ATC facility.

(d) *Launch notice.* Each person operating an unmanned free balloon shall notify the nearest FAA or military ATC facility of the launch time immediately after the balloon is launched.

#### § 101.39 Balloon position reports.

(a) Each person operating an unmanned free balloon shall—

- (1) Unless ATC requires otherwise, monitor the course of the balloon and record its position at least every two hours; and
- (2) Forward any balloon position reports requested by ATC.

(b) One hour before beginning descent, each person operating an unmanned free balloon shall forward to the nearest FAA ATC facility the following information regarding the balloon:

- (1) The current geographical position.
- (2) The altitude.
- (3) The forecast time of penetration of 60,000 feet standard pressure altitude (if applicable).
- (4) The forecast trajectory for the balance of the flight.
- (5) The forecast time and location of impact with the surface of the earth.

(c) If a balloon position report is not recorded for any two-hour period of flight, the person operating an unmanned free balloon shall immediately notify the nearest FAA ATC facility. The notice shall include the last recorded position and any revision of the forecast trajectory. The nearest FAA ATC facility shall be notified immediately when tracking of the balloon is re-established.

(d) Each person operating an unmanned free balloon shall notify the nearest FAA ATC facility when the operation is ended.

## APPENDIX B

### PUMPDOWN SPEED IN A STANDARD ATMOSPHERE

The net buoyant force  $F_b$  on the balloon system is given by:

$$F_b = [V\rho_a - V\rho_b - m] g \quad (B-1)$$

where  $V$  = volume of balloon system ( $m^3$ )  
(presumed constant),

$\rho_a$  = density of the ambient air at the  
altitude of the system ( $kg/m^3$ ),

$\rho_b$  = average density of gas contained in  
balloon,

$m$  = mass of balloon system exclusive of gas  
in balloon,

$g$  = acceleration due to gravity.

At the system's equilibrium altitude, the net buoyant force is zero, so:

$$V\rho_a = V\rho_b + m \quad (B-2)$$

If we pump air into the superpressure balloon for time  $dt$ , we add to the contained mass  $S\rho_a dt$  (where  $S$  is the pumping speed in  $m^3/s$ ), and hence change its density, so

$$d\rho_b = \frac{S\rho_a}{V} dt \quad (B-3)$$

But if we take the differential of Equation B2, we see

$$d\rho_a = d\rho_b \quad (B-4)$$

$$d\rho_a = \frac{S\rho_a}{V} dt \quad (B-5)$$

Assuming a standard atmosphere below the tropopause  
(Morris, 1975):

$$\rho_a = \rho_o \left[ 1 - \frac{\alpha}{T_o} z \right]^{\frac{Mg}{\alpha R} - 1} \quad (B-6)$$

where

$\rho_o$	=	1.2250 kg/m <sup>3</sup> ,
$M$	=	28.96 kg/(kg - mol), average molecular weight of air,
$g$	=	9.807 m/s <sup>2</sup> ,
$\alpha$	=	6.5 x 10 <sup>-3</sup> K/m, standard lapse rate,
$R$	=	8314.3 J/ K (kg - mol), universal gas constant; if pressures expressed in mb, then 83.143,
$\frac{Mg}{\alpha R}$	=	5.255,
$T_o$	=	288.15 K,
$z$	=	height in m MSL, or more strictly, "geopotential meters".

we can evaluate  $d\rho_a$ :

$$d\rho_a = \rho_o \left( -\frac{\alpha}{T_o} \right) \left[ \frac{Mg}{\alpha R} - 1 \right] \left[ 1 - \frac{\alpha}{T_o} z \right]^{\frac{Mg}{\alpha R} - 2} dz \quad (B-7)$$

Substituting this expression into Equation B5, and solving for  $dz/dt$ , we find:

$$\frac{dz}{dt} = \frac{-1}{(\alpha/T_o)} \frac{1}{(Mg/\alpha R - 1)} \frac{S}{V} \left( 1 - \frac{\alpha}{T_o} z \right) \quad (B-8)$$

or

$$v_p = \frac{dz}{dt} = -1.042 \times 10^4 \frac{S}{V} (1 - 2.256 \times 10^{-5} z) \quad (B-9)$$

## APPENDIX C

### SUPERPRESSURE AS A FUNCTION OF EQUILIBRIUM ALTITUDE

By definition, superpressure is given by

$$P_s = P_b - P_a \quad (C-1)$$

where  $P_b$  is the absolute pressure in the balloon, and  $P_a$  is the ambient pressure of the air at the balloon altitude.

$P_b(z)$  is given by the gas law coupled with the expression for temperature variation in a standard atmosphere:

$$P_b = \frac{\rho}{M_b} RT = \frac{n_b}{V} RT = \frac{n_b}{V} RT_0 \left(1 - \frac{\alpha}{T_0} z\right) \quad (C-2)$$

where  $n_b$  = total number of kg-moles of gas in the balloon (air and helium),  
 $M_b$  = average molecular weight of gas in balloon,  
 $T$  = temperature in K.

In a standard atmosphere,

$$P_a = P_0 \left(1 - \frac{\alpha}{T_0} z\right)^{\frac{Mg}{\alpha R}} \quad (C-3)$$

Here  $P_0 = 1013$  millibars or  $1.013 \times 10^5 \text{ N/m}^2$ .

In order to evaluate  $P_s$ , we need  $n_b(z)$ .

We have:

$$n_b = n_a + n_{\text{He}} \quad (C-4)$$

$n_a$  = kg-moles of air in balloon,

$n_{He}$  = kg-moles of helium in balloon.

In valving and pumping operations, only the quantity of air in the balloon is affected, not the helium. Hence, differentiating Equation C-4:

$$\frac{dn_b}{dz} = \frac{dn_a}{dz} \quad (C-5)$$

we can obtain  $n_a$  from the buoyancy condition, Equation B-2, if we note that

$$V\rho_b = n_a M + n_{He} M_{He} \quad (C-6)$$

where

$M_{He}$  = Molecular weight of helium  
(4 kg/[kg - mol]).

Then we find:

$$V\rho_a = n_a M + n_{He} M_{He} + m \quad (C-7)$$

If we differentiate this expression:

$$V \frac{d\rho_a}{dz} = M \frac{dn_a}{dz} \quad (C-8)$$

Thus

$$\frac{dn_b}{dz} = \frac{dn_a}{dz} = \frac{V}{M} \frac{d\rho_a}{dz} \quad (C-9)$$

and

$$n_b(z) = \frac{V}{M} \rho_a(z) + C \quad (C-10)$$

where C is an integration constant to be determined from a boundary condition. Combining Equations C1, C2 and C3 with 10:

$$P_s = \frac{RT_o}{V} \left(1 - \frac{\alpha}{T_o} z\right) \left[ \frac{V}{M} \rho_o \left(1 - \frac{\alpha}{T_o} z\right)^{\frac{Mg}{\alpha R} - 1} + C \right] - P_o \left(1 - \frac{\alpha}{T_o} z\right)^{\frac{Mg}{\alpha R}} \quad (C-11)$$

Expanding and collecting terms:

$$P_s = \left( \frac{RT_o \rho_o}{M} - P_o \right) \left(1 - \frac{\alpha}{T_o} z\right)^{\frac{Mg}{\alpha R}} + \frac{CRT_o}{V} \left(1 - \frac{\alpha}{T_o} z\right) \quad (C-12)$$

The quantity in the first parenthesis is zero by the gas law.  
Hence:

$$P_s = \frac{CRT_o}{V} \left(1 - \frac{\alpha}{T_o} z\right) \quad (C-13)$$

To express pressures in millibar, we take  $R = 83.14$ ;  
then

$$P_s = 2.396 \times 10^4 \frac{C}{V} (1 - 2.256 \times 10^{-5} z) \quad (C-14)$$

and

$$\frac{dP_s}{dz} = -.541 \frac{C}{V} \quad (C-15)$$

Using the expression for  $P_s$ , one can evaluate  $C$ .

$$C = \frac{VP_{so}}{2.396 \times 10^4 (1 - 2.256 \times 10^{-5} z_o)} \quad (C-16)$$

where  $P_{so}$  is the initial superpressure at some initial height  $z_o$ .

## APPENDIX D

### EFFECT OF TEMPERATURE SWING ON BALLOON PRESSURE

We may calculate the effect of a swing in balloon temperature caused by a change in the radiation environment from the gas law and Equation C10:

$$P_b = \frac{n_b RT}{V} \quad (D-1)$$

$$\Delta P_b = \frac{n_b R}{V} \Delta T \quad (D-2)$$

$$= \left[ \frac{\rho_a}{M} + \frac{C}{V} \right] R \Delta T \quad (D-3)$$

$$= R \Delta T \left[ \frac{1}{M} \rho_o \left( 1 - \frac{\alpha}{T_o} z \right)^{\frac{Mg}{\alpha R}} + \frac{C}{V} \right] \quad (D-4)$$

$$\Delta P = 3.52 \left[ (1 - 2.256 \times 10^{-5} z)^{4.255} + 83.14 \frac{C}{V} \right] \Delta T \quad (D-5)$$

## APPENDIX E

### ENERGY REQUIRED FOR PUMPDOWN

The incremental work done in bringing about a change in volume of gas  $dV$  is:

$$dW = P dV \quad (E-1)$$

$$= P \frac{dV}{dt} dt \quad (E-2)$$

for our system  $P = P_s$ , but  $P_s$  must be expressed in newtons/m<sup>2</sup>, where

$$1 \text{ mb} = 100 \text{ N/m}^2 \quad (E-3)$$

We interpret  $dV/dt$  as the pumping speed  $S$ . Then, choosing to keep  $P_s$  in mb, we have

$$dW = 100 P_s S dt \quad (E-4)$$

or

$$\frac{dW}{dz} = 100 P_s S \frac{dt}{dz} \quad (E-5)$$

finally

$$\frac{dW}{dz} = 100 \frac{P_s S}{v_p} \quad (E-6)$$

where  $v_p$  is the pumpdown speed. Combining with Equations B9 and C14, we obtain

$$\frac{dW}{dz} = 2.30 \times 10^2 C \quad (E-7)$$



Using Equation C14 to evaluate C, assuming some specified superpressure  $P_{so}$  at a specified altitude  $z_o$ , we find

$$\frac{dW}{dz} = \frac{9.60 \times 10^{-3} P_{so} V}{(1 - 2.256 \times 10^{-5} z_o)} \quad (E-8)$$

## APPENDIX F

### LIFT AND MAXIMUM ALTITUDE

During filling, initially one puts helium into the inner balloon. The lift  $L$  generated is

$$L = V' (\rho_a - \rho_{\text{He}}) g \quad (\text{F-1})$$

where  $\rho_a$  and  $\rho_{\text{He}}$  are the densities of air and helium respectively at the fill altitude, and  $V'$  is the volume of helium put into the balloon, and hence the (slack) volume of the balloon. Note that

$$\rho_a = \frac{n_a M}{V'} \quad \text{and} \quad \rho_{\text{He}} = \frac{n_{\text{He}} M_{\text{He}}}{V'} \quad (\text{F-2})$$

where  $n_a$  and  $n_{\text{He}}$  are the number of moles of air displaced, and the number of moles of helium occupying the volume  $V'$  respectively, and  $M$  and  $M_{\text{He}}$  are the molecular weights of air and helium respectively. However, since the balloon is slack, and the helium is presumed to be at ambient temperature,

$$n_a = n_{\text{He}} \quad (\text{F-3})$$

Thus

$$L = n_{\text{He}} (M - M_{\text{He}}) g \quad (\text{F-4})$$

So the lift from a slack (zero superpressure) balloon in thermal equilibrium with the ambient air is a function only of the number of moles of helium it contains.

One needs to put in enough helium to generate lift not only to carry the combined mass  $m$  of the balloon and payload, but also to carry the weight of excess air required to generate the desired amount of superpressure  $P_s$  at the surface where balloon fill is taking place. Thus, the

required lift is given by

$$L_R = (m + \Delta n M)g \quad (F-5)$$

where  $\Delta n$  is the number of moles of excess air. The term  $\Delta n$  can be obtained from application of the gas law. When the balloon is superpressured, the volume of the rigid balloon becomes  $V$ , and:

$$P_s V = \Delta n RT \quad (F-6)$$

so,

$$L_R = m + M \frac{P_s V}{RT} g \quad (F-7)$$

Thus, to fill the balloon properly, one first puts in helium until the gross lift is measured to be  $L_R$  as given by (F-7). Then, one seals the inner balloon, and inflates the outer balloon with air, until the desired superpressure  $P_s$  is reached. At that point, the balloon system, after attachment of the payload, should be approximately neutrally buoyant.

The question next arises as to what the ceiling altitude of this balloon system is. At maximum altitude, all of the air ballast will have been vented, leaving the balloon entirely filled with helium. Thus, at maximum altitude, the equilibrium condition becomes

$$V\rho_a = V\rho_{He} + m \quad (F-8)$$

but

$$V\rho_{He} = n_{He}M_{He} \quad (F-9)$$

Here  $n_{\text{He}}$  can be obtained by equating lift with required lift. From (F-4) and (F-7):

$$n_{\text{He}} (M - M_{\text{He}}) = m + M \frac{P_s V}{RT} \quad (\text{F-10})$$

$$n_{\text{He}} = \frac{m + M \frac{P_s V}{RT}}{M - M_{\text{He}}} \quad (\text{F-11})$$

So (F-8) becomes

$$V \rho_a = M_{\text{He}} n_{\text{He}} + m \quad (\text{F-12})$$

However, in a standard atmosphere (Equation B-6),

$$\rho_a = 1.2250 (1 - 2.256 \times 10^{-5} z)^{4.255} \quad (\text{F-13})$$

Substituting (F-13) into (F-12), one obtains

$$(1 - 2.256 \times 10^{-5} z_m)^{4.255} = \frac{n_{\text{He}} M_{\text{He}} + m}{1.255 V} \quad (\text{F-14})$$

where here  $z_m$  = maximum obtainable height.

$$1 - 2.256 \times 10^{-5} z_m = \left[ \frac{n_{\text{He}} M_{\text{He}} + m}{1.255 V} \right]^{0.2350} \quad (\text{F-15})$$

$$z_m = \frac{1}{2.256 \times 10^{-5}} \left[ 1 - \left( \frac{n_{\text{He}} M_{\text{He}} + m}{1.255 V} \right)^{0.2350} \right] \quad (\text{F-16})$$

This is the ceiling altitude.

## APPENDIX G

### TRAJECTORIES: ISENTROPIC AND ACTUAL

This discussion is based upon a paper by Danielson (1961). He postulates a balloon which follows an isentropic trajectory. If such a balloon is released from some point, it will in general trace out a somewhat different trajectory than the centroid of the volume of air initially surrounding it. The time-dependent positions of the balloon and the air parcel in which it was originally embedded are given by position vectors in three dimensions. However, the problem can be reduced to two dimensions by considering it in the vertical plane which contains the air parcel, the isentropic balloon, and the difference vector connecting them. In this coordinate system, the horizontal and vertical components,  $r'$  and  $z'$ , of the difference vector are given respectively by:

$$r' = \iint \left[ (W - W_{\theta}) \frac{\partial V}{\partial z} + \left( r' \frac{\partial}{\partial r} + z' \frac{\partial}{\partial z} + \dots \right) \frac{dV}{dt} \right] (dt)^2 \quad (G-1)$$

$$z' = \iint \left[ (W - W_{\theta}) + \left( r' \frac{\partial}{\partial r} + z' \frac{\partial}{\partial z} + \dots \right) W \right] dt \quad (G-2)$$

Here  $V = V(r, z, t)$  and  $W = W(r, z, t)$  are the horizontal and vertical components of the air velocity within the plane, and  $W_{\theta}$  is the vertical velocity of the balloon. The horizontal component of air velocity orthogonal to the plane does not enter. It does not affect horizontal or vertical separation. In (G-1), the horizontal acceleration of the air at the air parcel has been replaced with its Taylor expansion

about the position of the balloon (see Boas, 1966). Similarly in (G-2), the vertical velocity of the air at the air parcel has been replaced by its Taylor expansion about the position of the balloon.  $W$  and all derivatives of  $V$  and  $W$  in both equations are to be evaluated at the balloon position. Higher order terms in the expansions are denoted by dots.

The first term in (G-1) gives the effect of wind shear on horizontal separation; the second term, the effect on horizontal separation of differences in the temporal behavior of the wind at the balloon and at the air parcel. The expression under the integral in (G-2) is equivalent to the difference between the vertical velocity of the air at the air parcel, and the vertical velocity of the balloon.

The dominant terms in (G-1) and (G-2) can be expressed in terms of the diabatic heating rate,  $d\theta/dt$ :

$$(W - W_{\theta}) \frac{\partial V}{\partial z} = \frac{\partial V}{\partial \theta} \frac{d\theta}{dt} \quad (G-3)$$

$$W - W_{\theta} = \frac{\partial z}{\partial \theta} \frac{d\theta}{dt} \quad (G-4)$$

In (G-4), if  $d\theta/dt$  is of order  $1^{\circ}/\text{day}$  ( $1.16 \times 10^{-5} \text{ }^{\circ}/\text{s}$ ), and if  $\partial\theta/\partial z$  is taken as the standard atmosphere value of  $3.3 \times 10^{-3} \text{ }^{\circ}/\text{m}$ , then  $W - W_{\theta}$  becomes  $0.35 \text{ cm/s}$ . This compares with observed vertical velocities relative to isobars more than an order of magnitude higher. Hence, diabatic heating or cooling induces only small changes in vertical velocities. Note that in the absence of diabatic effects, the leading terms in the expression for the separation of an isentropic balloon from the centroid of the corresponding air parcel go to zero.

Danielson goes on to show that isentropic trajectories typically yield differences from actual air parcel trajectories an order of magnitude or more smaller than isobaric trajectories, such as those which CVBs might execute. He also reviews trajectory calculations based on actual meteorological data to illustrate the point. One such case is shown in Figure G-1.

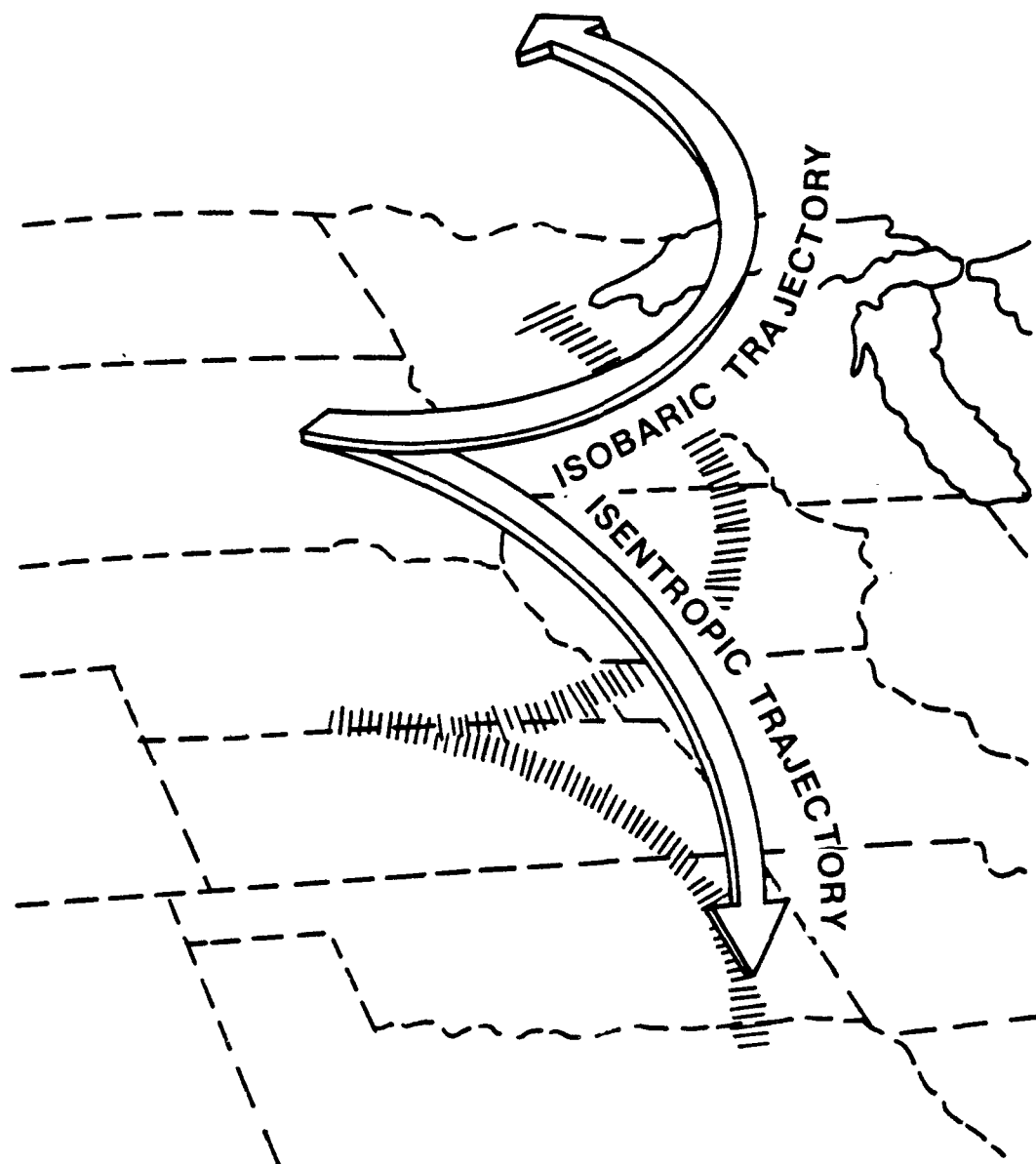


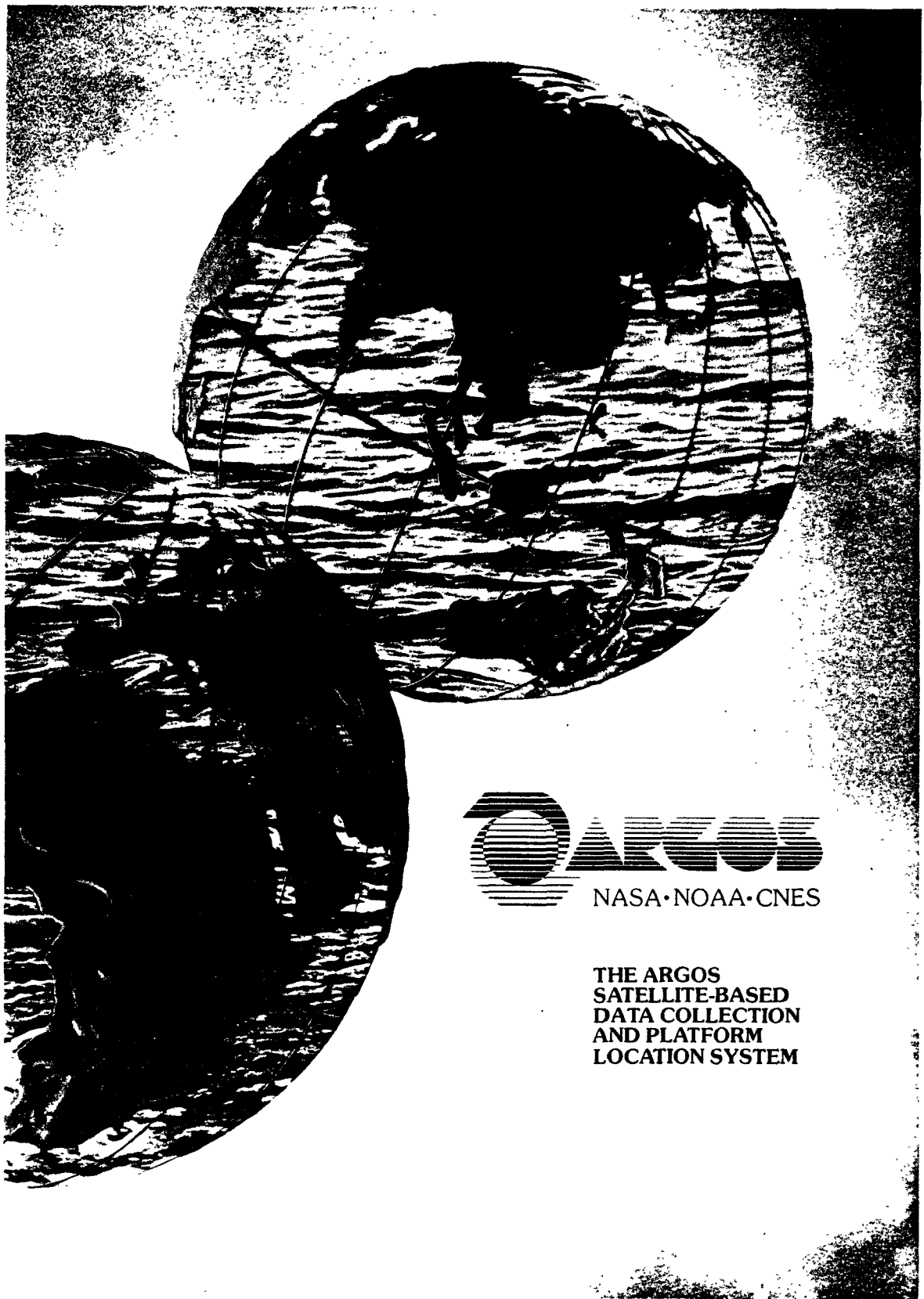
Figure G-1. Comparison of twelve-hour isobaric and isentropic trajectories originating at 700 mb at 0300 GCT 28 March 1956. Horizontal deviation is  $1300 \pm 200$  km. Passive constant volume balloons approximate isobaric trajectories, whereas air parcel trajectories are nearly isentropic.



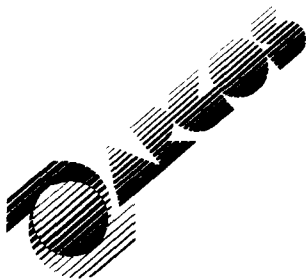
## APPENDIX H

### THE ARGOS SATELLITE-BASED DATA COLLECTION AND PLATFORM LOCATION SYSTEM

A pamphlet describing the ARGOS system is reproduced here courtesy of Service ARGOS.



THE ARGOS  
SATELLITE-BASED  
DATA COLLECTION  
AND PLATFORM  
LOCATION SYSTEM



**SERVICE ARGOS**  
CENTRE NATIONAL D'ETUDES SPATIALES  
18, AVENUE E. BELIN  
31055 TOULOUSE CEDEX - FRANCE  
Tel. (61) 531112 Telex 531081 F

**PRESENTS**  
**THE ARGOS SATELLITE-BASED  
DATA COLLECTION  
AND PLATFORM  
LOCATION SYSTEM**

## contents

<b>3</b>	<b>introduction</b>
<b>4</b>	<b>general description</b>
<b>4</b>	space segment
<b>5</b>	user platforms <ul style="list-style-type: none"><li>• data collection</li><li>• platform location</li></ul>
<b>9</b>	onboard data collection system
<b>9</b>	data processing centers
<b>11</b>	<b>applications of the Argos System</b>
<b>12</b>	<b>Service Argos</b>
<b>12</b>	Users - Service Argos relations

*Ce document a été édité  
par le Centre National  
d'Etudes Spatiales  
Service Argos  
18, avenue Edouard-Belin  
31055 Toulouse cedex*

*La maquette,  
la mise en page et l'illustration  
ont été réalisées  
par MM. François Boitana  
et Jean-Louis Reilles  
1 bis, rue Joseph Mangnac  
31300 St-Martin-du-Touch Toulouse*

*La photocomposition a été réalisée  
par Aquitaine Arts Graphiques  
5, allées de Tourny  
33000 Bordeaux*

*Il a été imprimé  
par l'imprimerie du Sud  
24, rue Négrenays à Toulouse*

*La traduction a été réalisée  
par M. Stephen Dyson*



(CNES) Toulouse  
Space Center  
Service Argos  
building in  
foreground

## introduction

*The Argos data collection and platform location system offers capabilities for the location of fixed and moving platforms and for the collection of sensor data transmitted by platforms located anywhere on the Earth's surface.*

*The Argos System is the fruit of a cooperative project between:*

- *the Centre National d'Etudes Spatiales (CNES, France),*
- *the National Aeronautics and Space Administration (NASA, USA), and*
- *the National Oceanic and Atmospheric Administration (NOAA, USA).*

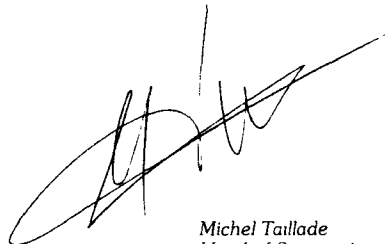
*CNES, NASA and NOAA are bound by a Memorandum of Agreement signed on December 10, 1974 which defines the responsibilities of each agency.*

*CNES, benefitting from the experience acquired in this type of activity through the EOLE program (1970-1974), is the prime contractor for the design, development and operation of the system.*

*The first Argos onboard equipment package (also known as the onboard data collection system or DCS) was carried by the TIROS-N satellite. The ten operational satellites designated NOAA-A thru NOAA-J, each equipped with the Argos DCS, will be launched at such times as to ensure that two operational satellites are available at all times.*

*Continuous service started in 1979 and is expected to continue through until 1990 at least.*

*The Argos System is primarily intended for applications concerned with environmental data collection (i.e. meteorology, oceanography, hydrology, ecology, remote sensing of earth resources, etc.). Satellite-based data collection and platform location is thus a new research tool... and frequently one offering unique features.*

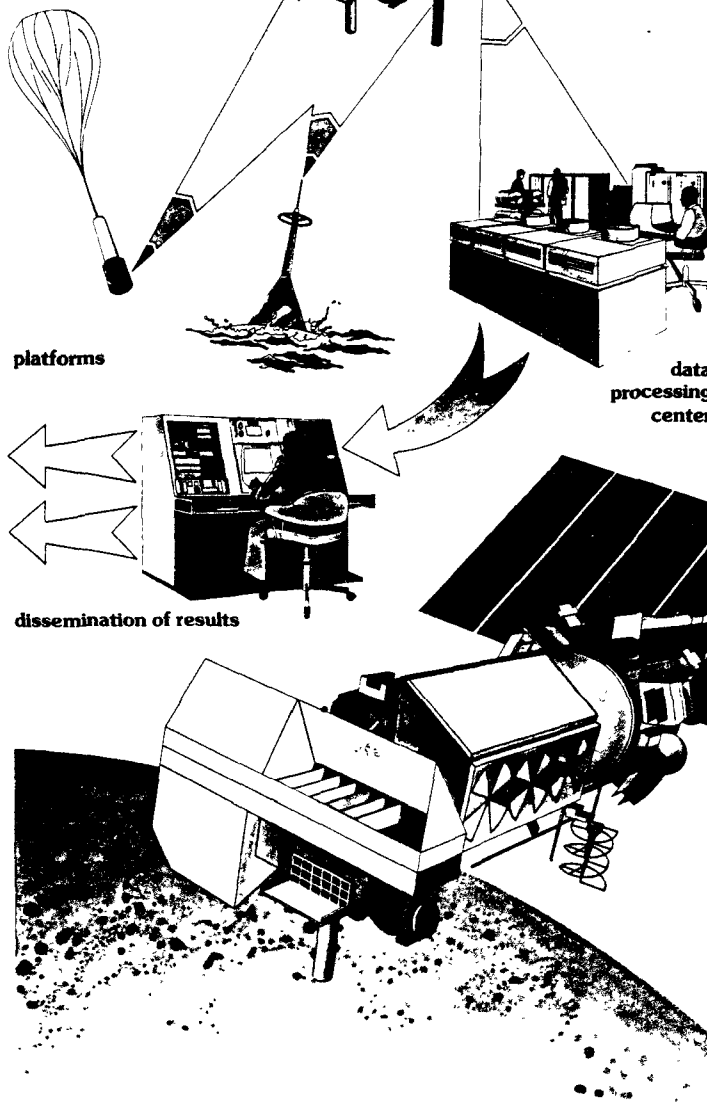


Michel Taillade  
Head of Service Argos

## general description

The Argos System comprises:

- a space segment consisting of two satellites in orbit at any one time, each being equipped with an onboard data collection system (or DCS) ensuring platform message reception, processing and retransmission.
- a set of user platforms, each being equipped with sensors and a platform



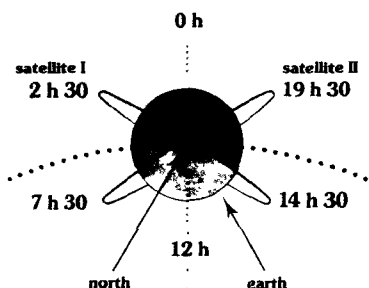
## space segment

At any given time, the space segment of the Argos System comprises two operational orbiting satellites.

### Orbit characteristics

- Configuration: circular.
- Altitude (satellite I):  $830 \pm 18$  km, (satellite II):  $870 \pm 18$  km.
- Inclination:  $98^\circ$  (polar orbits; during each orbit, each satellite "sees" both the North and South Poles).
- Period: 101 minutes (time required for each satellite to circle the Earth).
- Relative disposition: orbital plane of satellite I is inclined  $75^\circ$  relative to that of satellite II.
- Sun-synchronous orbits: the angle between the orbital plane of each satellite and the Sun direction is constant.

Each satellite crosses the equatorial plane at a fixed time (local solar time) each day. These times are:  
 satellite I: 14 h 30 (ascending node) and 2 h 30 (descending node).  
 satellite II: 19 h 30 and 7 h 30.  
 This characteristic is important from the user's viewpoint since, from one day to the next, a given platform comes within a satellite's coverage at the same time (local solar time).



The following table gives approximate data for satellite visibility, as a function of latitude, for a 24-hour period.

latitude	cumulative visibility time over 24 hours	number of passes in 24 hours			mean pass duration
		min.	mean	max.	
$\pm 0^\circ$	80 min.	6	7	8	10 min.
$\pm 15^\circ$	88 min.	8	8	9	
$\pm 30^\circ$	100 min.	8	9	12	
$\pm 45^\circ$	128 min.	10	11	12	
$\pm 55^\circ$	170 min.	16	16	18	
$\pm 65^\circ$	246 min.	21	22	23	
$\pm 75^\circ$	322 min.	28	28	28	
$\pm 90^\circ$	384 min.	28	28	28	

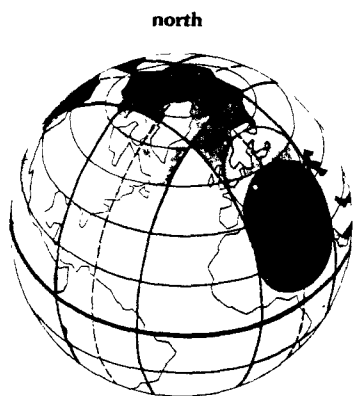


#### Technical data concerning orbit geometry

At any given moment, each satellite "sees" all the platforms located within a circle 5000 km in diameter.

As the satellite orbits, the ground track of this circle corresponds to a swath 5000 km in width encompassing the Earth. At each orbit, this swath covers both the North and South Poles (polar orbits). For a given satellite, the swath is displaced by  $25^\circ$  (i.e. 2800 km at the Equator) every 24 hours as a result of the rotation of the Earth.

Data collection performance, which is determined by orbit geometry, is thus a function of latitude.



#### user platforms

Each platform is equipped with a platform transmitter terminal (PTT) providing the up-link between platform and satellite.

Platform sensors are linked directly to the PTT. Analog or digital data from up to 32 sensors can be handled by each PTT.

The overall design of the Argos System is such that the PTTs providing up-links to the orbiting satellites offer the following features

- **simplicity** PTT electronics consists essentially of a transmitter
- **lightweight** less than 1.5 kg
- **low power consumption** approximately 200 mW on average
- **ease of implementation**
- **low cost**: FF 11,000 to FF 17,000 depending on type and options

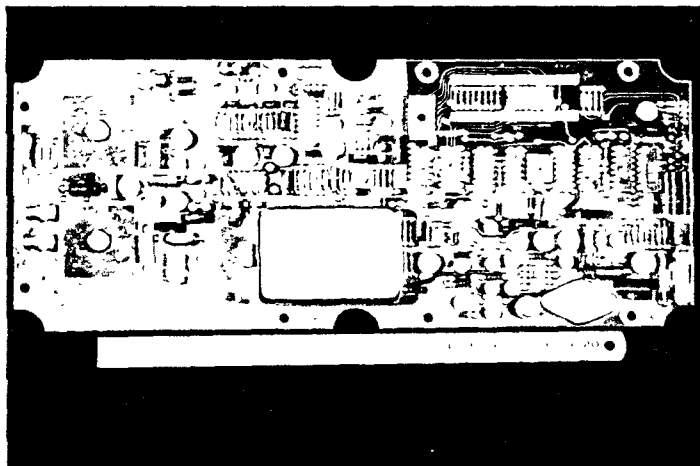


Photo CEIS Espace

All PTTs transmit on the same frequency (401.650 MHz) and at regular intervals: every 40 to 60 seconds in the case of "location" platforms and every 100 to 200 seconds for "data-collection-only" type platforms. Each message transmitted includes that particular platform's number and the sensor output values sampled at the time of transmission. Message duration is always less than 1 second.

#### certified PTTs

The list of manufacturers producing certified PTTs (i.e. satisfying Argos System requirements) is published regularly in Argos Newsletter or available from Service Argos on simple request.

## data collection

PTTs transmit their messages periodically, on the same frequency, independently of each other, and without the need for satellite interrogation.

The only communication links between users' platforms and the satellites are one-way platform-to-satellite links (or up-links).

Messages from platforms within view of a satellite appear at the input to the onboard receiver in a random fashion:

- message separation in time is obtained through the asynchronization of transmissions and the use of different repetition periods.
- message separation in frequency is achieved as a result of the different Doppler shifts in the carrier frequency transmitted by the various platforms.

In the event of a number of messages reaching the receiver input simultaneously, up to four can be acquired provided they are separated in frequency.

The probability of acquisition of a message transmitted by a platform during a satellite pass is 0.99 provided all messages transmitted during periods of about 10 minutes are identical.

## Random access

## platform location

### Principle of platform location

The location of each platform is determined solely by measuring the Doppler effect on the carrier frequency of in-coming messages (the transmitting frequency being fixed and the same for all platforms).

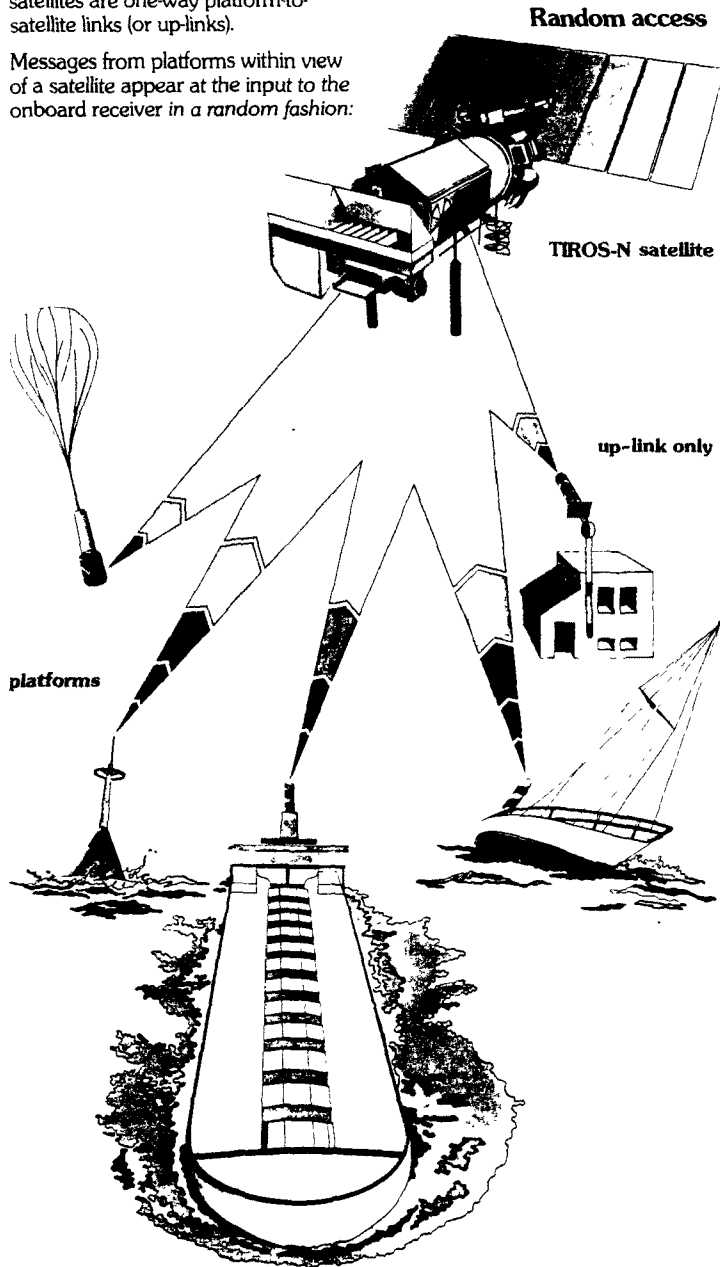
Each measurement made by the satellite corresponds to a field of possible positions of the platform under consideration. This field takes the form of a cone with the satellite at its apex and the velocity vector as the axis of symmetry.

The altitude of the satellite being assumed to be known, the intersection of several of these cones (each corresponding to a separate measurement) with the altitude sphere yields the solution.

Taking into account the nature of the geometrical fields concerned (cones with the orbits as their axes of symmetry), the statistical processing of the measurement data obtained by the satellite yields two symmetrical solutions relative to the ground track. One of these points is the required solution, the other its "image".

The ambiguity cannot be resolved without additional information, e.g. previous positions, range of possible speeds, etc.

The slower the platform moves, the more easily the ambiguity can be resolved.

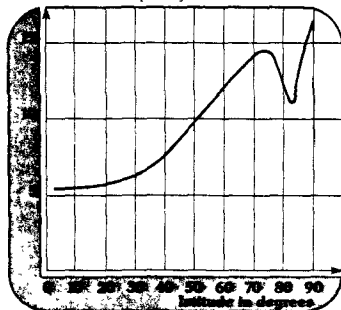




### Platform location performances

The following curve gives the number of locations per day you may expect with the Argos System as a function of the latitude.

Number of locations per day



performance data for 99% of cases	Drifting buoys	Drifting balloons
location accuracy	1 km	3 km
accuracy of speed determination	0.3 m/s	1.5 m/s

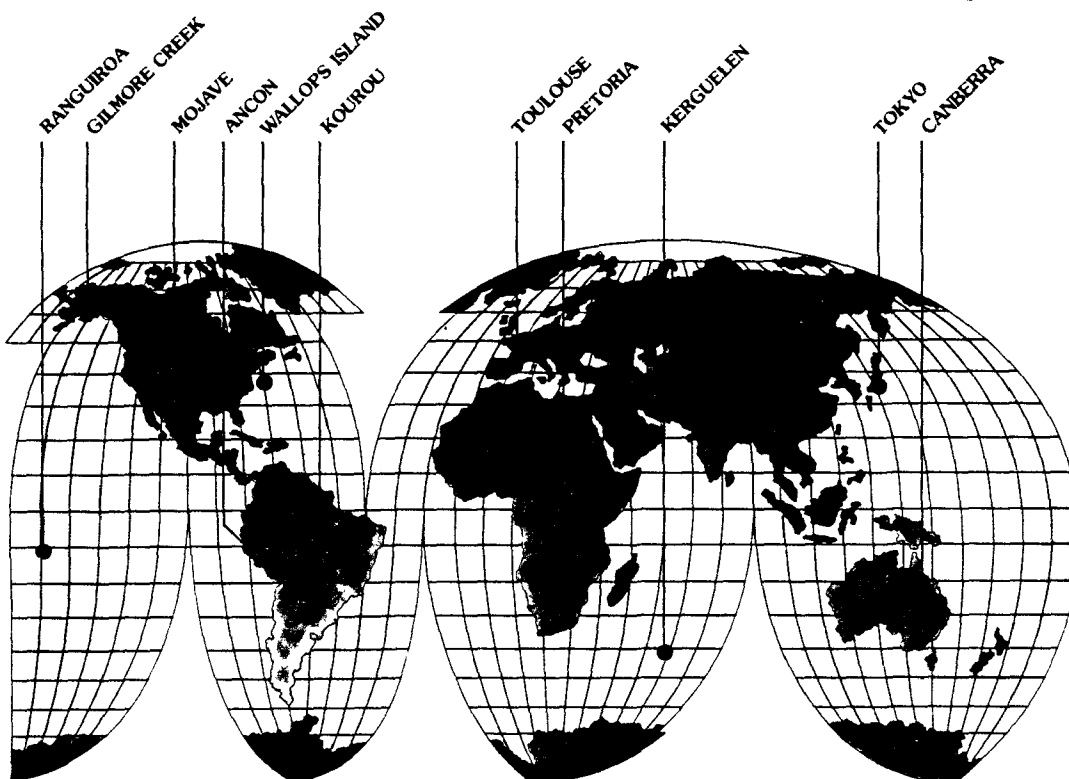
### Errors associated with platform location

The main sources of error regarding platform location are:

- the accuracy with which the platform altitude is known. This is relatively unimportant in the case of drifting buoys, but may be very important in the case of balloons;

- the stability of the PTT oscillator, in particular the drift in transmitting frequency during a satellite pass (approximately 10 minutes);

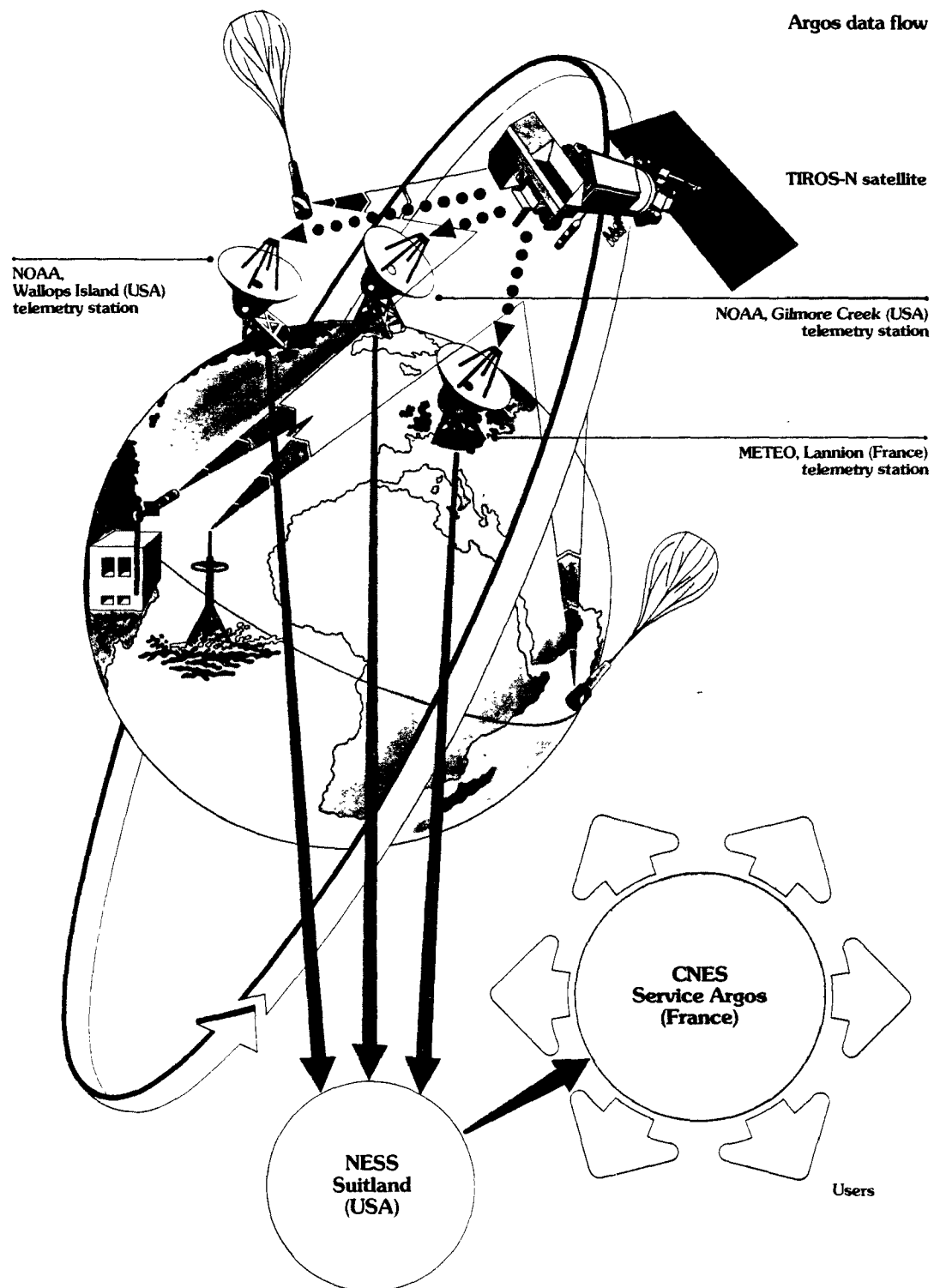
### orbit determination platforms



### Orbit determination platforms

Eleven special orbit determination platform are installed at appropriate locations. The geodetic position of each of these sites have been accurately determined

These platforms are used for the high-precision determination of each satellite's orbit, within 300 m along the orbit and within 250 m along the two other axes  
The resultant data being in turn employed for platform location



## onboard data collection system

The onboard DCSs are equipped with receivers that pick up messages transmitted by platforms within the satellite's coverage. Message reception is on a random access basis. As each message is acquired, the DCS records the time and date, measures the carrier frequency and demodulates the platform identification number and sensor data.

Four messages can be received and processed at any one time.

These data are then formatted and stored by one of the onboard magnetic tape recorders. Each time the satellite passes over one of the three telemetry stations, the data recorded on tape are read out and transmitted to ground.

### capacity of the Argos DCS

The onboard data collection system maintains nominal performance with 920 data collection only platforms or 230 platform location only platforms (plus minimal data collection) respectively that falls simultaneously within satellite coverage.

### direct transmission

In addition to recording the DCS data, the spacecraft transmits it in real-time on 136.770 or 137.770 MHz. The DCS data is multiplexed with other instrument data at a low bit rate. Users can receive sensor data from platforms within the satellite's coverage at the time of transmission.

### breakdown of interval between data collection and availability

component			
orbital interval		0 to 100'	
transmission to NESS			45'
transmission to Service Argos			20'
processing at Service Argos			40'
total interval			
min.			1 h 45'
max.			3 h 25'

## data processing centers

Data are read out once every orbit, i.e. every 100 minutes for each satellite.

Once a satellite has completed telemetry data transmission for a particular pass, the received data are transmitted to the NESS (National Environmental Satellite Service) Center at Suitland (Maryland, USA). Data concerning the Argos System are separated from those concerning other satellite systems and transmitted to the CNES Toulouse Space Center where the Argos Data Processing Center is located.

The processing performed at the Center permits the determination of platform positions and the extraction of sensor data.

### breakdown of interval between data collection and availability

The minimum interval between data collection and data availability in a nominal system can be evaluated as follows:

- a particular message collected during a single orbit may have been stored up to 100 minutes before the onboard tape is played back to the ground telemetry station.
- the time required for data transmission between the receiving telemetry station and the NESS

facility is estimated at 45 minutes while the time required to retransmit Argos data to Service Argos is estimated at 20 minutes

- the time required to process the data generated by a single orbit is 40 minutes at the maximum.

The interval between the time when a given platform message is acquired by the satellite and the time when the data is processed and available to users will vary between 1 hour 45 minutes and 3 hours 25 minutes depending on the platform's position.

These figures thus represent the ultimate possibilities of the system.

### Argos data availability

About two third of the results are made available to users at the Toulouse Space Center within 3 hours after the onboard recording of the corresponding message.

## results supplied to users

In the case of data-collection-only platforms, the results supplied to users include:

- experiment identification code (project n°).
- platform number (Argos ID n°).
- time of data collection.
- sensor data after conversion to pure binary code or to physical units.

In the case of location-and-data-collection platforms, the results include all the above plus:

- time of location.
- position data (latitude and longitude).
- latitudinal and longitudinal velocity components in degrees per day.

## data dissemination options

Each user can choose between various modes of data dissemination to achieve an optimal time/cost trade-off for his particular requirements and circumstances.

### off-line data distribution

Results, in this case, are made available to users from the data bank. Data stored in the bank are read out once a week for all users and held available for a period of three months only.

Results are available in the following forms once a fortnight or once a month:

- computer print-out.
- magnetic tapes.

The normal mode of distribution is by the fastest postal means.

### on-line data distribution

Results, in this case, are supplied the moment they become available, i.e. immediately the corresponding data flow has been processed. A suitable high-speed means of communication must then be chosen from among the following:

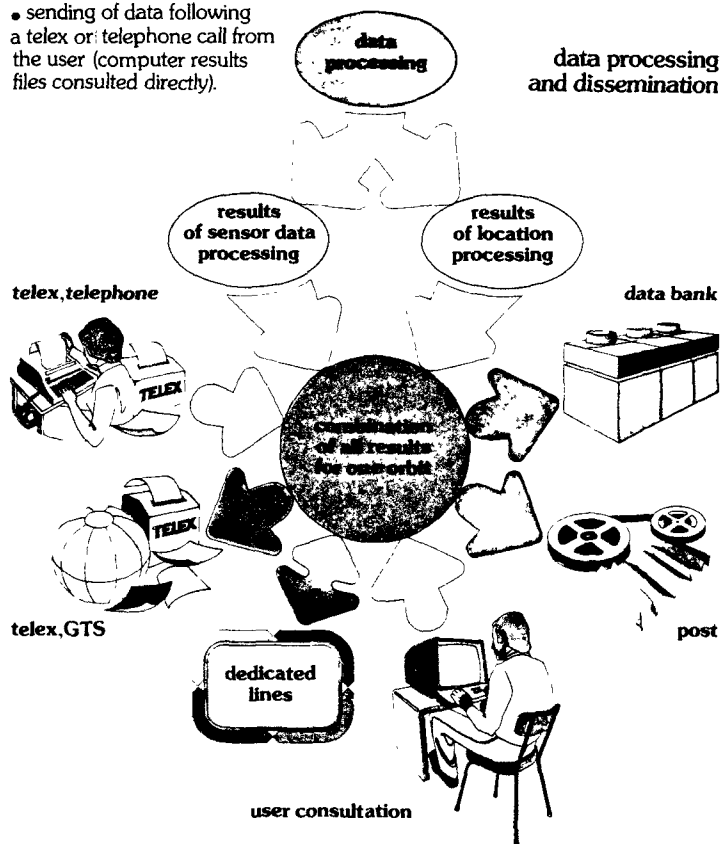
- permanent links:
- dedicated lines hired by the user.
- dedicated network through the French TRANSPAC and other dedicated networks such as EURONET and TIMENET...
- the Global Telecommunications System (GTS) operated by the



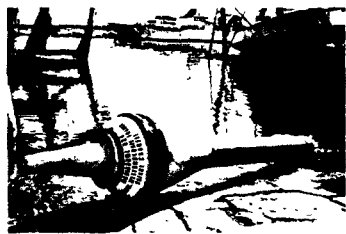
World Meteorological Organization (W.M.O).

Service Argos data processing Center in Toulouse (France)

- links via switched networks (telex or telephone):
- sending of telex messages generated automatically by the Argos Data Processing Center,
- sending of data following a telex or telephone call from the user (computer results files consulted directly).



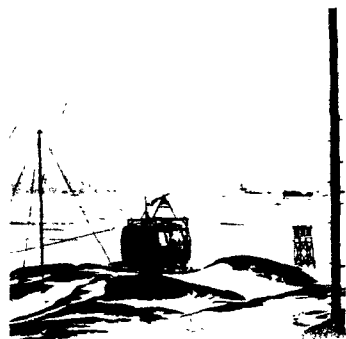
# applications of the Argos System



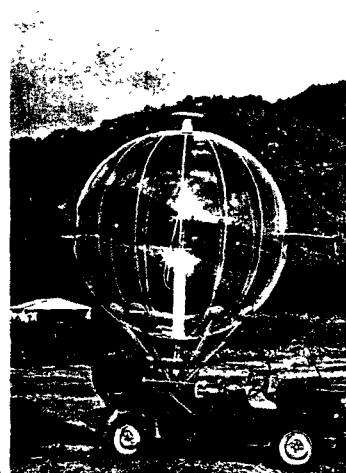
1



2

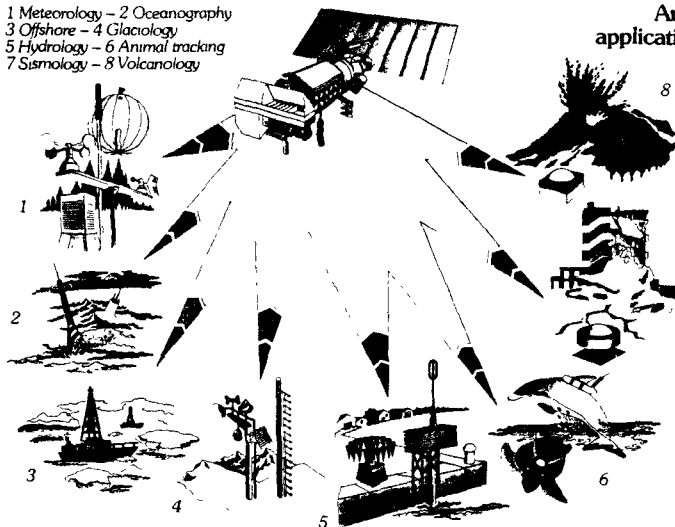


3



4

1 Meteorology - 2 Oceanography  
3 Offshore - 4 Glaciology  
5 Hydrology - 6 Animal tracking  
7 Sismology - 8 Volcanology



Argos  
applications

The Argos System is particularly suitable for gathering environmental data in various areas such as:

## Meteorology

Worldwide data collection of observations concerning the state of the atmosphere is possible. Meteorological applications include:

- world meteorological and oceanographic networks (e.g. FGGE, First Garp Global Experiment) using mainly buoys and balloons,
- anchored meteorological buoy networks,
- land based stations used for meteorological measurements,

- meteorological keyboard terminals for vessels,
- automatic mini weather stations for merchant ship developed pursuant to a WMO recommendation. This kind of equipment is also successfully used for offshore yacht races,
- studies on surface currents using rapid drifting buoys.

## Oceanography

represents a wide variety of current and potential applications for the Argos System. Typical examples include:

- regional experiments such as the EEC's COST 43,
- courses, studies, width and speed of major currents,
- subsurface studies with measurements of water temperature at various depths, of drogue line parameters, of acoustic parameters. Such oceanographic research is also of great use to the fishing industry,
- ocean swells and waves (formation, spectrum, propagation, correlation with underwater ambient noise levels studies)

1 French Marseilles buoy  
(photo Sefare-Crouzet)

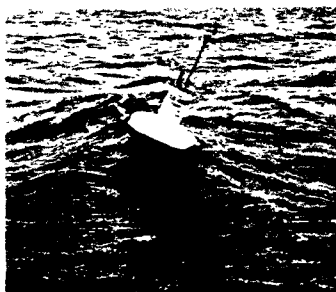
2 Mini weather station on a sail boat  
(photo CEIS Espace)

3 Automatic weather station  
in Greenland (Norway)  
(photo Danish Meteorological Institute)

4 French BALSAMINE Experiment  
(Balloon to study the monsoon circulation)  
(photo LMD)



1 Hydrological station for river monitoring  
(photo ORSTOM)



2 Norwegian Meteo-Oceanographic buoy  
(photo IKU)

3 Animal tracking  
(photo NOAA - South West Fisheries Center)



### Offshore

in connection with meteorological, oceanographic and glaciology utilization, for prospection studies, environmental control, oil spill tracking, pollution studies, ocean climate studies, operation monitoring, mooring failure monitoring

### Glaciology

to study polar currents and compare buoys and iceberg trajectories. Operational avalanche risk forecast program can be included in glaciology application.

### Biology

is used to cover animal tracking. Experiments were conducted on the following species to improve hardware problems: dolphins, basking sharks, turtles, whales and polar bears

### Hydrology

covers a wide range of potential applications due to the low cost of the Argos compatible hydrologic station: management of hydrologic networks, water survey and supply and assessment of water resources.

### Geology

monitoring and prediction of earthquakes and volcanic eruptions, prediction of fault movements, study of the thermal inertia of soil types

The Argos System is strongly recommended to all WMO (World Meteorological Organization)/IOC (UNESCO Intergovernmental Oceanographic Commission) participating countries for utilization in future international climate programs.

## Service Argos

Supervised by the Argos Operations Committee, Service Argos is a bilateral Franco-American (CNES, NOAA, NASA) organization set up by CNES at the Toulouse Space Center in France. Service Argos is the contact point for all system users.

The main responsibilities of Service Argos are:

- coordination of the operation and monitoring of the entire Argos System,
- promotion activities to extend the use of the system,
- preparation and dissemination of documentation,
- maintenance of the orbit determination network,
- technical certification of prototype PTTs submitted by manufacturers,
- provision of technical assistance services concerning the implementation and operation of transmission equipment for use with Argos System satellites.

### Users-Service Argos relations

Telephone      Telex  
• (61) 53.11.12      • 531081 F

### General Documentation

- Argos Newsletter, published periodically by Service Argos and available on request.
- Argos System User's Guide.

### Access to the Argos System

- the document entitled "Argos application form" is available, on request, to any individual or group in the process of preparing a project or program.

### Visits

- persons with a professional interest in the Argos System can arrange to visit the Argos facilities

### Manufacture and Certification of PTTs

- specification for PTT manufacture and details concerning the certification procedure are available either from Service Argos or from manufacturers



CONCEPTION F. BOLZINA AL. BELLES / PHOTO L. JAMES / PHOTOMONTAGE

## APPENDIX I

### PUMPDOWN SPEED WITH AN ARBITRARY LAPSE RATE

Consider the density  $\rho_a$  of the ambient air in the vicinity of the balloon as it is pumped down. The gas law gives:

$$\rho_a = \frac{MP_a}{RT} \quad (I-1)$$

where  $M$  is the average molecular weight of air.

The rate of change of ambient air density during pumpdown is given by

$$\begin{aligned} \frac{d\rho_a}{dt} &= \frac{M}{R} \left[ \frac{1}{T} \frac{dP_a}{dz} \frac{dz}{dt} - \frac{P_a}{T^2} \frac{dT}{dz} \frac{dz}{dt} \right] \\ &= \frac{M}{R} \left[ \frac{1}{T} \frac{dP_a}{dz} - \frac{P_a}{T^2} \frac{dT}{dz} \right] \frac{dz}{dt} \end{aligned} \quad (I-2)$$

where here  $dz/dt$  is the rate of change of altitude, and  $-dT/dz = \gamma$ , the lapse rate. To evaluate  $dP_a/dz$ , note that

$$dP_a = -\rho_a g dz \quad (I-3)$$

so

$$\frac{dP_a}{dz} = -\frac{MP_a}{RT} g \quad (I-4)$$



Substituting:

$$\frac{d\rho_a}{dt} = \frac{M}{R} \left[ \frac{1}{T} \left\{ \frac{-MP_a g}{RT} \right\} + \frac{P_a}{T^2} \gamma \right] \frac{dz}{dt} \quad (I-5)$$

If the balloon remains in equilibrium during pumpdown, then by definition  $dz/dt$  is the pumpdown speed,  $v_p$ , and the equilibrium condition applies:

$$V\rho_a = V\rho_b + m \quad (I-6)$$

Taking the time derivative

$$\frac{d\rho_a}{dt} = \frac{d\rho_b}{dt} \quad (I-7)$$

But  $d\rho_b/dt$  is given by Equation (B-3),

$$\frac{d\rho_b}{dt} = \frac{S\rho_a}{V} \quad (I-8)$$

Substituting,

$$\frac{S\rho_a}{V} = \frac{S}{V} \frac{MP_a}{RT} = -\frac{M}{R} \left[ \frac{1}{T} \left\{ \frac{-MP_a g}{RT} \right\} + \frac{P_a}{T^2} \gamma \right] v_p \quad (I-9)$$

Solving for  $v_p$ :

$$v_p = -ST/[V(Mg/R - \gamma)] \quad (I-10)$$

## APPENDIX J

### DIFFUSIVE SPREAD OF A MARKED AIR PARCEL AND ITS IMPLICATIONS FOR LAGRANGIAN EXPERIMENTS

A design goal for the PLT is that it be capable of following mean vertical flows as low as 1 cm/s with "acceptable" fidelity. The questions to answer are, how is the "mean flow" to be interpreted, and what is "acceptable" fidelity?

To answer these questions, it is useful to consider a discrete initial volume of air in which the balloon is embedded. If one conceptually marks every molecule in that volume, and follows each through subsequent time, one finds that diffusion will increase the RMS separation of this set of marked molecules from the mean in both the horizontal and the vertical; that is,  $\sigma_x$ ,  $\sigma_y$ , and  $\sigma_z$  will grow with time. Here the  $\sigma$ s are the root mean square deviations of the marked molecules from the centroid of the cloud. Each marked molecule may be viewed as a perfect Lagrangian tracer. These perfect tracers end up throughout the cloud at subsequent times. If an artificial Lagrangian tracer such as the PLT remains within  $\pm\sigma_x$ ,  $\pm\sigma_y$ , and  $\pm\sigma_z$  of the centroid of the cloud, there is little doubt that it follows the flow in both the horizontal and the vertical with "acceptable" fidelity -- it has followed the centroid as well as, or better than, a significant fraction of the perfect Lagrangian tracers -- the marked molecules themselves.

In this conceptual framework, the term "mean vertical flow" has a straightforward interpretation: the vertical motion of the centroid of the cloud. The question of how to interpret the "mean" then reduces to how to choose the

dimensions of the volume one desires to follow. Clearly that choice is experiment-dependent. In air pollution experiments, there is a physical puff or plume one desires to follow, the dimensions of which determine the choice. The principle is that the volume should be "representative" of the puff or plume. If one is interested in following the plume from some industrial facility in complex terrain over a few kilometres, the volume of interest might be some tens of metres in size -- perhaps comparable in scale to the plume cross section during the transport of interest. If one is interested in following the urban plume from Chicago, the volume might be 100 km in horizontal dimension, and the depth of the mixing layer in the vertical.

This interpretation of the mean flow leads to the practical question of how one can in fact follow the centroid of the volume of interest. Here, we borrow an idea from statistical mechanics. Under certain broad conditions, ensemble averages and time averages can be assumed to be equal (Reif, 1965). This suggests that the time average of the vertical velocity of the air evaluated at the PLT over an appropriately-chosen time interval may approximate the average vertical velocity of the air integrated over some volume surrounding the PLT. It is certainly plausible that the time average at the PLT is more characteristic of the motion of the centroid than the instantaneous velocity. It is also plausible that the longer the averaging time, the larger the associated equivalent averaging volume.

A characteristic time associated with a volume is the time required for molecules emitted from a central point within the volume to diffuse throughout. For lack of a better choice, we take this as an estimate of the appropriate averaging time for a PLT intended to follow the centroid of the specified volume.

To evaluate the time required to diffuse throughout the specified volume, we take the approach of MacCready et al (1974). From MacCready's derivation, it can be shown that:

$$\sigma_z = 0.88 L_w D \quad (J-1)$$

where  $\sigma_z$  is the root mean square position deviation of either a puff or a plume in the vertical<sup>†</sup>,  $L_w$  is the vertical correlation length estimated from the LO-LOCAT data by MacCready to be about 90 m, and D is the square root of a dimensionless velocity power spectrum integral. MacCready evaluated D as a function of a dimensionless quantity T proportional to time (Figure J-1):

$$T = Ut/2L_w\beta \quad (J-2)$$

where U is the mean wind velocity, t is time, and  $\beta$  is a constant connecting Eulerian and Lagrangian correlation times.

MacCready uses Pasquill and Smith's (1970) estimate,  $\beta = 0.44/i$ , where i is intensity of turbulence  $\sigma_w/U$ . We may also follow MacCready in using the inertial subrange relation:

$$\sigma_w = L_w^{.33} \epsilon^{.33} \quad (J-3)$$

to find

$$T = 1.14 L_w^{-.67} \epsilon^{.33} t \quad (J-4)$$

where here  $\epsilon$  is the turbulence dissipation rate, and  $\epsilon^{1/3}$  serves as a measure of the intensity of turbulence.

We are now in a position to find  $\sigma_z$  as a function of time

---

<sup>†</sup> MacCready comments in MacCready and McMullen (1977) that in the vertical, meander and large scale eddies are not dominant. Hence, total diffusion and relative diffusion are about the same. For simplicity's sake, we adopt this approximation.

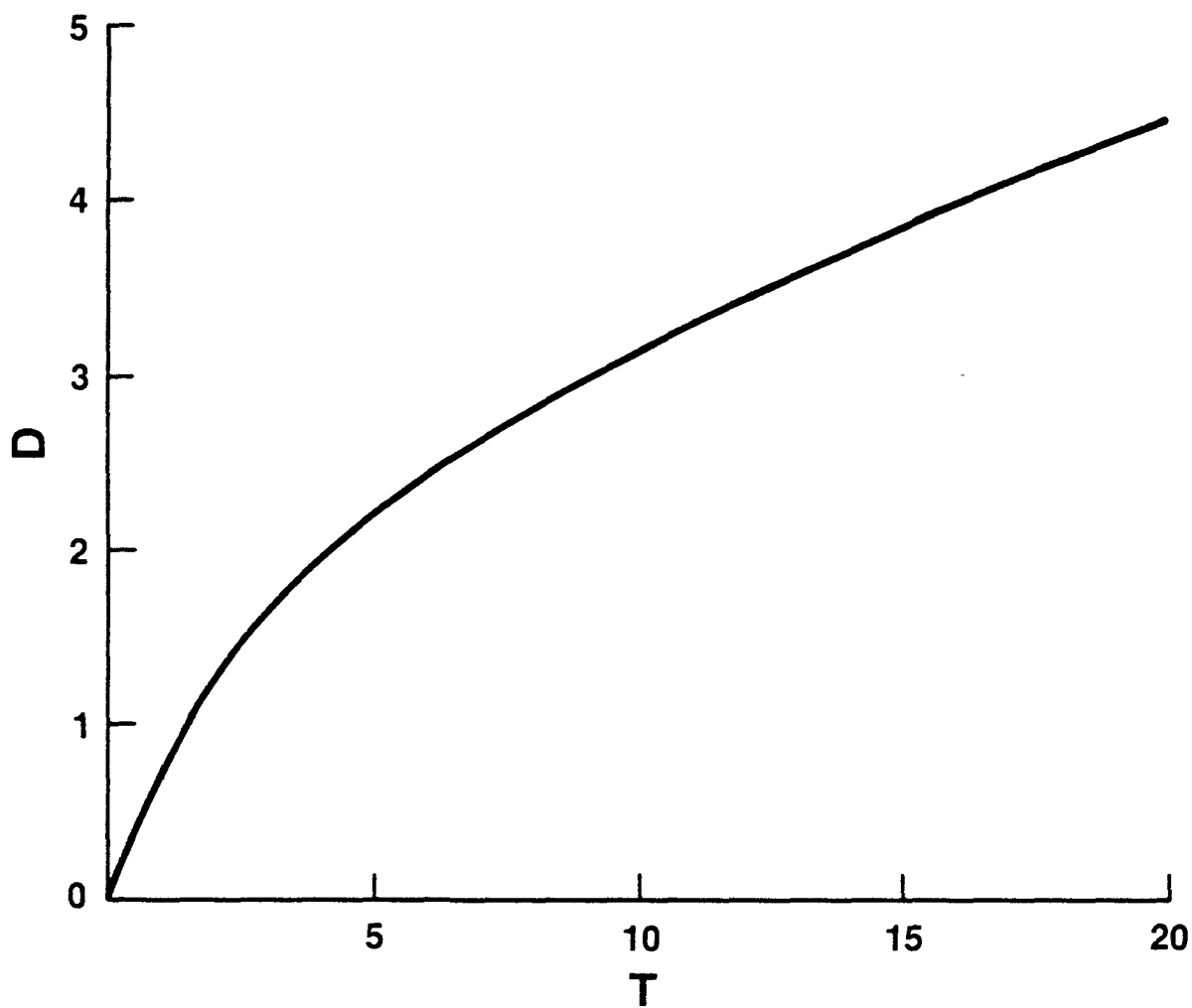


Figure J-1. Dimensionless diffusion parameter  $D$  versus dimensionless parameter  $T$  proportional to time. For  $T < 0.5$ ,  $D \approx T$ ; for  $T > 3$ ,  $D \approx \sqrt{T}$ .

based on values of  $\epsilon^{1/3}$  measured aloft on the DaVinci II balloon flight (Zak, 1981) over a 24-hour period (Figure J-2). During the convective portion of the day,  $\epsilon^{1/3}$  averaged about 2; during the evening and early night, about 0.5; and during the post-midnight hours, sometimes as low as 0.1. Here the units are  $\text{cm}^{2/3}\text{s}^{-1}$ . A sketch of the device used to make these measurements is shown in Figure J-3.

It can be shown that:

$$T_{\epsilon} = 2.64 \times 10^{-3} \epsilon^{1/3} t \quad (\text{J-5})$$

if  $\epsilon^{1/3}$  is left in units of  $\text{cm}^{2/3}\text{s}^{-1}$ .

---

TABLE J-1  
T as a Function of  $\epsilon^{1/3}$  and Time

t (s)	$\epsilon^{1/3} \text{ (cm}^{2/3}\text{s}^{-1}\text{)}$		
	<u>2.0</u>	<u>0.5</u>	<u>0.1</u>
10	.053	.013	.0026
30	.16	.040	.0079
100	.53	.13	.026
300	1.58	.40	.079
1,000	5.28	1.32	.26
3,000	15.8	3.96	.79
10,000	52.8	13.2	2.64
30,000	158.4	39.6	7.92

---

# DA VINCI II - ONE MINUTE AVERAGED DATA

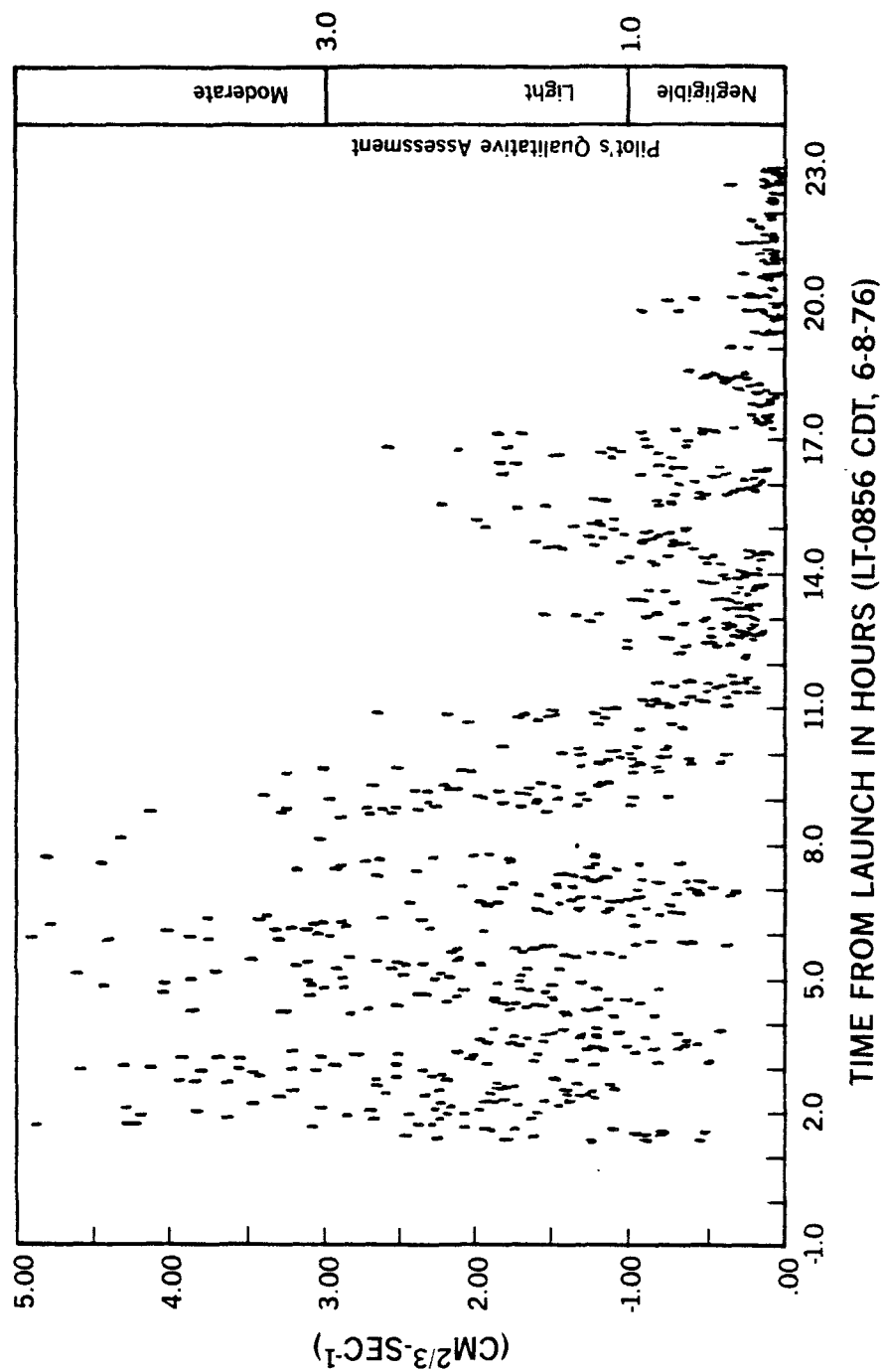


Figure J-2.  $\epsilon^{1/3}$  versus time for the DaVinci II flight. Time is given in hours from launch. Launch time was 0856 CDT.

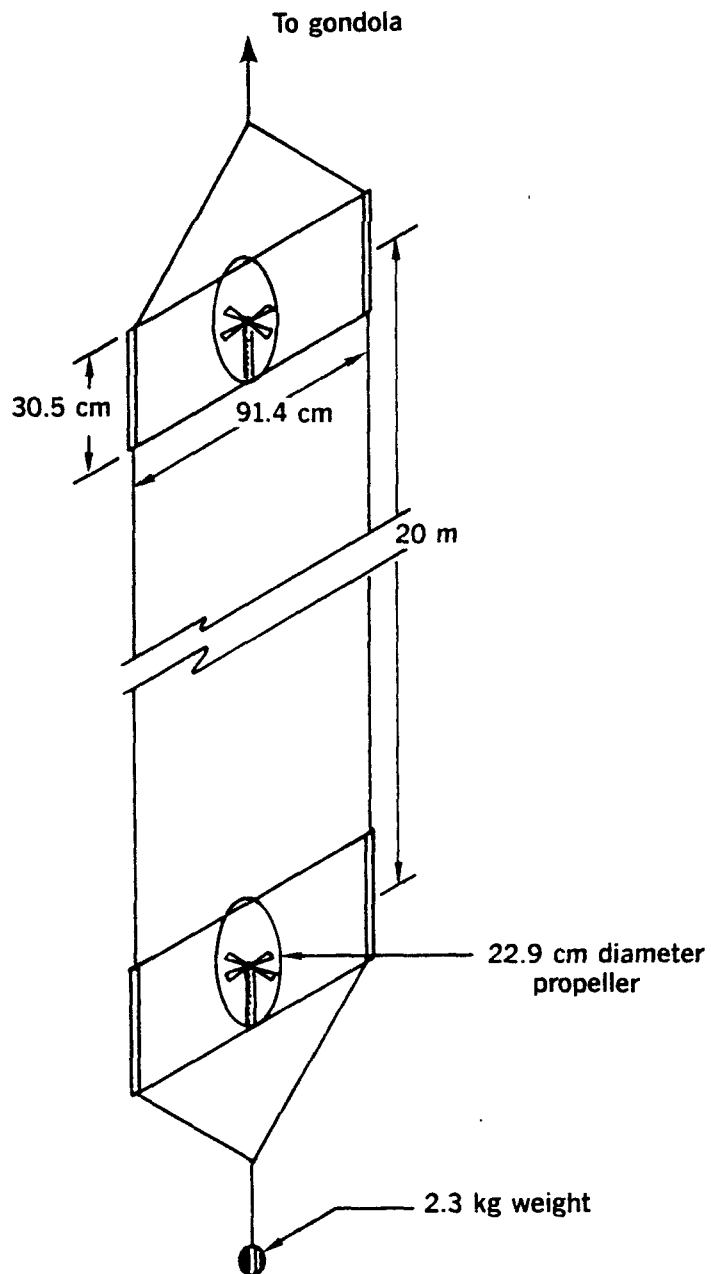


Figure J-3. "ε-meter" used to make turbulence measurements on DaVinci II. The two wind sensors are identical to the one shown in Figure 4-6, with the exception of supporting electronics.



Knowing  $T$ , we may use Equation J-1,  $\sigma_z = 0.88 L_w D$  and Figure J-1 to evaluate  $\sigma_z$ . However, it should be noted that for  $T \leq 0.5$ ,  $D \approx T$ , and that for  $T \geq 3$ ,  $D \approx \sqrt{T}$ .

TABLE J-2

$\sigma_z$  (metres) as a Function of  $\epsilon^{1/3}$  and Time

<u>t (s)</u>	<u><math>\epsilon^{1/3}</math> (cm<sup>2/3</sup>s<sup>-1</sup>)</u>		
	<u>2.0</u>	<u>0.5</u>	<u>0.1</u>
10	4.2	1.0	.21
30	13.	3.2	.63
100	42.	10.	2.1
300	87.	32.	6.3
1,000	182.	77.	21.
3,000	315.	158.	49.
10,000	575.	288.	126.
30,000	997.	498.	223.

For the convective period, a rough check is available on the rate of diffusive spread. On the day of DaVinci II, sunrise occurred at 5:36 am. Between sunrise and noon, the mixed layer grew to about 2 km. A puff originating at ground level at sunrise would have continuously grown to fill the mixed layer in the vertical to its maximum height. We assume that the mixed depth is at most  $2 \sigma_z$ , so that at  $t = 2.3 \times 10^4$  s,  $\sigma_z \approx 1000$  m.

Using our technique, we predict  $\sigma_z = 870$  m for this time. In view of the approximations made, this is quite reasonable agreement.

If the reasoning presented earlier is valid, the data in Table J-2 allow one to crudely estimate the thickness of the volume characterized by a specified averaging time. For an averaging time of 300 seconds (5 minutes), during a period of convective mixing with  $\epsilon^{1/3} = 2$ , the volume is about 173 m thick. During the decay of convective mixing characteristic of evening, the same averaging time corresponds to a layer of 63 m thickness. In the hours before dawn in the presence of minimal turbulence, a 5-minute averaging time characterizes a layer at least 12 m thick. If under any of these conditions the volume of interest is in fact thicker than the dimensions given above, then either the averaging time should be appropriately increased to attempt to follow the centroid more faithfully, or one must accept having a "better" Lagrangian tracer, that is, one which acts more like an individual gas molecule and which follows motions of smaller scale than the scale of interest, and hence simulates the motion of the centroid of the volume less well.

Table J-2 also casts light on the question of "acceptable" fidelity. Even with  $\epsilon^{1/3} = 0.1 \text{ cm}^{2/3} \text{ s}^{-1}$ , which is close to the minimum turbulence believed to be commonly present in the atmosphere for sustained periods, a puff spreads in the vertical from its centroid at an initial rate of about 2.1 cm/s. Only after hours of diffusion does the rate of spread fall to 1 cm/s (see Figure J-1). Consequently, even in extremely light turbulence, following the mean flow to within  $\pm 1$  cm/s will keep the marker balloon within  $\pm \sigma_z$  of the centroid of the ensemble of molecules which started out in its immediate vicinity. On the other hand, during active

daytime convective mixing, the initial rate of diffusive spread is about 42 cm/s. This falls to 3.3 cm/s in eight hours. Consequently, if a marker balloon follows the mean flow to within  $\pm 3.3$  cm/s over eight hours under convective conditions, even if the deviation is systematic, the balloon will remain within  $\pm \sigma_z$  of the centroid of the point source puff it started with.

It should be pointed out that the arguments presented above are approximate, and furthermore, depend upon relationships for the inertial subrange of turbulence. As the scale of the volume of interest increases...say beyond a kilometre or so...these relationships become less accurate. However, we have been applying these arguments to motion in the vertical. Here, the region of interest is usually limited to only about 2 km. Thus the arguments should be reasonably sound throughout this region. We do not consider the horizontal because, for the horizontal, there is no mechanism analogous to buoyancy which could lead to systematic bias in the balloon motion.

Note also that for validating long range transport and transformation models, even the condition that the PLT remain within  $\pm \sigma_x$ ,  $\pm \sigma_y$ , and  $\pm \sigma_z$  of the centroid of the volume of interest may be stronger than is necessary. Lamb (1984) has pointed out that the meteorological data available do not uniquely define the atmospheric flow field present at the time of an experiment. Rather, the data merely limit the flow field to some ensemble of flow fields consistent both with the data and with physical principles. What models really seek to do is predict ensemble average pollutant concentrations, rather than the concentrations produced by the flow field actually present on a given day. Analogously, for model validation, perhaps the trajectory of the PLT need only

approximate the mean trajectory over the ensemble of flow fields consistent with the data, rather than the trajectory of the centroid of the volume of interest under the action of the flow field actually present. Because the meteorological data usually available admits of quite a range of flow fields, this is likely to be a considerably less demanding requirement.

Consideration of Lamb's views leads to yet another perspective of the PLT. Clearly, the PLT itself yields information on the flow field, quasi-continuous information in the immediate vicinity of the volume of interest. This is in marked contrast to the widely-spaced grid of data available every 12 hours from the winds-aloft network. The information from the PLT can be used to narrow the ensemble of flow fields consistent with the available meteorological data. If these data are appropriately used, the flow field entered into a model would likely approximate the actual flow field in the vicinity of the volume of interest much more accurately. This could be of considerable value in experiments which include both a gaseous tracer species and a PLT for model validation. The PLT would minimize uncertainties arising from the flow field, and the gaseous tracer would allow measurements of concentrations to be directly compared with model predictions. In the experiment configuration shown in Figure 7-1, such experiments could be done with a single PLT, and a single instrumented aircraft, and would not necessarily require extensive ground sampler arrays.

<b>TECHNICAL REPORT DATA</b> <i>(Please read Instructions on the reverse before completing)</i>		
1. REPORT NO.	2.	3. RECIPIENT'S ACCESSION NO.
4. TITLE AND SUBTITLE DEVELOPMENT OF AN ADJUSTABLE BUOYANCY BALLOON TRACER OF ATMOSPHERIC MOTION Phase I. Systems Design and Demonstration of Feasibility		5. REPORT DATE
		6. PERFORMING ORGANIZATION CODE
7. AUTHOR(S)		8. PERFORMING ORGANIZATION REPORT NO.
9. PERFORMING ORGANIZATION NAME AND ADDRESS B.D. Zak, H.W. Church, A.L. Jensen, G.T. Gay, and M.D. Ivey Sandia National Laboratories Albuquerque, NM 87185		10. PROGRAM ELEMENT NO. CDTAID/08/3005 (FY-85)
		11. CONTRACT/GRANT NO. IAG DW930214
12. SPONSORING AGENCY NAME AND ADDRESS Atmospheric Sciences Research Laboratory - RTP, NC Meteorology and Assessment Division U. S. Environmental Protection Agency Research Triangle Park, NC 27711		13. TYPE OF REPORT AND PERIOD COVERED Interim
		14. SPONSORING AGENCY CODE EPA/600/09
15. SUPPLEMENTARY NOTES		
16. ABSTRACT <p>An Adjustable Buoyancy Balloon Tracer of Atmospheric Motion is a research tool which allows one to follow atmospheric flows in both the horizontal and the vertical, including the weak, sustained vertical motion associated with meso- and synoptic- scale atmospheric disturbances. The design goals for the Balloon Tracer to be developed here specify a lifetime &gt; 3 days, tracking range &gt; 1000 km, a ceiling altitude &gt; 500 mb (5.5 km), and the capability to respond to mean vertical flows as low as 1 cm/s. The balloon tracer is also to measure and telemeter selected meteorological variables, to be sufficiently inexpensive to permit use in significant numbers, and to be serviced by a ground system capable of handling several balloon tracers at a time. While the balloon tracer has applications throughout the atmospheric sciences, the immediate motivation for this effort is to meet the need to evaluate the accuracies of existing air pollution transport models, to establish source-receptor relationships to distances of order 1000 km, and to assess the inherent limits on the predictability of source impact at long distances. The authors have proposed a generic design for such a system. They also have subjected the proposed design to theoretical analysis, have constructed a prototype, and have conducted a series of tests with the prototype to evaluate the concept. They conclude, without reservation that a system meeting the design goals is feasible, and are proceeding to build that system in Phase II of this project.</p>		
17. KEY WORDS AND DOCUMENT ANALYSIS		
a. DESCRIPTORS	b. IDENTIFIERS/OPEN ENDED TERMS	c. COSATI Field/Group
18. DISTRIBUTION STATEMENT  RELEASE TO PUBLIC	19. SECURITY CLASS (This Report) UNCLASSIFIED 20. SECURITY CLASS (This page) UNCLASSIFIED	21. NO. OF PAGES  22. PRICE